

Republic of Iraq  
Ministry of Higher Education and Scientific Research  
University of Technology  
Laser and Optoelectronics Engineering Department



***CALCULATION OF MTF FOR OPTICAL DISK  
MODULATOR BY USING FRACTAL  
FUNCTION***

A Thesis Submitted to the  
Laser and Optoelectronics Engineering Department, University of  
Technology in a Partial Fulfillment of the Requirements for the  
Degree of Master of Science in Optoelectronics Engineering

By  
***Ahmed Seleman Abdula***

Supervisor  
***Dr. Abdulrazak A.S. Mohammad***

April 2008 A.D.

Rabea Al-Awal 1429 A.H



جمهورية العراق  
وزارة التعليم العالي والبحث العلمي  
الجامعة التكنولوجية  
قسم هندسة الليزر والبصريات الالكترونية

## حساب دالة الانتقال المعدلة لقرص التضمين البصري باستخدام الدالة الكسورية

رسالة مقدمة إلى

قسم هندسة الليزر والبصريات الالكترونية الجامعة التكنولوجية  
وهي جزء من متطلبات نيل درجة الماجستير علوم في هندسة  
البصريات الالكترونية

تقدم بها

احمد سليمان عبدالله

بإشراف

الدكتور عبدالرزاق عبدالسلام

## *Abstract*

Optical modulator is an important component in optical systems. It is a device, which changes the angle between the vision line to the target and coordinate to electrical signal. The optical modulator modulates the optical signal by a frequency depending on the shape and number of sectors.

The optical modulator takes various circular shapes due to the need for it. Through this study we have designed an optical modulator consisting of three concentric circles ( $C_0$ ,  $C_1$ ,  $C_2$ ). Each circle is divided to transmittance and oblique sectors, the numbers of sectors chosen equal to (20,40,60) respectively, and increases progressively with increasing the number of circles. And thickness of each circle chosen equal to ( $R_0=1.5$ ) cm, that means the radius of optical disk is ( $R_r=4.5$ )cm.

The central circle was designed using fractal geometry with a modified program to draw and enhance fractal figures including the fractal optical disk. The final shape of the proposed disk was designed using (Auto-CAD) software.

The efficiency of this optical modulator disk was tested by applying the modulation transfer function (MTF), where we found that the results converge, the maximum chopping frequencies in circles ( $C_0$ ,  $C_1$ ,  $C_2$ ) are (2.5,5,10)KHZ at ( $t=0.004$ )sec, and minimum chopping frequencies are (0.05,0.1,0.2)KHZ at ( $t=0.2$ )sec, and the best modulation at spot light size equal to ( $2 \text{ mm}^2$ ), and that the proposed optical modulator disk could be used in optical systems.

```
CLS
5 INPUT "enter number of sectors="; q
10 INPUT "enter time="; t
REM (t=sec)
15 INPUT "enter number of initial circle="; A
20 INPUT "enter number of final circle="; B
25 INPUT "enter spot size="; a
30 FOR N= A TO B
35 FOR n= 1 TO 3
REM (n= number of circle)
40 r=1.5
REM (r= radius of circle in mm)
45 s = ((2 * 3.14 * r) / q)
REM (k=s/r)
50 k = ((2 * 180 * r) / (r * n*q))
REM (k=angel with degree =s/r=360/n*q)
55 V=(s/t)*(1/r)
REM ( V the angular velocity in rev/min)
60 Fcn= n*q*V
65 Sn=(3.14*((2*N)-1)*r^2)
REM (Sn the area of circle n in mm2)
70 Scn= Sn/N*q
75 Imax=a/Scn
80 Imin=a/(Sn-Scn)
85 Z=(Imax-Imin)/(Imax+Imin)
REM(Z=MTF)
90 PRINT "Scn="; Scn;, "Fcn=KHZ"; Fcn; "T=sec"; t; , "Z="; Z,
95 NEXT
100 END
```

## Equation solving for Triangle Transformations

```

#include <float.h>
#include "fdestria.h"
#include "fdesign.h"
#include "fdesfile.h"
#include "fdesmenu.h"
#include "fdesmous.h"
#include "fdesplot.h"
/*****
*****

SOLVING EQUATIONS FOR TRIANGLE TRANSFORMATION
TO IFS CODE
*****/

Compute the IFS array for the given triangles
Float det(float a, float b, float c, float d)
Return (a*d-b*c);
Float solve3 (float x1, float x2, float x1h, float y1, float y2, float y1h,
Float z1, float z2, float z1h, float *a, float *b, float *e) /* solve linear
system
Format for the equations is this:
x1*a + x2*b + e = x1h
y1*a + y2*b + e = y1h
z1*a + z2*b + e = z1h
float det1;
det1 = x1 * det(y2,1.0,z2,1.0) - x2 * det(y1,1.0,z1,1.0) + det(y1,y2,z1,z2);
if (det1 == 0.0) return (det1);
a = (x1h * det(y2,1.0,z2,1.0) - x2 * det(y1h,1.0,z1h,1.0) +
det(y1h,y2,z1h,z2))/det1;
*b = (x1 * det(y1h,1.0,z1h,1.0) - x1h * det(y1,1.0,z1,1.0) +
det(y1,y1h,z1,z1h))/det1;
e = (x1 * det(y2,y1h,z2,z1h) - x2 * det(y1,y1h,z1,z1h) +
x1h*det(y1,y2,z1,z2))/det1;
Return (det1);

Compute IFS of triangle and place codes at IFS pointer
t1 is the transform triangle, t0 is the reference triangle

Void IFS_compute (float IFS, triangle t1, triangle t0)
Solve3 ((t0). col [0], (t0). row [0], (t1). col [0],
(t0). Col [1], (t0). row [1], (t1). col [1],
(t0). Col [2], (t0). row [2], (t1). col [2],

```

---

```
&IFS [0], &IFS [1], &IFS [4]);  
  Solve3 ((t0). Col [0], (t0). row [0], (t1). row [0],  
          (t0). Col [1], (t0). row [1], (t1). row [1],  
          (t0). Col [2], (t0). row [2], (t1). row [2],  
          &IFS [2], &IFS [3], &IFS [5]);
```

**Compute IFS codes for all of the triangles**

```
Void IFS_compute_all (int how many, triangle t, triangle *t0)  
Int i;  
Float total area;  
IFS [0] = how many;  
Total area = 0.0;  
For (i=0; i<how many; i++)  
  IFS_compute (&IFS [1+i*7], &t [i], t0);  
  Pseudo-probability measure */  
Total area += (IFS [1+i*7+6] = triangle area (&t [i]));  
  Normalize probabilities to 1.0 */  
For (i=0; i<how many; i++)  
  IFS [1+i*7+6] /= total area;  
End
```

# ***CONTENTS***

Seq.	<i>Contents</i>	Page
	Dedication	I
	Acknowledgment	II
	Abstract	III
	List of Symbols	IV
	List of Abbreviation	VI
	Contents	VII
<i>Chapter One: General Introduction</i>		
1.1	Introduction	1
1.2	Lens Testing	2
1.2.1	Qualitative Test	2
1.2.2	Quantitative Test	3
1.3	Diffraction	5
1.4	Aberration	7
1.4.1	Monochromatic Aberration	7
1.4.2	Spherical Aberration	8
1.4.3	Coma	9
1.4.4	Astigmatism	9
1.4.5	Field Curvature	10
1.4.6	Chromatic Aberrations	11
1.5	Resolution of Optical System	12
1.6	Depth of Focus	13
1.7	Electro-Optic Modulators	14
1.8	Acousto-Optic Modulators	15
1.9	Opto-Mechanical Chopper	16
1.10	Literature Survey	17
1.11	Aim of this Work	19

<i>Chapter Two: Theoretical Background</i>		
2.1	Modulation	20
2.1.1	Amplitude Modulation (AM)	20
2.1.2	FM Modulation	25
2.1.3	Optical Modulator	26
2.1.4	AM and FM Optical Modulator	28
2.2	Image Resolution	30
2.2.1	Optical Transfer Function	35
2.2.2	Modulation Transfer Function	37
2.3	Fractal Geometry	39
2.3.1	Fractal Word	39
2.3.2	Fractal Dimension	43
2.3.3	Iterated Function Systems (IFS)	44
2.3.4	Random IFS Algorithm	46
<i>Chapter Three: Modulator Design</i>		
3.1	General Modulator Design	50
3.1.1	The Optical Modulator Movements	54
3.2	AM Modulator Design	57
3.3	FM Modulator Design	58
3.4	Fractal Modulator Design	59
<i>Chapter Four: Results &amp; Discussions</i>		
4.1	Introduction	62
4.2	Evaluation of MTF	69
4.2.1	MTF of Central Circle (C0) (Fractal Modulator)	70
4.2.2	MTF of Circle One (C1) (Acquisition Modulator)	74
4.2.3	MTF of Circle Two (C2) (Detection Modulator)	78
4.3	Discussion	82
<i>Chapter Five: Conclusions and Suggestion For Future Work</i>		
5.1	Conclusions	84



5.2	Suggestions for Future Work	84
<i>References</i>		85
<i>Appendixes</i>		
Appendix (A)		89
Appendix (B)		90

**1.1 Introduction**

The production of the optical system has passed through several stages, the optical design is the first one, after this stage is completed, the optical components manufacturing will be the next stage and then, the evaluation and the testing of these components will be the last stage before the lens is being used.

The optical design includes specification for the radii of the surfaces curvature, the thickness, the air spaces, the diameters of the various components, the type of glass to be used and the position of the stop. These parameters are known as "*degrees of freedom*" since the designer can change them to maintain the desired system.

The image that is formed by these optical systems will be approximately corrected from the aberrations. But there isn't ideal image which corresponds to the object dimensions because of the wave nature of the light, which is mostly affected by several factors like the type of illumination that is used (*incoherent, coherent and partially coherent*), the object shape (*Point, Line or Edge*) and the aperture shape [1].

There are several factors that affect the evaluation of the image quality which is formed by the optical system. Of these important factors that have effect on evaluation of the image quality is measured spread function (*Point, Line and Edge*) [1,2,3] which describes the intensity distribution in image plane for an object (*Point, Line and Edge*). The spread function depends on diffraction that is produced by the lens aperture and the amount of the aberrations and its type in lens or in the optical system. The point spread function is an important parameter that is used for identification of the efficiency of the optical system, where several of the other functions are derived from the point spread function or in differential relation or integral relation with it.

## 1.2 Lens Testing

There are generally three basic reasons for carrying out series of tests on lenses:

1. To determine if the lens is suitable for a given purpose.
2. To determine whether a lens which has been constructed fulfills the design characteristics.
3. To study the limitation on accuracy of optical imagery and the relation among various methods of assessing image quality [4].

There are two ways to test the lenses and optical systems.

### 1.2.1 Qualitative Test

By the qualitative test we have the ability to know the type of aberrations in the tested lens, without measuring it, and the *star test* is classified under the qualitative test. In the *star test* a collimator is used to produce plane waves which fall directly on the tested lens. The image formed by the tested lens is examined through a microscope as shown in Fig. (1-1). The lens rotates about its axis through the test to examine the decentering aberrations and asymmetric aberrations in the point image. If the tested lens is perfect the observer sees bright circle surrounded by several rings rapidly diminishing in brightness which is called Airy pattern [5]. This process of examination helps in the deduction of some aberrations which reach  $(1/10)$  of the wavelength that is used.

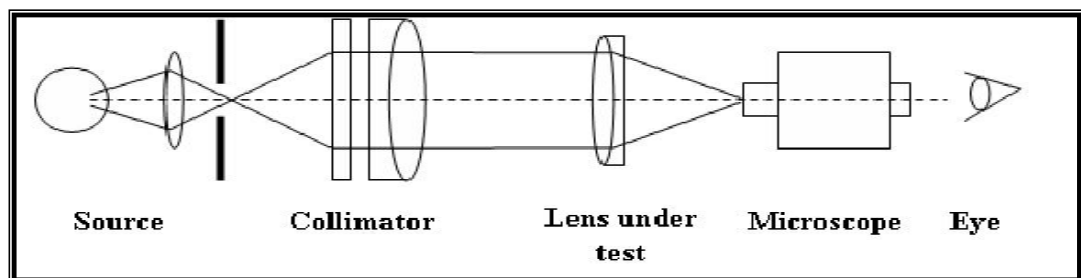


Fig. (1-1), star test

In this process the human eye is used which is practically a good detector for asymmetric and for the change in the form, but it can not show the exact difference in value of the intensity and the distance between the fringes.

### ***1.2.2 Quantitative Test***

The quantitative test is divided in two types:

#### ***1- Visible Test***

It is the test that contains all the required measurements that are designed on the basis principle of interference between the wave front coming from the lens through using ideal wave of mono wavelength from point source (the ideal wave is considered as a reference to the wave coming from the testing lens).

The instruments used for this purpose is Twyman-Green interferometer [6] which is widely used in examination of the lenses and prisms, and the interferometer is a good instrument to find out the amount of moving away from the ideal state, starting from  $(1/20) \lambda$  part from the wavelength until little wavelength ( $3\lambda$ ). When the wavelength moves away for hundred wavelengths the interferometer will be useless. The Twyman-Green interferometer is essentially a variation of the Michelson interferometer. It is an instrument of great importance in the domain of modern optical testing as shown in Fig. (1-2).

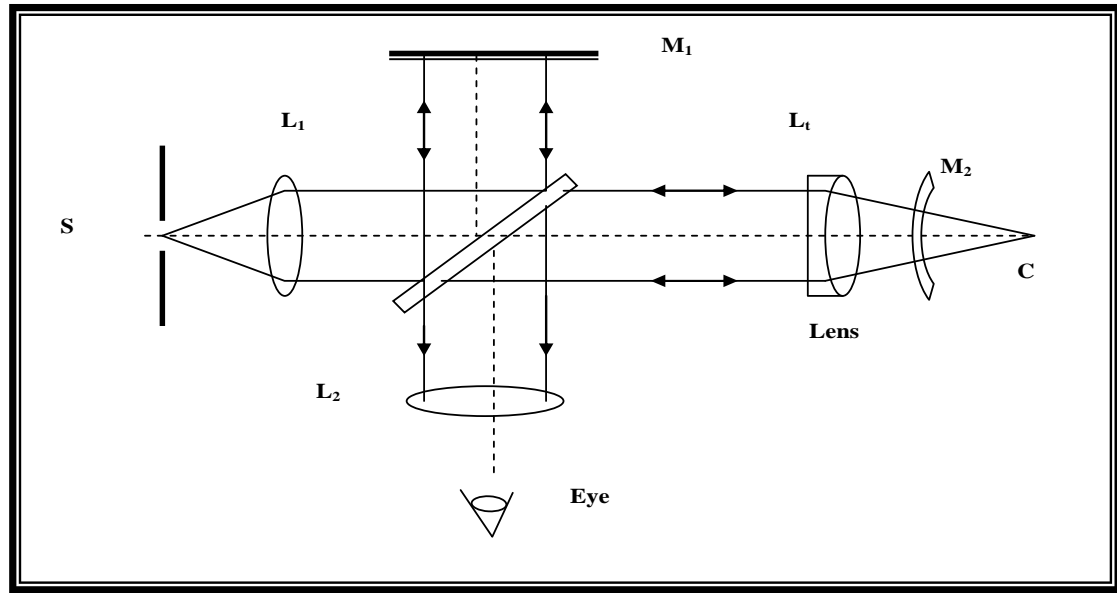


Fig. (1-2): Twyman-Green interferometer [6]

This device is setup to examine lenses. The spherical mirror **M1** has its center of curvature tested found free of aberrations (which is usually plane mirror), the emerging reflected light returning to the beam splitter will again be plane wave. In case, astigmatism, coma, or spherical aberrations deformation, the waveform, fringe pattern will manifest these distortions which can be seen and photographed. When **M2** is replaced by plane mirror, a number of other elements (*primes, optical flats*) can be equally tested as well [7].

## 2- The Photometer Test

This way of examination includes the measurement of special function that explains the lens efficiency, its ideality, and the amount of aberrations that is present in it.

Some of these functions e.g. point spread functions (**PSF**), line spread function (**LSF**), disk spread function (**DSF**) and other spread functions give good description of the intensity distribution in the image plane of an object by the optical system to be examined. The spread function depends on the aperture lens diffraction and the aberrations type and the amount of aberrations in the lens or in the optical components.

There is another important function which is used to examine the optical system like the optical transfer function (**OTF**). We can define the **OTF** as the ability of the optical system to transfer the different frequencies from the object plane to the image plane [8]. One of the other important functions used to evaluate the image specificity is the contrast transfer function (**CTF**) and (MTF). and we will explain this functions carefully in chapter two.

### **1.3 Diffraction**

Diffraction is a phenomenon or effect resulting from the interaction of the radiation wave with the limiting edges of the aperture stop of optical system [5, 9]. Diffraction is a natural property of light arising from its wave nature, and possesses fundamental limitation on any optical system. Diffraction is always present, although its effects may be made clear if the system has significant aberrations. When an optical system is essentially free from aberrations, its performance is limited solely by diffraction, and it is referred to as diffraction-limited. The image of a point source formed by diffraction-limited optics is blurred, which appears as a bright central disk surrounded by several alternately bright dark rings [5,10,11]. this diffraction blur or Airy disk, is named in honor of Lord George Biddel Airy, one of those who analyzed the diffraction process. The energy distribution and the appearance of Airy disk are shown in Fig. (1-3).

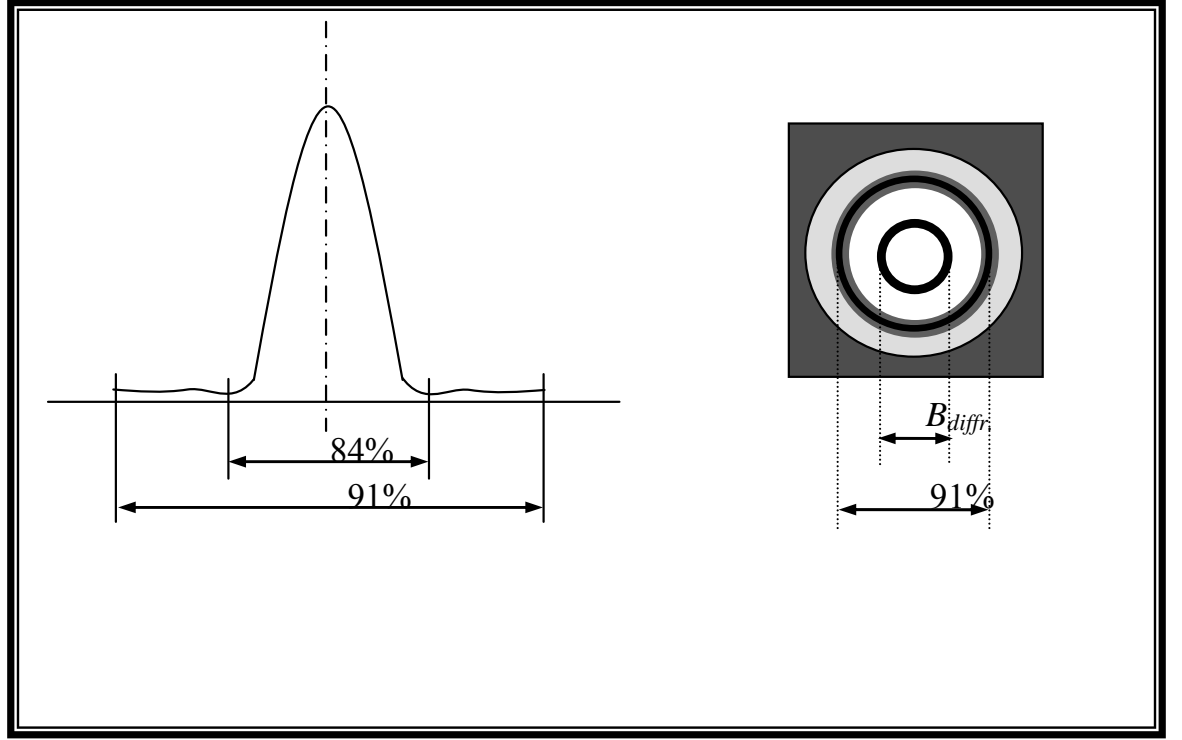


Fig. (1-3): Airy disk, energy distribution and appearance [5].

If the aperture of the lens is circular, approximately (**84%**) of the energy from an image point energy is spread over the central disk and the rest is surrounding rings of the Airy pattern [5]. The angular diameter of Airy disk ( $B_{ang}$ ) which is assumed to be the diameter of the first dark ring is [5,10,12].

$$B_{ang} = 2.44 \lambda / D \quad (1-1)$$

The Airy disk diameter  $B_{diff}$  is then:

$$B_{diff} = B_{ang} f = 2.44 \lambda f / D = 2.44 \lambda (f / \#) \quad (1-2)$$

where  $\lambda$  is light wavelength that is used. The angular diameter is expressed in radians if  $\lambda$  and  $D$  are in the same units. Since the blur size is proportional to the wavelength as indicated in Equation (1-2) the diffraction effect can often become the limiting factor for optical system.

## 1.4 Aberration

For a perfect lens and monochromatic point source the wave aberrations (**Wa**) measure the optical path difference (OPD) of each ray compared with that of the principal ray [13].

The wave aberration polynomial in polar coordinates is [14]

$$Wa = W(\sigma^2, r^2, r \cos \phi) \quad (1-3)$$

$$Wa = \sum_i \sum_m \sum_j W_{imj} \sigma^i \cdot r^m \cdot \cos \phi \quad (1-4)$$

where (i,m,j) represents the power of ( $\sigma$ ,  $r$ ,  $\cos \phi$ ) respectively [14]

$r$ : represents the radius distance  $B'$ ,  $E'$  in exit plane

$\phi$ : the angle between the two variable  $x$ ,  $r$ .

$\sigma$ : represents the amount of principal ray high on the optical axis in the image plane.

### 1.4.1 Monochromatic Aberration

The most important aberrations in the majority of applications are **Seidel** aberrations [15]. The aberrations of any ray are expressed in terms of five sums  $S_1$  to  $S_5$  called **Seidel** sums [16]. **Seidel** was the first one who studied this type of aberration. If a lens is to be free of all defects all five of these sums would be equal to zero. No optical system can be made to satisfy all these conditions at once. Therefore it is customary to treat each sum separately, and certain ones vanish, thus, if for a given axial object point the **Seidel** sum  $S_1=0$ , there is no spherical aberration at the corresponding image point. If both  $S_1=0$  and  $S_2=0$ , the system will also be free of coma. If, in addition to  $S_1=0$  and  $S_2=0$  there are the sums  $S_3=0$  and  $S_4=0$  as well the images will be free of astigmatism and field curvature. If finally  $S_5$  could be made to vanish, there would be no distortion of the image. These aberrations are also known as the five monochromatic aberrations because they exist for any specified color and refractive index.



Additional image defects occur when the light contains various colours. We shall first discuss each of the monochromatic aberrations and then take up the chromatic effects.

### ***1.4.2 Spherical Aberration***

In paraxial region (and with monochromatic light) all rays originating from an axial point again pass through a single point after traversing the system. This is not generally true for larger angle of divergence; different zones of the aperture have different focal lengths, depending on their distance from the axis. This difference is called spherical aberration when the separation of these foci is taken as a measurement of the aberration, it is referred to as longitudinal, and where the accompanying aberration spread in the image point is referred to as transverse aberration [4]. The primary spherical aberration is seen in Fig. (1-4).

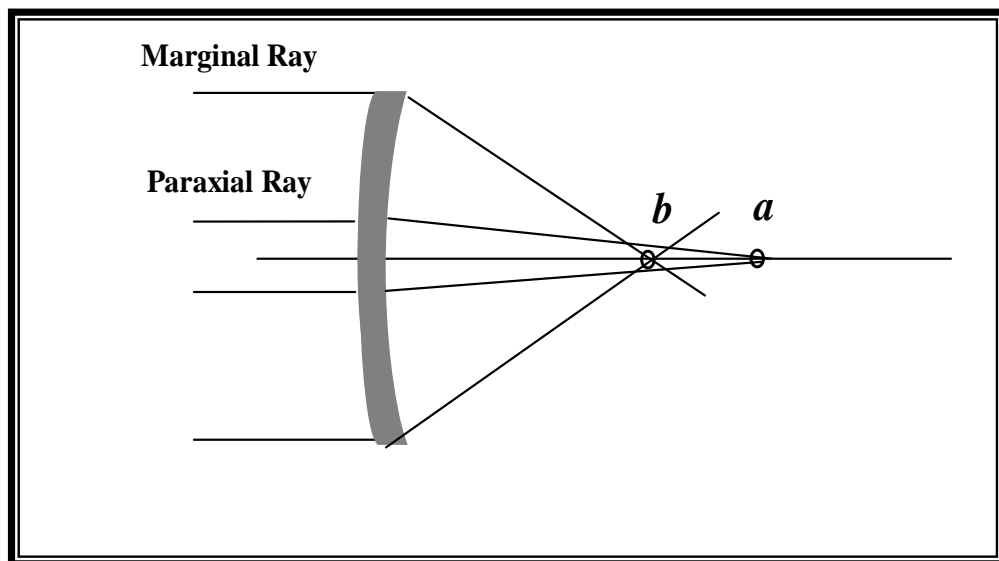


*Fig. (1-4): Spherical aberration [5]*

### 1.4.3 Coma

Coma is the first of the lens aberration that appears as the conjugate points moved away from the optical axis [17]. Parallel input beam approaching the lens at an oblique angle is shown in Fig. (1-5)

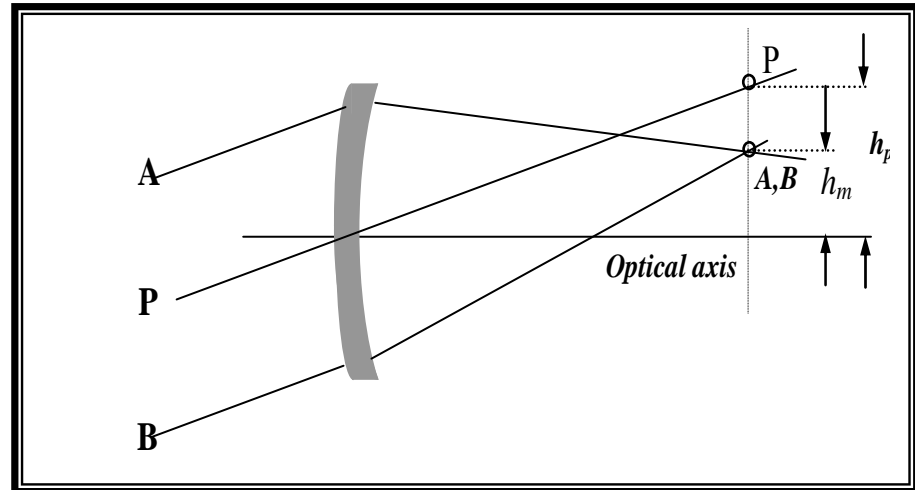


Fig. (1-5): Coma aberration [5]

The ray at the upper edge of the lens has higher angle of incidence with the curved surface than the ray at the lower edge. The deflection of the upper ray will be greater, and it will intersect the chief ray closer to the lens than the ray from the lower edge [13].

### 1.4.4 Astigmatism

The word (Astigmatism) is derived from the Greek a-means not, and stigma means spot or point [12]. When a narrow beam of light is obliquely incident on reflecting surface, astigmatism is introduced and the image of the point source is formed by small lens aperture becomes a pair of focal lines. [14]:

Astigmatism is off-axis and asymmetric aberration and it is controlled by lens curvature, by choosing the refractive indexes of the lens components, and by the location of the iris and the refractive surfaces are selected, Astigmatism is shown in Fig. (1-6).

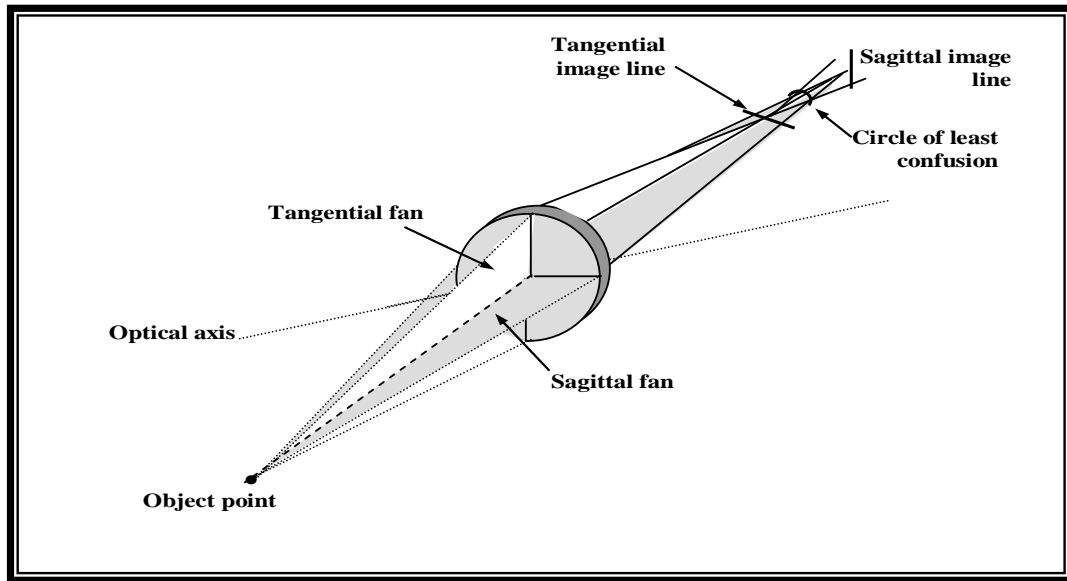


Fig. (1-6): Astigmatism aberration [5].

#### 1.4.5 Field Curvature

When a plane surface, normal to the optical axis is imaged by a lens, in which all the above aberrations have been eliminated, the image will not be plane but will lie on curved surface, This image defect is known as curvature of the field, Fig.(1-7)[13].

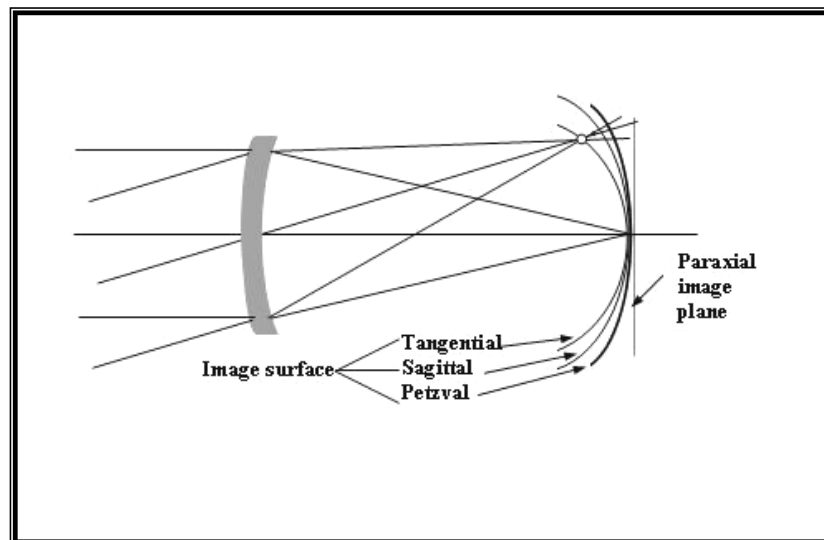


Fig. (1-7): Field curvature aberration [5].

### 1.4.6 Chromatic Aberrations

The presence of material dispersion causes the refractive index to vary with wavelength [18]. The aberrations previously described are purely functional of the shape of the lens surface, and can be observed with monochromatic light. There are however other aberrations that arise when this optics is used to transform light containing multiple wavelengths. Chromatic aberrations are caused by variation in the index of refraction of the lens material with wavelength. The first two chromatic errors are variation of the paraxial image plane position and image height with wavelength. These are known respectively as longitudinal axial and lateral chromatic. Fig. (1-8) illustrates these two types of aberrations.

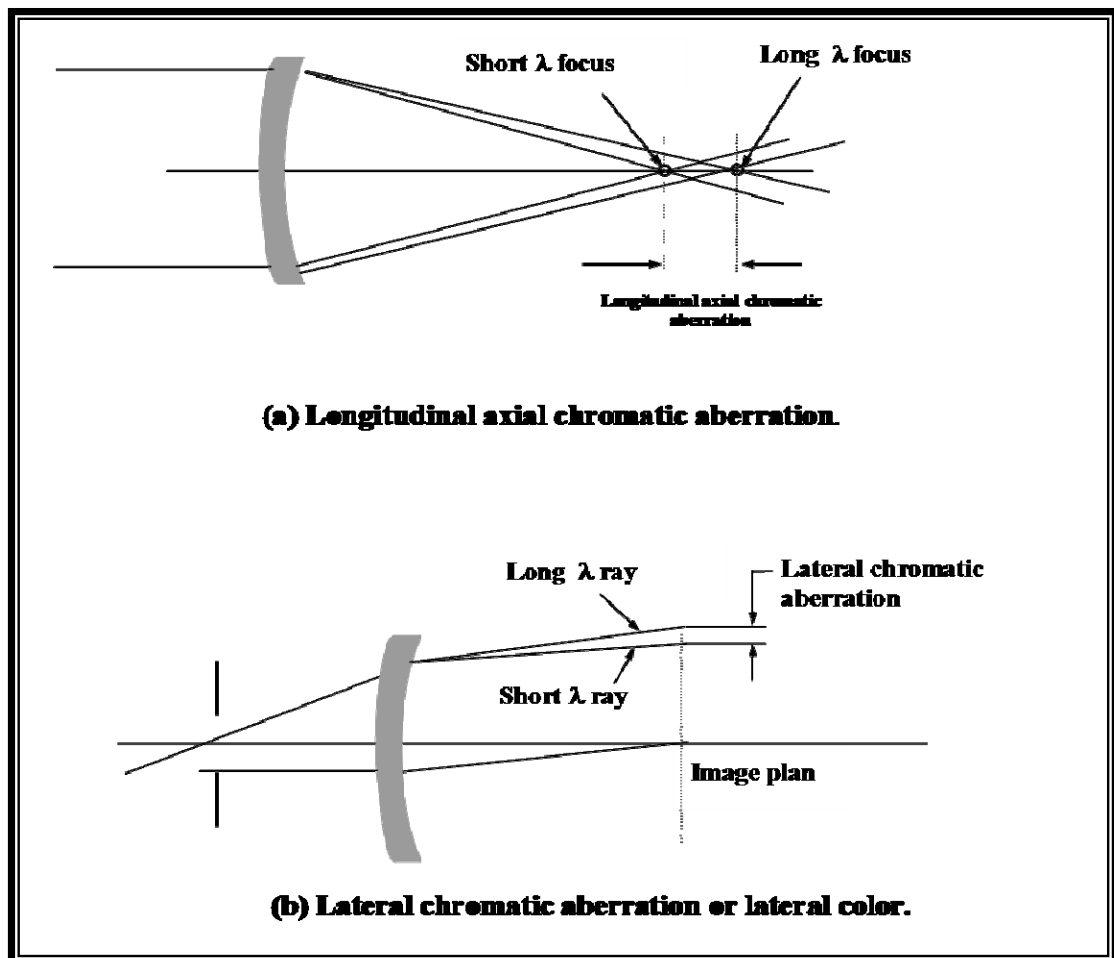


Fig. (1-8): Chromatic aberration [5].

### 1.5 Resolution of Optical System

Consider an optical system which images two equally bright point source of light, each point, is imaged as an Airy disk with the encircling rings, and if the points are close, the diffraction patterns will overlap. When the separation is such that it is just possible to determine that there are two points and not one, the points are said to be resolved [19]. The most widely used value for the limiting resolution of an optical system is **Rayleigh's** criterion. **Rayleigh** suggested that the image formed by an aberration free system of two self luminous points of the same brightness may be regarded as resolved if the central maximum of one image falls on the first minimum of the other.

This minimum resolvable separation known as "limit of resolution" is given by [20]

$$Z = \frac{0.61\lambda}{n' \sin u'} = 1.22\lambda(f/\#) \quad (1-5)$$

This represents Airy disk [19]. If rectangular slit aperture has been used **Rayleigh's** criterion for resolving power will be in the new form:

$$Z = 1.0 \lambda (f/\#) \quad (1-6)$$

Dawes criterion is used only for circular and annular aperture and gives the separation between point image centers for circular aperture:

$$Z = 1.02 \lambda (f/\#) \quad (1-7)$$

Both of Rayleigh's and Dawes criteria apply only to incoherent source. But Sparrow gives special criterion for resolving power. He states that the second intensity derivation between half distance of point image center equals zero [21]. This criterion applies to coherent and incoherent source, according to the separation distance for circular aperture [20]:

$$Z = 0.947 \lambda (f/\#). \quad \text{Incoherent} \quad (1-8)$$

$$Z = 1.464 \lambda (f/\#) \quad \text{Coherent} \quad (1-9)$$

For slit aperture:-

$$Z=0.829\lambda (f/\#) \quad \text{Incoherent} \quad (1-10)$$

$$Z=1.325\lambda (f/\#) \quad \text{Coherent} \quad (1-11)$$

Therefore the resolution power of slit aperture performs more than the circular aperture for the two types of light source (coherent and incoherent), Fig. (1-9) represents the criterion discussed.

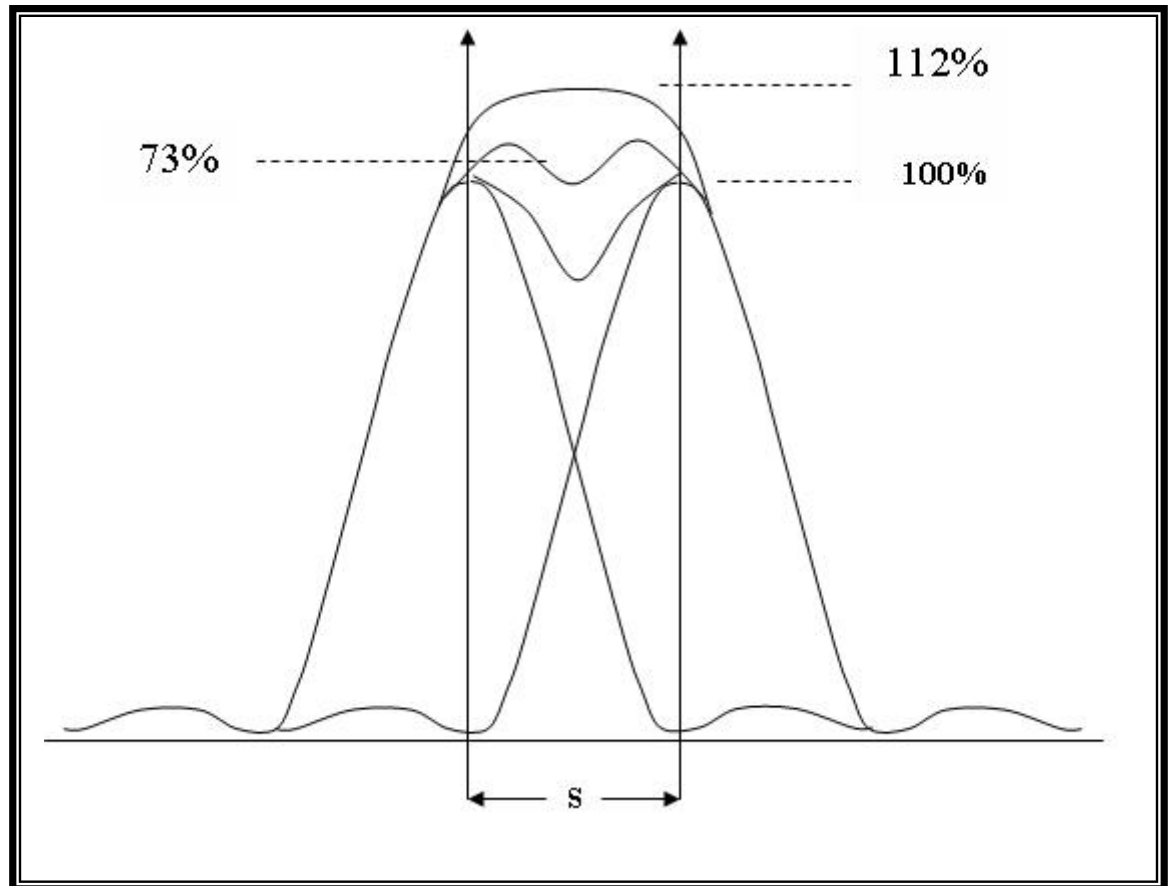


Fig. (1-9): Raleigh's and Dawes criterions[20].

## 1.6 Depth of Focus

The concept "depth of focus" rests on the assumption that for an optical system, there exists blur (due to defocusing) of small enough size such that it will not adversely affect that performance of the system. The depth of focus is the amount by which the image may be shifted longitudinally with respect to some reference plane and introduces no more than the acceptable blur. This is the amount of shifted image which is

corresponds to being out of focus by one quarter wavelength. The depth of focus ( $\delta$ ) which corresponds to an optical path difference of  $\pm \frac{1}{4}\lambda$  is [22]

$$\delta = \pm 2\lambda (f/\#)^2 \quad (1-12)$$

### 1.7 Electro-Optic Modulators

The electro-optic device which is used as a light-beam modulator is shown schematically in Fig.(1-10). Polarized light is incident on the modulator.[23,24] The light may be polarized originally or a polarizer may be inserted. The analyzer, oriented at  $90^\circ$ , to the polarizer, prevents any light from being transmitted when no voltage is applied to the electro-optic material. When the correct voltage is applied to the device, the direction of the polarization is rotated by  $90^\circ$ . Then the light will pass through the analyzer.[23]

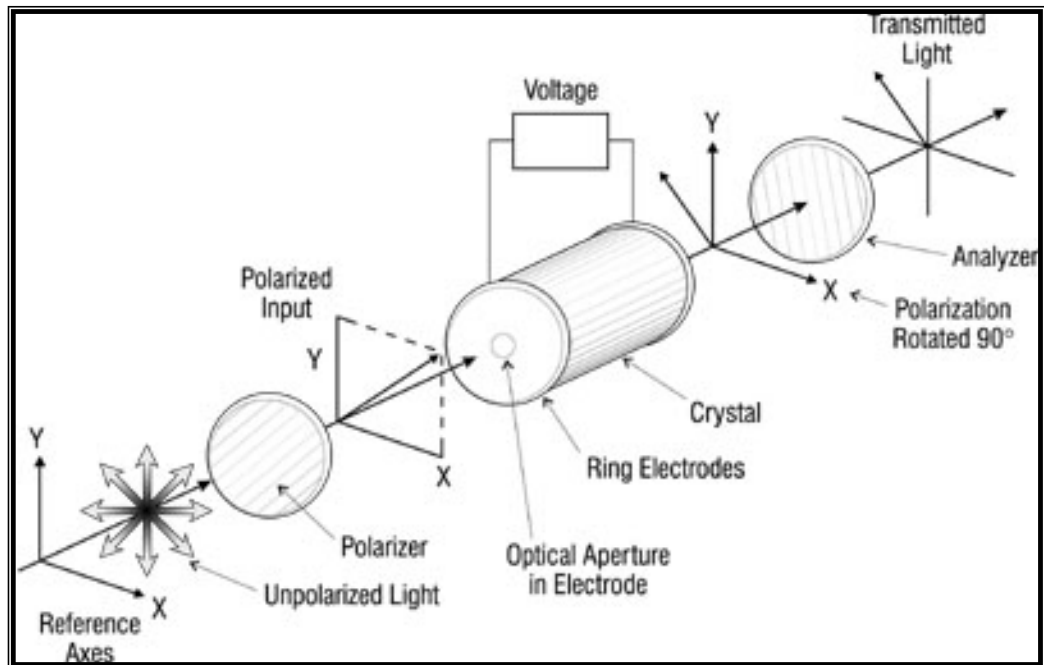


Fig.(1-10) Schematic diagram of the operation of a modulator based on the electro-optic effect.[23]

Electro-optic modulators may be fabricated in different physical forms. In one form, voltage is applied parallel to the light propagation, as shown in Fig.(1-10). One uses transparent electrodes or electrodes with central apertures. This is called a longitudinal electro-optic modulator[24].

The speed of electro-optic modulators is expressed as a bandwidth, i.e., the rate at which the device can be turned on and off. The bandwidth of electro-optic modulators can be very large, up to hundreds of megahertz. The speed is limited mainly by the ability to produce voltage pulses of sufficient amplitude at high frequency[25].

### ***1.8 Acousto-Optic Modulators***

A different approach to modulator technology uses the interaction between light and sound waves to produce changes in optical intensity, phase, frequency, and direction of propagation. Acousto-optic modulators are based on the diffraction of light by a column of sound in a suitable interaction medium[23,24,25].

When a sound wave travels through a transparent material, it causes periodic variations in the index of refraction. The sound wave can be considered as a series of compressions and rarefactions moving through the material. In regions where the sound pressure is high, the material is compressed slightly. This compression leads to an increase in the index of refraction. The increase is small, but it can produce large cumulative effects on a light wave passing some distance through the compressed material[23,26].

The elasto-optic properties of the medium respond to the acoustic wave so as to produce a periodic variation in the index of refraction. A light beam incident on this disturbance is partially deflected in much the same way that light is deflected by a diffraction grating. The operation is shown



in Fig. (1-11). The alternate compressions and rarefactions associated with the sound wave form a grating that diffracts the incident light beam. No light is deflected unless the acoustic wave is present[23,24].

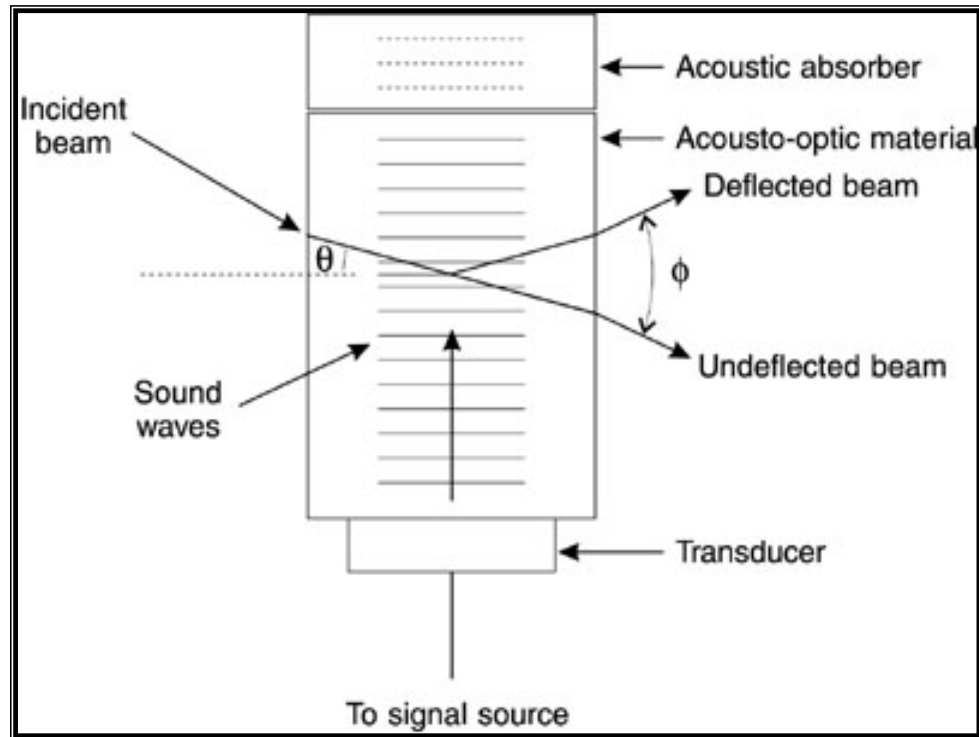


Fig. (1-11) Diagram showing the principles of operation of an acousto-optic light-beam modulator[24]

### 1-9 Opto-Mechanical Chopper

Optical choppers are mechanical or electronic devices that pass and then interrupt a beam of light for a known brief interval. Technologies used for optical choppers include liquid crystals, rotating shutters, tuning forks, etc. Rotating disk optical choppers are used in situations where frequency, aperture size, or mark/space ratios (duty cycle) are variable[27]. The variable frequency rotating disks resemble small fans. They have a slotted disk mounted on a motor head, and can be used at a variety of frequencies by adjusting the motor speed. An optical switch senses disk position and provides a reference output to automatically adjust the chopping frequency. The entire device is often connected to an external signal so

that the optical chopper maintains the same speed and frequency as the system in which it is placed[28].

Tuning fork choppers, also called resonant choppers, are appropriate for optical chopping when a single known fixed frequency is desired and small size is required, or long life needed. Tuning fork optical choppers resemble musical tuning forks with small vanes mounted on the tines. They vibrate in response to an AC signal at a specific resonant frequency. Their vibration occurs at a frequency fixed by the mechanics of the structure. Fork optical choppers are extremely durable and have no wearing parts. As a result they are often used in high acceleration and vibration applications, in which they provide a long service life. Tuning fork optical choppers are versatile and are usable at extreme temperature or in a vacuum[27]

### ***1.10 Literature Survey***

The first recorded instance of optical modulator use was in **1928** by **A.H. Pfund**. He used mechanical pendulum to chopping the incident radiation, that is incident in the thermal detector (**Thermopile**) in a period of 1.5 sec. And he did that in radiation measurement [10]. The first employment of optical modulator in military applications used in the second world war by the **German scientist**[29], They discovered that the proposed optical modulator could be used in **Tracking** and **Guidance** operation[30]. After the end of the war, some of the Tracking and Guidance system has been produced in the German war machine [31].

In **1946**, **Zahl** has published the first patent in how to find the object position, by its thermal radiation emitted. The patent has been eliminated for ten years, because it was very important in military application.

In **1946**, **Clark** published research into (**Sun-Seeker**) system[10]. Then the (**Star-Tracker**) systems has been designed to be used in astronomical applications. Then the (**IR-seeker**) systems of thermal guidance head have

been used in thermal missile[29]. In the 1960s, **Benoit Mandelbrot** started investigating self-similarity, which was built on earlier work by **Lewis Fry Richardson**. Finally, in 1975 Mandelbrot coined the word "**fractal**" [32]. In 1984 Liedtke [33], proposed a systematic approach for modulation identification; the classifier used signal features such as amplitude, frequency, and phase histograms. In 1999 P. Lallo [34], developed an algorithm based on the Discrete Fourier Transform (DFT) where the carrier frequency was estimated, then the modulation rate is estimated, the correlation of the received unknown signal with all signals in a signal database was done. A distance measure is used to identify the received unknown signal. In 2003 Y. Fukui [35], clarified that there is a significant loss in contrast in acquired image of high frequency grating, i.e., our eye appears to resolve each line. To assure that each line is resolved, the output intensity was measured and illustrated as sinusoidal curve. The intensity measurement shows that 95% contrast was achieved for low frequency grating, thus both spatial and intensity resolution can be transferred nearly perfect from specimen to the image using this optical system. In contrast, only 40% contrast was achieved for high frequency grating. This decrease in contrast was due to overlap of the sinusoidal intensity curves. In 2007 M. L. Gebbar [36] Designed an optical fractal modulator (Reticle) which is made of semiconductors material by using fractal function, and Evaluated the effect of the refractive index and transmittance for the circular aperture on the output signal. The efficiency of the output signal was tested by applying the modulation transfer function (MTF).

***1.11 Aim of This Work***

This research, aims to study and design optical modulator disk by using classical method and fractal function method at the same time. The efficiency of the proposed optical modulator disk is tested by applying the modulator transfer function (MTF). The disk is divided into three circles, The central circle ( $C_0$ ) is designed by the fractal function and other two circle ( $C_1, C_2$ ) are designed by using (AUTO-CAD) software.

**2.1 Introduction**

The operation of determining the object position with respect to a reference coordinate of Electro-optical systems was usually measured by using modulation rule. We have explained some of its parameters and principle of modulation theory[37,25,39].

The Continuous-Harmonic-Modulation is of two types:-

- 1- Amplitude Modulation(AM)
- 2- Angular Modulation(Frequency-Modulation (FM) and Phase-Modulation (PM).

This classification is dependent on the parameters of the optical wave that will be modulated.

**2.1.1 Amplitude Modulation (AM)**

The parameter that will be changed in this type of modulation is(Optical Flux Amplitude). That will be emitted from the target .If the carrier beam flux is represented by the harmonic relation[37] :-

$$\Phi_c(t) = \Phi_0 \sin \omega_c t \quad (2-1)$$

where:-

$\Phi_0$  = the maximum amplitude of carrier pulse.

$\omega_c$  = the angular frequency of carrier wave .

And the Modulation Signal flux:-

$$\mu_m(t) = \mu_{m0} \sin \omega_m t \quad (2-2)$$

where

$\mu_{m0}$  = the modulation signal .

$\mu_m(t)$  = the modulation signal flux function.

$\omega_m$  = the angular frequency of modulation wave.

The maximum amplitude of carrier pulse is given by:-

$$\Phi_0 = m_{AM} \mu_{mo} \quad (2-3)$$

$m_{AM}$  = the amplitude modulation Index .

The resultant of amplitude modulated pulse is given by:-

$$A = \Phi_0 (1 + m_{AM} \sin \omega_m t) \quad (2-4)$$

So that the flux of carrier pulse radiance that is modulated in amplitude modulation is given by:-

$$\begin{aligned} \Phi_m(t) &= A \sin \omega_c t \\ &= \Phi_0 (1 + m_{AM} \sin \omega_m t) \\ &= \Phi_0 \sin \omega_c t + m_{AM} \frac{\Phi_0}{2} \cos(\omega_c - \omega_m)t - m_{AM} \frac{\Phi_0}{2} \cos(\omega_c + \omega_m)t \end{aligned} \quad (2-5)$$

There are three parts in Equation (2-5)[4].

- First part represents the formula of un-modulated carrier pulse wave, and its angular frequency is  $\omega_c$ .
- Second part represents the formula of the waves modulated in Upper-Side-Band (USB). And its angular frequency is equal to the sum of carrier wave frequencies, and modulation signal  $(\omega_c + \omega_m)$ .
- Third part is the formula of the waves modulated in Lower-Side-Band (LSB). And its angular frequency is equal to the difference

between carrier waves frequencies, and modulation signal  $(\omega_c - \omega_m)$ .

Usually amplitude modulation of optical beam radiation can be produced by generated flux of continuous pulses, whose shapes are dependent on the radiance waves and modulation parameter. The frequency of these pulses represents the carrier frequency  $(\omega_c)$ .

The ratio between the time-interval  $(T_p)$  and the band width of the single pulse is given by:-

$$\Gamma = \frac{T_p}{\tau_p} \quad (2-6)$$

where:-  $\Phi(t)$

$T_p$  = the time-interval between pulses.

$\tau_p$  = the band width of the single pulse.

When  $\Gamma \leq 2$ , the modulation will be continuous modulation, as shown in Fig.(2-1).

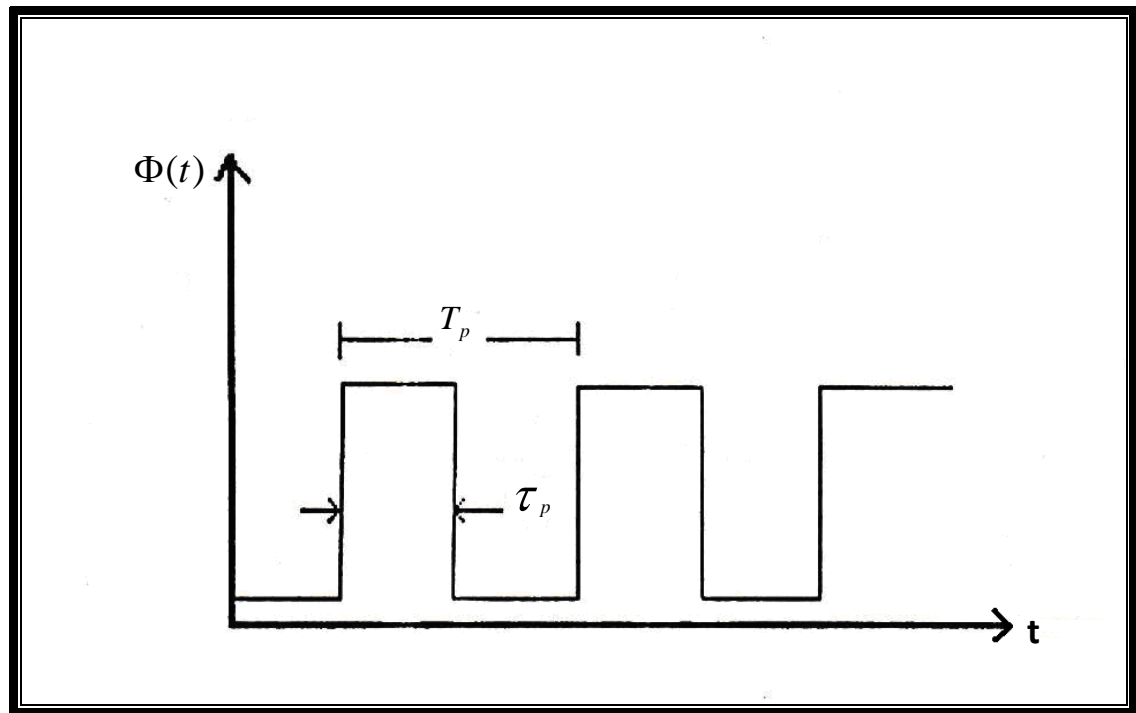


Fig. (2-1) The supposed shape of the optical signal produced from the modulation disk[39].

Generally the flux of the modulated pulses can be represented in the mathematical equation given below[31]:-

$$\Phi_m(t) = \frac{\Phi_0}{2} [1 + m_{AM} \mu_m(t)] \cos(\omega_c t) \quad (2-7)$$

The maximum power of optical modulated signals is found when ( $m_{AM} = 1$ ). The periodic function ( $\mu_m(t)$ ) limits the time change of the Electro-Mechanical Modulator (Reticle) transmittance. This function produced as a result of field scan, in both of the object and its image. That is done through moving between the object image and modulation disk. While the function ( $\Phi_c(t)$ ) is produced by chopping operation in the radiant beam.[31]

The optical modulation signal of the detector can be given by:-

$$\Phi_m(t) = \Phi_c(t) \cdot \mu_m(t) \quad (2-8)$$

The most modulated signals functions are subordinate to the Fourier-Transform. And by using Fourier-Transform the function ( $\Phi_m(t)$ ) is given by:-

$$\Phi_m(\omega) = \int_{-\infty}^{\infty} \Phi_m(t) \text{Exp.}(-i \omega_c t) dt \quad (2-9)$$

If modulation function ( $\mu_m(t)$ ) is expanded as Fourier series then:-

$$\mu_m(t) = \mu_{m0} + \sum_{n=1}^{\infty} \mu_{mn} \cos(n \omega_m t) \quad (2-10)$$

After expansion of modulation function, it is found the modulated signal produced from the optical detector of electro-optical system.

$$\Phi_m(\omega) = \int_{-\infty}^{\infty} \Phi_c(t) [\mu_{m0} + \sum \mu_{mn} \cos(n \omega_m t)] \text{Exp.}(-i \omega_c t) dt \quad (2-11)$$

And this relation is similar to Equation (2-5), which represents the double Side AM, as shown in Fig. (2-2) .



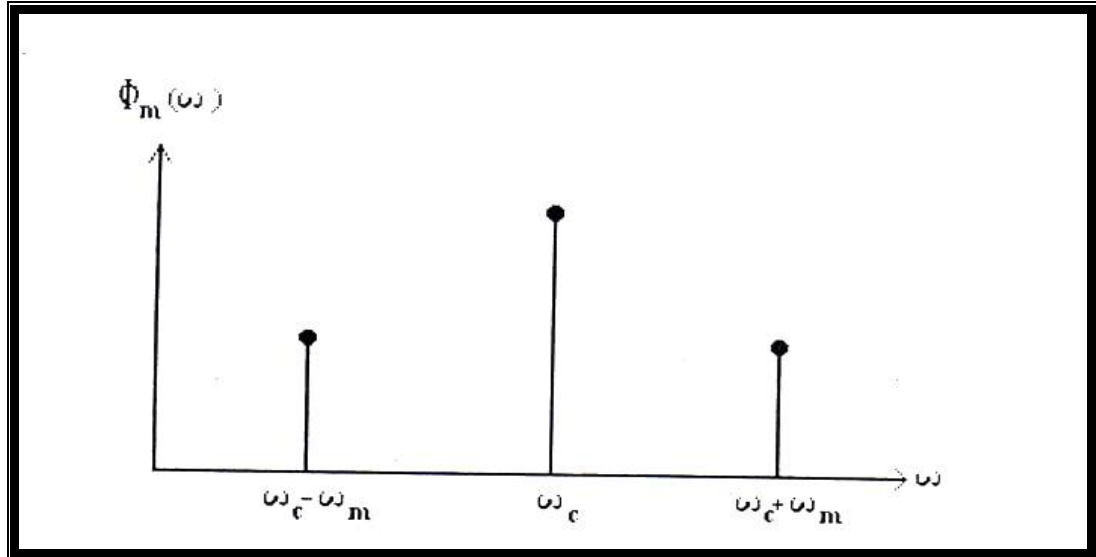


Fig. (2-2) Double Side AM [39].

The series of rectangular pulses ,whish have pulse duty factor equal to( $\gamma = \frac{1}{\Gamma}$ ) and amplitude ( $\Phi_0$ ), can be represented as Fourier series [32,25]:-

$$\Phi_m(t) = \gamma\Phi_0 + 2\Phi_0 \sum_{n=1}^{\infty} \left[ \frac{\sin(\pi n \gamma)}{\pi n} \right] \cos(n\omega_c t) \quad (2-12)$$

Where:-

$\gamma$ =the pulse duty factor

These pulses can be generated when the optical beam band width ,which through from the modulation disk, is smaller than the band width of transmittance sectors of the modulation disk.

When  $\gamma = 0.5$ , the 80% of total half power is carried by the first harmonic ( $n=1$ ). While the half spokes of modulation disk are transmittance and other are oblique .That means, the half power of the incident radiation beam is lost before its transformation from continuous state to the pulse state, that is at the best state.

And with increasing ( $\Gamma$ ) or decreasing ( $\gamma = \frac{1}{\Gamma}$ ),the band width spectrum will be increasing. And the power carried by the first harmonic

will be decreasing. At the end the modulation becomes pulse type modulation.

### 2.1.2 FM Modulation

The modulation signal frequency can be represented by using average change of carrier wave frequency . If the carrier wave function is given by[25,37,39]:-

$$\Phi_c = \Phi_0 \sin(\omega_c t + \varphi) \quad (2-13)$$

where:-

$\varphi$  = the phase wave.

and the modulation signal function shape is given by:-

$$\begin{aligned} \mu_m(t) &= \mu_{m0} \cos(\omega_m t) \\ \omega_c &= 2\pi f_c \\ \omega_m &= 2\pi f_m \end{aligned} \quad (2-14)$$

then the modulation wave frequency can be given by [39] :-

$$f_m = f_c [1 + k \mu_{m0} \cos(\omega_m t)] \quad (2-15)$$

where the constant (k) is proportion constant. And the second part of Equation (2-15) represents the maximum deviation in frequency ( $\Delta\delta$ ) .

$$\Delta\delta = f_c k \mu_{m0}$$

The carrier wave function after its modulation can be given by :-

$$\begin{aligned} \Phi_m(t) &= \Phi_0 \sin \vartheta \\ \vartheta &= \omega_c t + \frac{\Delta\delta}{f_m} \end{aligned} \quad (2-16)$$

The factor of second part of the equation (2-16) represents the FM-modulation index ( $m_{FM}$ ) and is given by :-

$$m_{FM} = \frac{\Delta\delta}{f_m} \quad (2-17)$$

The frequency modulation wave becomes :-

$$\Phi_m(t) = \Phi_0 \sin[\omega_c t + m_{FM} \int_0^t \sin(\omega_m t) dt] \quad (2-18)$$

The FM wave has many frequencies. While the AM wave has two frequencies (USB&LSB). That will be clear when we write the FM function in (Bessel function expansion ). The Fourier transform of the function  $\Phi_m(t)$  is given by [32] :-

$$\begin{aligned}\Phi_m(t) = & \Phi_0 [J_0(m_{FM}) \sin(\omega_c t) \\ & + J_1(m_{FM}) \{ \sin(\omega_c + \omega_m)t - \sin(\omega_c - \omega_m)t \} \\ & + J_2(m_{FM}) \{ \sin(\omega_c + 2\omega_m)t + \sin(\omega_c - 2\omega_m)t \} \\ & + \dots\dots\dots \\ & + J_n(m_{FM}) \{ \sin(\omega_c + n\omega_m)t + (-1)^n \sin(\omega_c - n\omega_m)t \}]\end{aligned}\quad (2-19)$$

### 2.1.3 Optical Modulator

Optical modulator is a device ,which changes the angle between the vision line to the target and coordinate to electrical signal [10].An optical modulator is used to provide directional information for target , and to suppress unwanted signal from background [40].

It is a device used for chopping the emitted light from the source. And this will be done by choosing the best shape and size . The optical modulator takes many various circular shapes due to its need[36]. The position of the optical modulator in front of the optical source, as shown in Fig. (2-3).

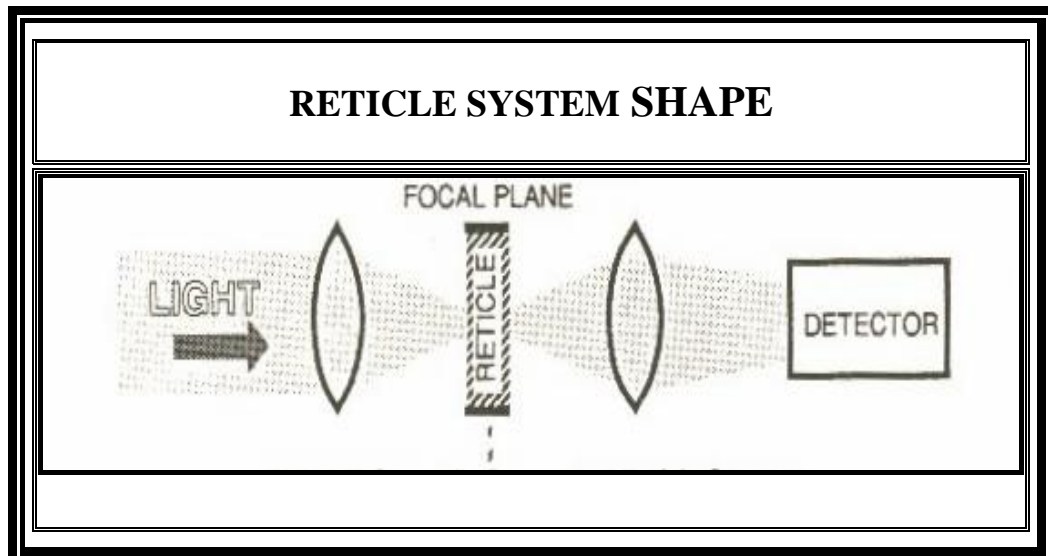


Fig. (2-3) The Position of the modulator in the optical system[41]

The optical modulator is called in many different names :-

- 1- Optical modulator .
- 2- Reticle.
- 3- Chopper.
- 4- Raster

The modulation operation in optical modulator depends on the movement between image object and optical modulator . In this concept the optical modulator can be classified in two types :-

- 1- Rotating Reticle Disk :- In this type the disk rotates about its axis ,while the object image rotates within the disk area. Sometimes the disk axis has been rotated about the optical axis of the Electro-Optical-System, in circular path. This type of disk is called (Nutating Reticle) [10].
- 2- Stationary Reticle Disk :- In this type the disk is stationary, while the image object has been rotated on the disk surface by using rotational optical system.

The optical modulator has two important operations in detection, tracking and guidance system ,and this operations is to:-

- 1- Provide directional information about tracking and to suppress unwanted signal from background .This operation is called (Spatial-Filtering).[42,43]
- 2- Change the optical signals parameter ,which is produced from the object, by designing suitable disk pattern.[10,37,44]

The modulation can be done by using two types of mode Active and Passive modes [5]. The two operations can be applied in the active mode in the same time, while just the second operation can be applied in the passive mode.

The spatial filtering property depends on assuming that, most objects have angular extent, it is reduced from the angular extent of the background objects . As an example, the airplane represents point- source of thermal

radiation, and in the sky there are a lot of reflected sun radiation and cloud, whose dimensions are more than the airplane size. Fig. (2-4) explains this concept.[17,18]

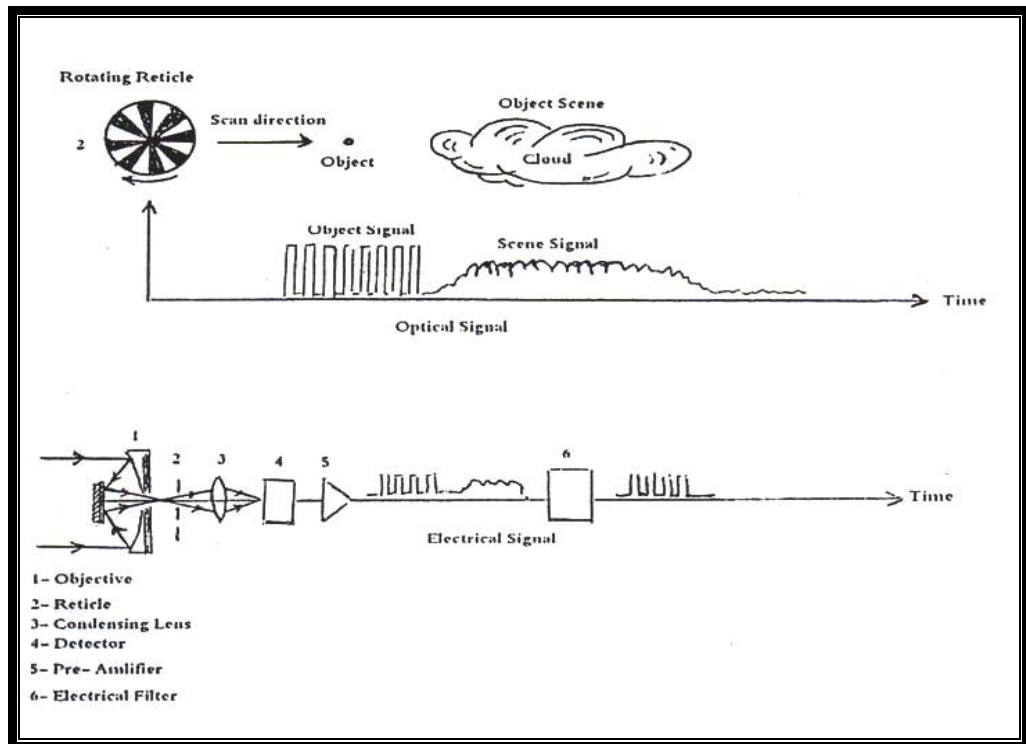


Fig.(2-4)The principles of the optical modulator action[10]

The better efficiency of the optical modulator can be produced when the spot size is not larger than three times the object image size. The real efficiency is produced when the spot size is equal to the object image. When the object image approaches the optical system, its size will be increased.

#### 2.1.4 AM and FM Optical Modulator

One of the optical modulator shapes is (**Fan Shape**), and sometimes called (Wagon Wheel), it is shown in Fig. (2-5) and it is used in many optical applications. In radiation measurement system, it is used as optical chopper. Therefore it is used in optical modulation in most Tracking and Guidance systems. This type of optical modulator works in two modes[38].

- The first , is when the optical modulator is rotated around its axis, then the incident radiation will be modulated in amplitude modulation **AM** .
- The second, is when the optical modulator is stationary ,while the object scene rotates about the disk axis by nutating movement. Or the optical modulator center will be rotated about the optical axis of the tracking system. then the incident radiation will be modulated in frequency modulation **FM** .[45]

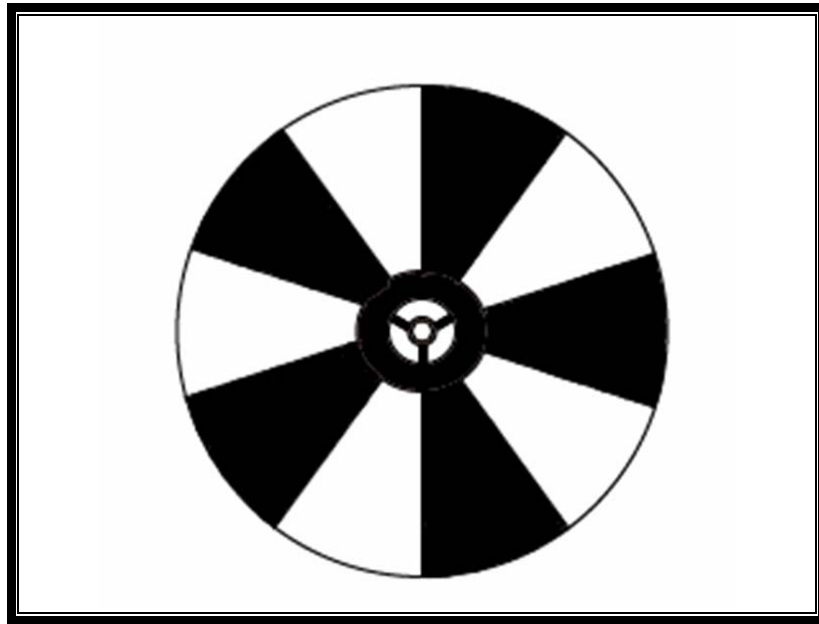


Fig. (2-5) optical modulator[45]

The optical modulator divides in (**q**) couple of transparent and opaque spokes as shown in Fig. (2-5) . The rotating frequency of optical modulator (**fr**) is given by[10] :-

$$fr = \frac{\omega r}{2\pi} \quad (2-20)$$

where :-

$\omega r$  = the angular velocity.

The Chopping frequency of the transmitted rays is given by :-

$$fc = q \cdot fr \quad (2-21)$$

where :-

$q$  = the number of pairs of clear opaque segment.

## 2.2 Image Resolution

The impulse response  $h(x,y)$  is the smallest image detail that an optical system can form. It is the blur spot in the image plane when a point source is the object of an imaging system. The finite width of the impulse response is a result of the combination of diffraction and aberration effects.  $h(x,y)$  is interpreted as an irradiance ( $\text{W}/\text{cm}^2$ ) distribution as a function of position. Modeling the imaging process as a convolution operation (denoted by  $*$ ), we express the image irradiance distribution  $g(x,y)$  as the ideal image  $f(x,y)$  convolved with the impulse response  $h(x,y)$  [46]:-

$$g(x,y)=f(x,y)*h(x,y) . \quad (2-22)$$

The ideal image  $f(x,y)$  is the irradiance distribution that would exist in the image plane (taking into account the system magnification) if the system had perfect image quality, a delta-function impulse response. The ideal image is thus a magnified version of the input-object irradiance, with all details preserved.[47] For conceptual discussions, we typically assume that the imaging system has unit magnification, so that we can directly take  $f(x,y)$  as the object irradiance distribution, albeit as a function of image-plane coordinates. It can be seen from Equation (2.22) that if  $h(x,y) = \delta(x,y)$ , the image is a perfect replica of the object. It is within this context that  $h(x,y)$  is also known as the point-spread function (PSF). A perfect optical system is capable of forming a point image of point object. However, because of the blurring effects of diffraction and aberrations, a real imaging system has an impulse response that is not a point. For any real system  $h(x,y)$  has finite spatial extent. The narrower the PSF, the less blurring occurs in the image-forming process. A more compact impulse response indicates better image quality.[48]

As Fig. (2.6) illustrates, a point object is represented as a delta function at location  $(x',y')$  in object-plane coordinates.

$$f(x_{\text{obj}},y_{\text{obj}}) = \delta(x' - x_{\text{obj}},y' - y_{\text{obj}}) \quad (2-23)$$

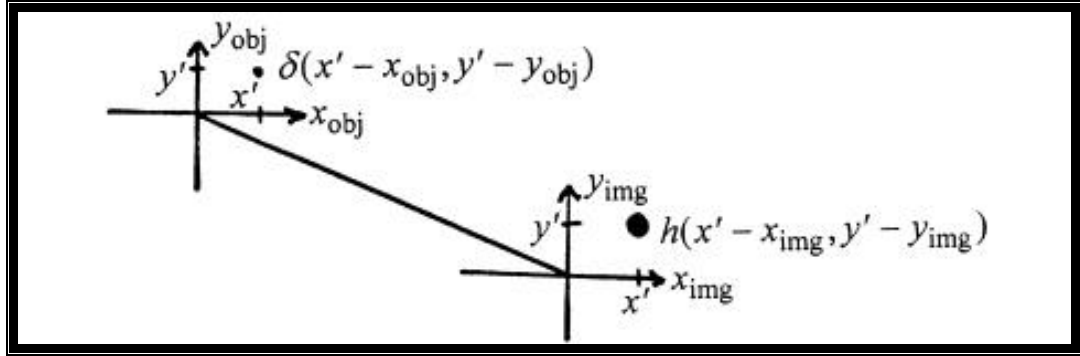


Fig.( 2-6) A delta function in the object is mapped to a blur function, the impulse response, in the image plane[46].

Assuming that the system has unit magnification, the ideal image is a delta function located at  $(x', y')$  in image-plane coordinates[46]

$$g(x_{\text{obj}}, y_{\text{obj}}) = \delta(x' - x_{\text{img}}, y' - y_{\text{img}}) \quad (2-24)$$

In a real imaging system, instead of a delta function at the ideal image point, the impulse response is centered at  $x' = x_{\text{img}}$  and  $y' = y_{\text{img}}$  in the image plane

$$g(x_{\text{img}}, y_{\text{img}}) = h(x' - x_{\text{img}}, y' - y_{\text{img}})$$

In response to the delta-function object of Equation (2.23), we represent a continuous function  $f(x_{\text{obj}}, y_{\text{obj}})$  of object coordinates, by breaking the continuous object into a set of point sources at specific locations, each with a strength proportional to the object brightness at that particular location. Any given point source has a weighting factor  $f(x', y')$ , which is found using the sifting property of the delta function:-

$$f(x', y') = \iint \delta(x' - x_{\text{obj}}, y' - y_{\text{obj}}) f(x_{\text{obj}}, y_{\text{obj}}) dx_{\text{obj}} dy_{\text{obj}}. \quad (2.25)$$

The image of each discrete point source will be the impulse response of Equation (2.22) at the conjugate image-plane location, weighted by corresponding object brightness. The image irradiance function  $g(x_{\text{img}}, y_{\text{img}})$



becomes the summation of weighted impulse responses. This summation can be written as a convolution of the ideal image function  $f(x_{\text{img}}, y_{\text{img}})$  with the impulse response.[46,47]

$$g(x_{\text{img}}, y_{\text{img}}) = \iint h(x' - x_{\text{img}}, y' - y_{\text{img}}) f(x_{\text{img}}, y_{\text{img}}) dx' dy' \quad (2.26)$$

which is equivalent to Equation (2.22). Fig.(2.7) illustrates the imaging process using two methods: the clockwise loop demonstrates the weighted superposition of the impulse responses and the counterclockwise loop demonstrates a convolution with the impulse response. Both methods are equivalent.

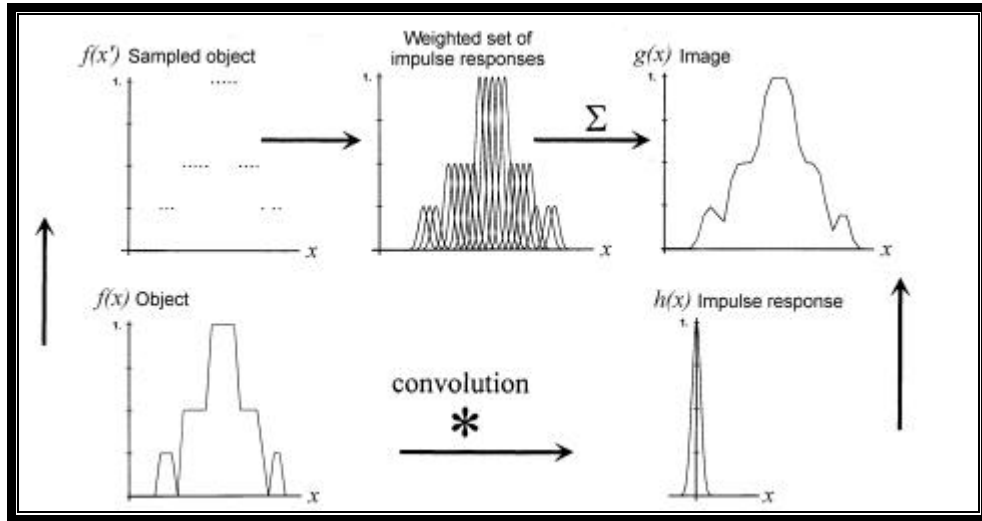


Fig. (2.7) Image formation in convolutional process[46].

Representing image formation as a convolutional process assumes linearity and shift invariance (LSI). To model imaging as a convolutional process, we must have a unique impulse response that is valid for any position or brightness of the point-source object. Linearity is necessary for us to be able to superimpose the individual impulse responses in the image plane into the final image[46]. Linearity requirements are typically accurately satisfied for the irradiance distribution itself (the so-called aerial image). However, certain detectors such as photographic film, detector

arrays (especially in the IR band ), and xerographic media are particularly nonlinear in their impulse response. In these cases, the impulse response is a function of the input irradiance level. We can only perform LSI analysis for a restricted range of input irradiances[48]. Another linearity consideration is that coherent optical systems (optical processors) are linear in electric field (V/cm), while incoherent systems (imaging systems) are linear in irradiance (W/cm<sup>2</sup>). We will deal exclusively with incoherent imaging systems. Note that partially coherent systems are not linear in either electric field or irradiance and their analysis, as a convolutional system, is more complicated, requiring definition of the mutual coherence function.[46,47]

Shift invariance is the other requirement for a convolutional analysis. According to the laws of shift invariance, a single impulse response can be defined that is not a function of image-plane position. Shift invariance assumes that the functional form of  $h(x,y)$  does not change over the image plane. This shift invariance allows us to write the impulse response as  $h(x' - x_{\text{img}}, y' - y_{\text{img}})$ , a function of distance from the ideal image point, rather than as a function of image-plane position in general. Aberrations violate the assumption of shift invariance because typically the impulse response is a function of field angle.[2] To preserve a convolutional analysis in this case, the image plane is segmented into isoplanatic regions over which the functional form of the impulse response does not change appreciably.[3,5]

It can be considered that the imaging process from a frequency-domain (modulation transfer- function) viewpoint, as an alternative to the spatial-domain (impulse response) viewpoint. An object- or image-plane irradiance distribution is composed of “spatial frequencies” in the same way that a time-domain electrical signal is composed of various frequencies: by means of a Fourier analysis. As seen in Fig. (2.8), a given

profile across an irradiance distribution (object or image) is composed of constituent spatial frequencies. By taking a one-dimensional profile across a two-dimensional irradiance distribution, you obtain an irradiance-position waveform, which can be Fourier decomposed in exactly the same manner as if the waveform was in the more familiar form of volts time. A Fourier decomposition answers the question of what frequencies are contained in the waveform in terms of spatial frequencies with units of cycles (cy) per unit distance, analogous to temporal frequencies in cy/s for a time-domain waveform. Typically for optical systems, the spatial frequency is in cy/mm[46].

An example of one basis function for the one-dimensional waveform of Fig.(2.8) is shown in Fig.(2.9). The spatial period  $X$  (crest-to-crest repetition distance) of the waveform can be inverted to find the  $x$ -domain spatial frequency denoted by  $\xi \equiv 1/X$ .

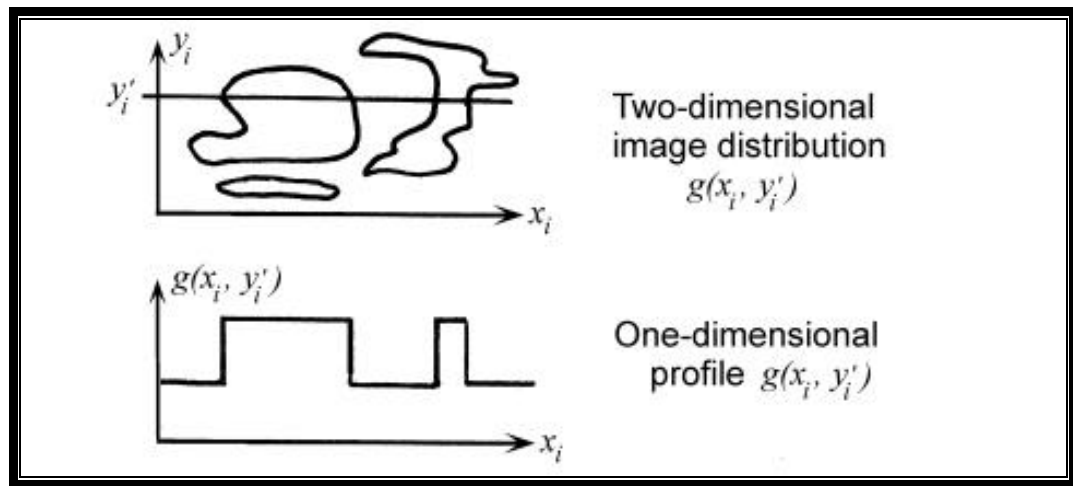


Fig. (2.8) Definition of a spatial-domain irradiance waveform[46].

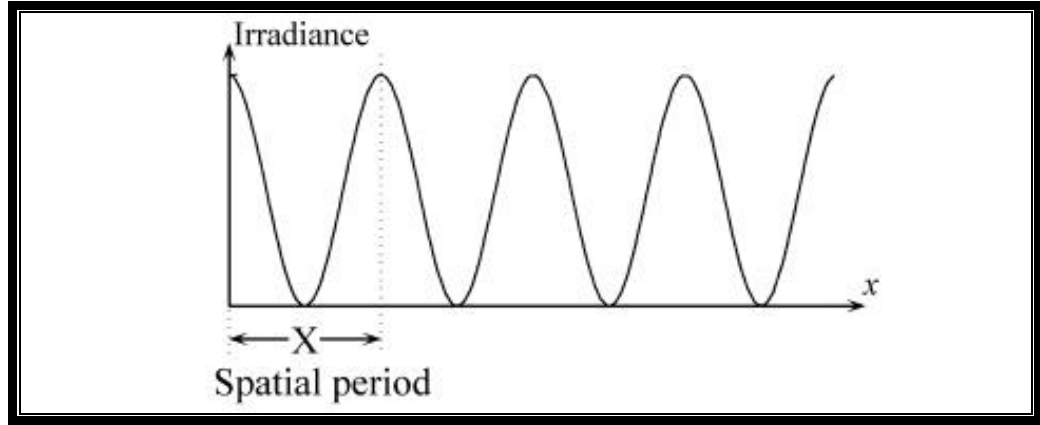


Fig. (2.9) One -dimensional spatial frequency[46].

### 2.2.1 Optical Transfer Function

The optical transfer function is an important function defined as the ability of an optical system to transfer different frequencies of object to image, and sometimes defined as (Frequency Response Function).[8] The OTF is a complex function that measures the loss in contrast in the image of a sinusoidal target, as well as any phase shifts. The MTF is the amplitude (i.e.  $MTF = |OTF|$ ) and the Phase Transfer Function (PTF) is the phase portion of the OTF.[5,8]

Equation (2.22) describes the loss of detail inherent in the imaging process as the convolution of the ideal image function with the impulse response. The convolution theorem<sub>2</sub> states that a convolution in the spatial domain is a multiplication in the frequency domain. Taking the Fourier transform (denoted  $\mathcal{F}$ ) of both sides of Equation (2.22) yields [47,8]:-

$$\mathcal{F} [g(x,y)] = \mathcal{F} [f(x,y) * h(x,y)] \quad (2.27)$$

and

$$G(\xi,\eta) = F(\xi,\eta) \times H(\xi,\eta) \quad (2.28)$$

The appeal of the frequency-domain viewpoint is that the multiplication of Equation (2.28) is easier to perform and visualize than the convolution of Equation (2.22). This convenience is most apparent in the analysis of imaging systems consisting of several subsystems, each with its own

impulse response. As Equation (2.29) demonstrates, each subsystem has its own transfer function as the Fourier transform of its impulse response. The final result of all the subsystems operating on the input object distribution is a multiplication of their respective transfer functions. Fig. (2.10)[48] illustrates that you can analyze a combination of several subsystems by the multiplication of transfer functions of Equation (2.30) rather than the convolution of impulse responses of Equation (2.29)[48]:-

$$f(x, y) * h_1(x, y) * h_2(x, y) * \dots * h_n(x, y) = g(x, y) \quad (2.29)$$

and

$$F(\xi, \eta) \times H_1(\xi, \eta) \times H_2(\xi, \eta) \times \dots \times H_n(\xi, \eta) = G(\xi, \eta) \quad (2.30)$$

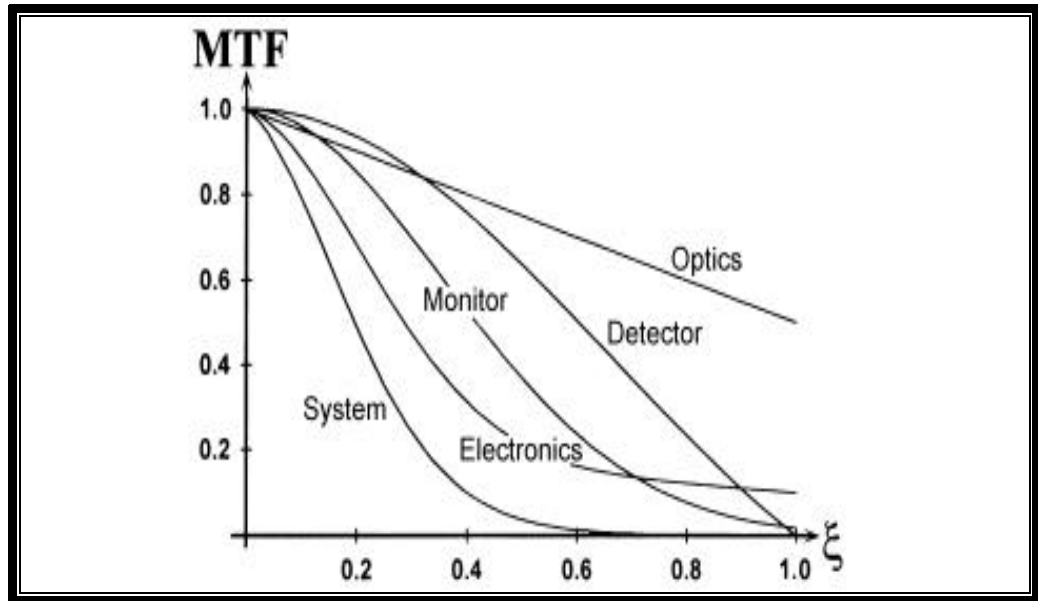


Fig. (2.10) :The aggregate transfer function of several subsystems is a multiplication of their transfer functions[48].

It is typically assumed that  $H(\xi, \eta)$  has been normalized to have unit value at zero spatial frequency (a uniform image irradiance distribution). This normalization yields a relative transmittance for the various frequencies and ignores attenuation factors that are independent of spatial frequency, such as Fresnel reflections or material absorption. Although this

normalization is common, when you use it, information about the absolute signal levels is lost. For some cases you may want to keep the signal-level information, particularly when electronics noise is a significant factor.[49]

With this normalization,  $H(\xi, \eta)$  is referred to as the optical transfer function (OTF). Unless the impulse response function  $h(x, y)$  satisfies certain symmetry conditions, its Fourier transform  $H(\xi, \eta)$  is in general a complex function, having both a magnitude and a phase portion, referred to as the modulation transfer function (MTF) and the phase transfer function (PTF) respectively:-[8,49]

$$\text{OTF} \equiv H(\xi, \eta) \exp[-j\theta(\xi, \eta)] \quad (2.31)$$

### 2.2.2 Modulation Transfer Function

Modulation transfer function is the ability of an optical system to transfer various levels of details from object to image .[8,49] The modulation transfer function is the magnitude response of the optical system to sinusoids of different spatial frequencies. When you analyze an optical system in the frequency domain, you consider the imaging of sine wave inputs (Fig. 2.11) rather than point objects.[5,49]

From the equation(2-31):-

$$\text{PTF} \equiv \theta(\xi, \eta)$$

$$\text{CTF} \equiv H(\xi, \eta) = \frac{I_{\max} - I_{\min}}{I_{\max} + I_{\min}} \quad (2-32)$$

where:

=the maximum intensity.  $I_{\max}$

=the minimum intensity.  $I_{\min}$

When the OTF is real function there is no change in phase where:-

$$\text{PTF} \equiv \theta(\xi, \eta) = 0$$

then the equation (2-31) becomes:-

$$\text{OTF} \equiv H(\xi, \eta) = \text{MTF}$$

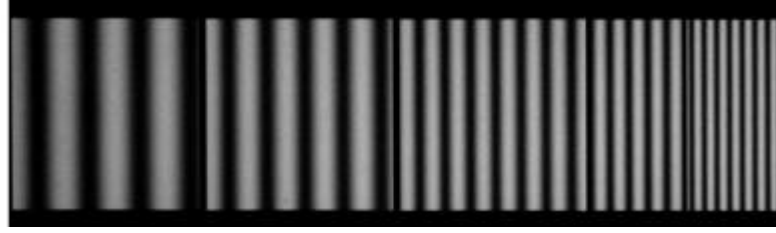


Fig. (2.11) Sine wave target of various spatial frequencies[49].

A linear shift-invariant optical system images a sinusoid as another sinusoid. The limited spatial resolution of the optical system results in a decrease in the modulation depth  $M$  of the image relative to what it was in the object distribution (Fig. 2.12). Modulation depth is defined as the amplitude of the irradiance variation divided by the bias level [49]:-

$$M = \frac{A_{\max} - A_{\min}}{A_{\max} + A_{\min}} = \frac{2 \times ac - \text{component}}{2 \times dc - \text{component}} = \frac{ac}{dc} \quad (2-33)$$

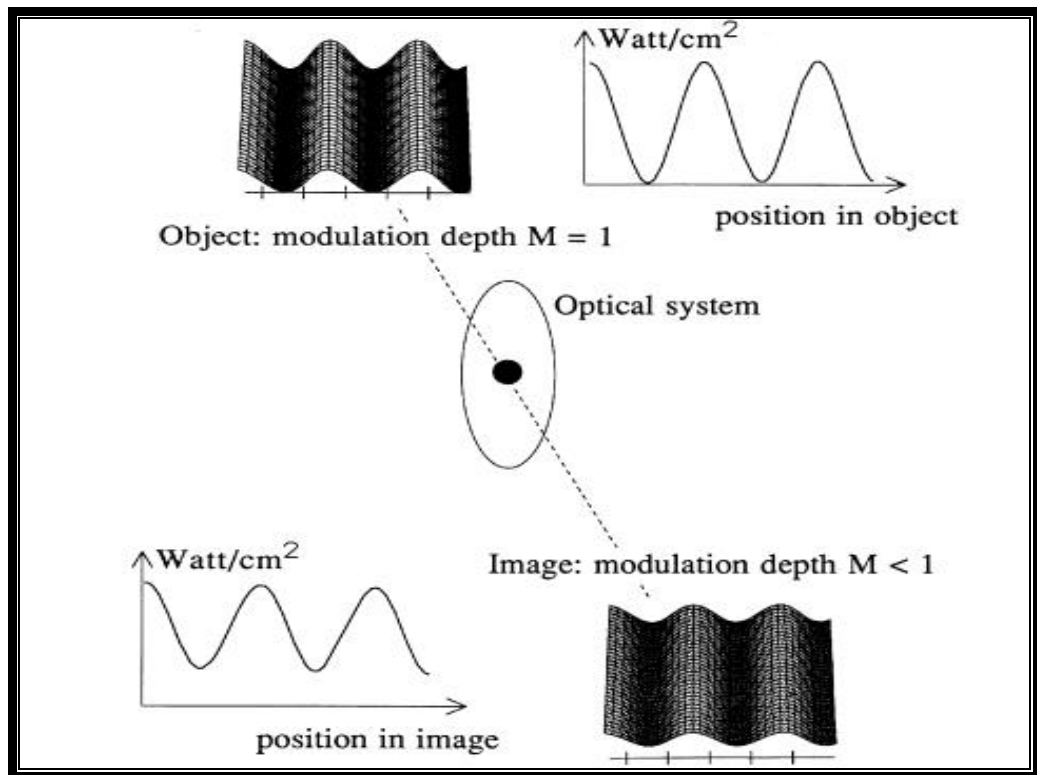


Fig. (2.12): Modulation depth decreases going from object to image[49].

### **2.3 Fractal Geometry**

Fractal Geometry is the study of sets called fractals. When drawn, a fractal is very rough-looking. Also, it can be cut into parts which look quite like a smaller version of the set that was started with. Another thing that fractals have is a dimension which is not what people would expect - often it is not an whole number. Fractals have very simple descriptions. Last of all, even in very small parts of the set, the set will still look very rough.[32]

A fractal often has the following features:-

- It has a fine structure at arbitrarily small scales.
- It is too irregular to be easily described in traditional Euclidean geometric language.
- It is self-similar (at least approximately or stochastically).
- It has a Hausdorff dimension which is greater than its topological dimension (although this requirement is not met by space-filling curves such as the Hilbert curve).
- It has a simple and recursive definition.[50]

Because they appear similar at all levels of magnification, fractals are often considered to be infinitely complex (in informal terms). Natural objects that approximate fractals to a degree include clouds, mountain ranges, lightning bolts, coastlines, and snow flakes. However, not all self-similar objects are fractals, for example, the real line (a straight Euclidean line) is formally self-similar but fails to have other fractal characteristics.

#### **2.3.1 Fractal Word**

A fractal is generally "a rough or fragmented geometric shape that can be subdivided into parts, each of which is (at least approximately) a reduced-size copy of the whole,"[32,50] a property called self-similarity. The term was coined by Benoît Mandelbrot in 1975 and was derived from the Latin *fractus* meaning "broken" or "fractured."



**Georg Cantor** gave examples of subsets of the real line with unusual properties, these Cantor sets Fig.(2-13 ) are also now recognized as fractals.

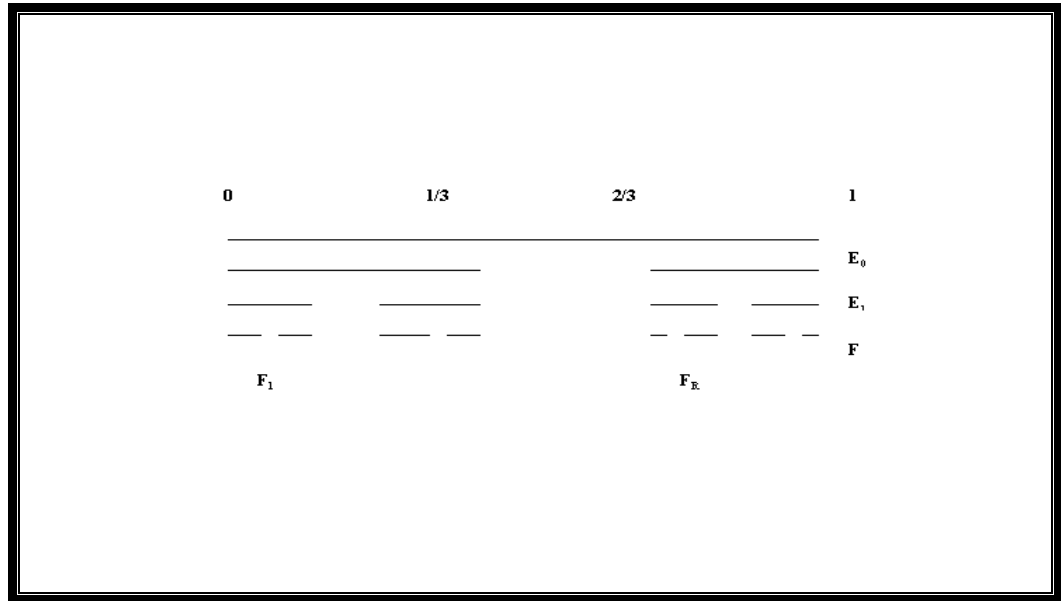
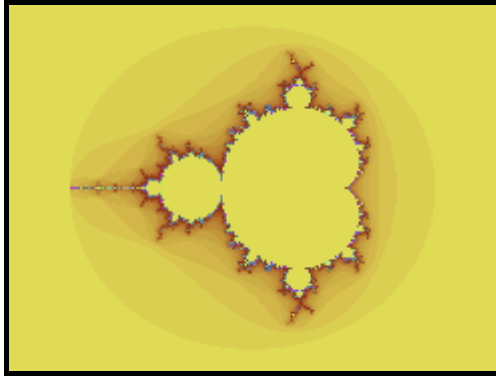
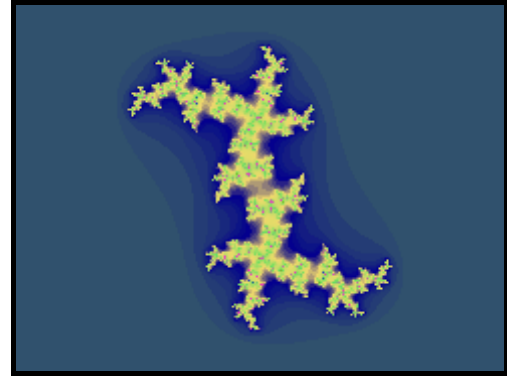


Fig. (2-13) Cantor sets [51]

Chaotic dynamical systems are sometimes associated with fractals. Objects in the phase space of a dynamical system can be fractals. Objects in the parameter space for a family of systems may be fractal as well. An interesting example is the Mandelbrot set Fig. (2-14)(a). This set contains whole discs, so it has a Hausdorff dimension equal to its topological dimension of two. Another example is the Julia set Fig. (2-14)(b).



(a)- Mandelbrot set



(b)- Julia set

Fig. (2-14) Samples of non linear Fractal [52]

The Koch Curve is a simple example of a fractal. Koch's Snowflake is another geometric iterative fractal, based this time on an equilateral triangle. It was first published in 1906 by the Swede. The iterative step, like Cantor's Set, is applied to any remaining line segments. This step consists of splitting a line in 3, removing the middle third and replacing it with two copies of itself angled 60 degrees apart, to make a kink in the line similar to the equilateral triangle. An interesting feature of this curve is how quickly it grows in complexity - the number of edges increases by 4 with every iteration, with the length of the perimeter increasing by  $4/3$ . This means that the actual Koch Snowflake has an infinite perimeter[52].

The length of the Koch Curve is infinity, and the area of the Koch Curve is zero. This is quite strange. A line segment (with dimension 1) could have a length of 1, but it has an area of zero. A square of length 1 and width 1 (with dimension 2) will have area 1 and length of infinity as show in Fig.(2-15).

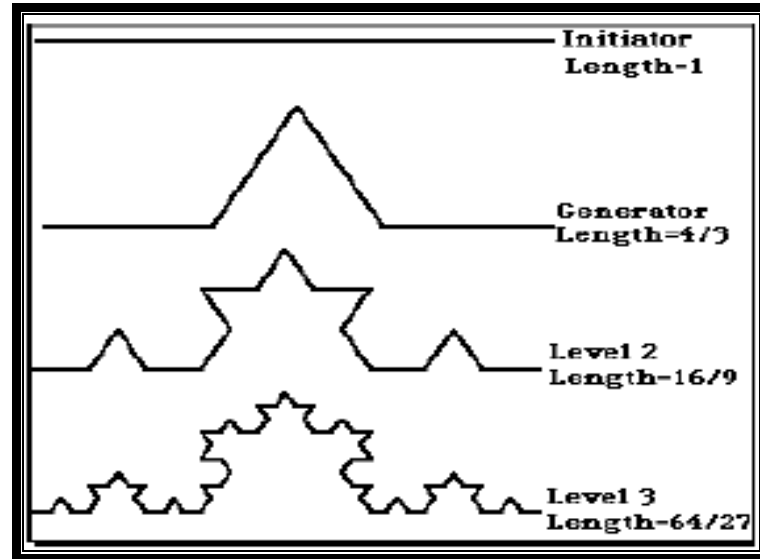


Fig. (2-15) The steps of the Koch Curve[52].

So, the Koch Curve seems to be bigger than something of dimension 1, and smaller than something of dimension 2. The idea of the similarity dimension is to give a dimension which gives a better idea of length or area for fractals. So, for a Koch Curve, we want a dimension between 1 and 2.

The Koch Curve can be cut into 4 pieces, each of which are  $\frac{1}{3}$  of the size of the original. The number of pieces that a fractal can be cut into is called  $N$ , and the size difference is represented by ( $r$ ). These are put into equation[52]:-

$$N = r^D \quad (2-34)$$

Where the exponential is the Hausdorff Dimension of the fractal Fig. (2-16). In the Koch Curve, this is as we wanted.

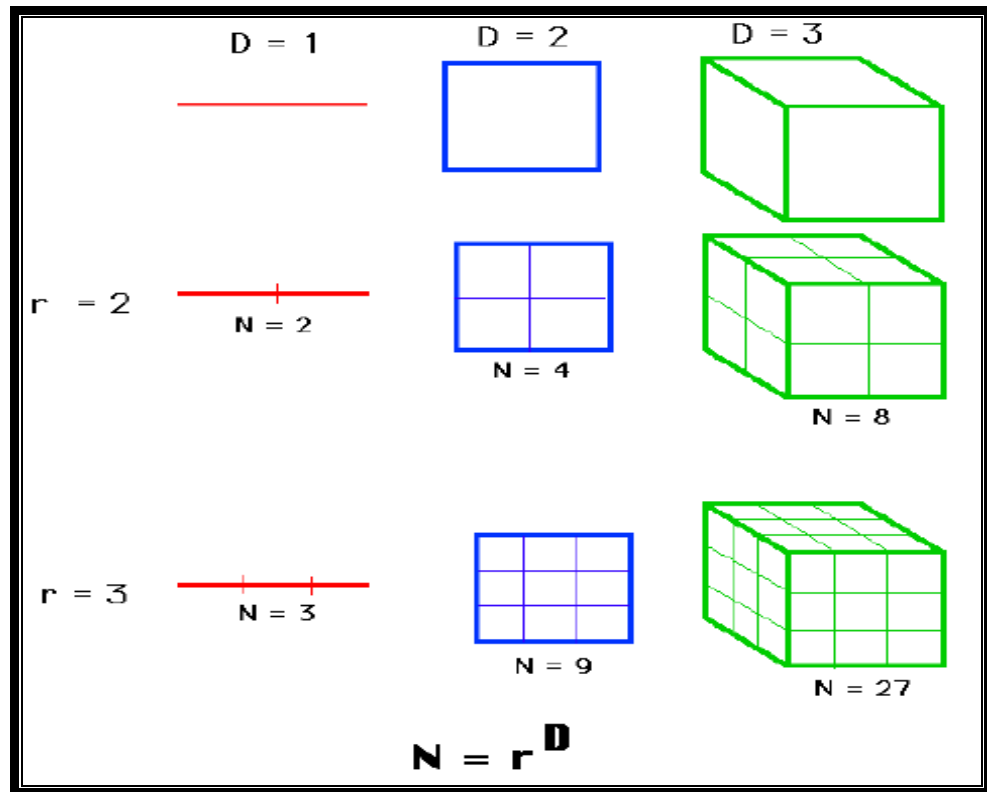


Fig. (2-16) The Hausdorff Dimension of the fractal [52]

### 2.3.2 Fractal Dimension

It is easy to assign a dimension. The square has two dimensions, a line has one dimension, and a cube has three dimensions. Because there are two directions in which we can move on a square, one direction on a lines, and three directions in a cube, but what about fractals? Sometimes can be move in a certain number of directions and sometimes can be move in a different number of directions. This is what causes fractal dimensions to be non-integers.[51]

To derive a formula which will work with all figures, let's first look at how to calculate the dimensions for the figures which we already know. A line can be divided into  $(n^1)$  separate pieces. Each of those pieces is  $(\frac{1}{n})$  the size of the whole line and each piece, if magnified  $(n)$  times, would look exactly the same as the original. Repeating the process for a square, we find that is can be divided into  $(n^2)$  pieces. The same concept holds

true for a cube, we need  $(n^3)$  pieces to reassemble a cube. Each of the pieces would be  $(n^{\frac{1}{3}})$  the size of the whole figure. The exponent in each of these examples is the dimension. For fractals, we need a generalized formula, which can be derived from what we already know.

If we take a straight line, its length (L), and divide it to set pieces, these pieces have length (K), then the number of these pieces equal to :-

$$N = L / K \quad (2-35)$$

To measured the curve of fractal, first we divide it to many pieces, increased exponentially to have high quality .[50] As Fig. (2-17) shows.

$$N = (L / K)^{D'} \quad (2-36)$$

$$D' = \log(N) / \log(L / K) \quad (2-37)$$

where  $D'$  represents the fractal dimension.

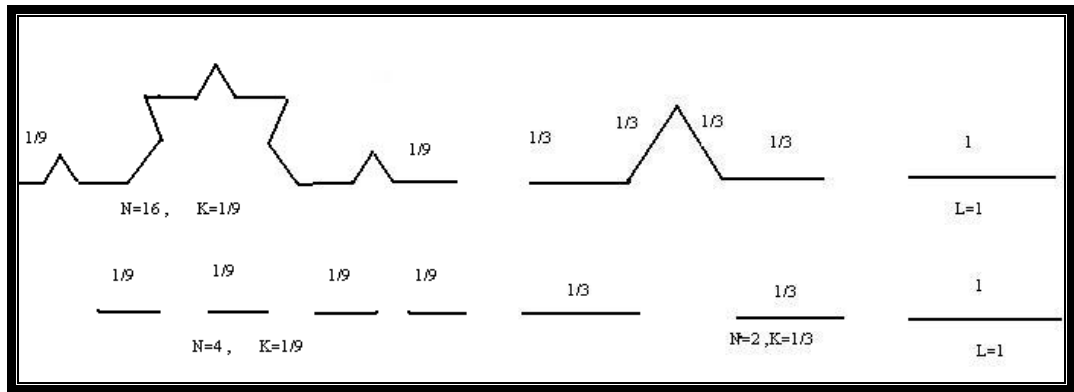


Fig. (2- 17) Fractal curve deviation method[50]

### 2.3.3 Iterated Function Systems (IFS)

In mathematics, **iterated function systems** or **IFSs** are a method of constructing fractals; the resulting constructions are always self-similar.

**IFS** fractals as they are normally called can be of any number of dimensions, but are commonly computed and drawn in 2D. The fractal is

IF the  $(x,y)$  is mapping space of an matrix ,then  $f(x)$  represents the space ,that all points are part of  $(x)$ .

IF  $(W_i : i = 1,2,3,4,\dots,m)$  . Then:-

$$W_i(x) = W \begin{pmatrix} x_i \\ y_i \end{pmatrix} = \begin{pmatrix} a_i & b_i \\ c_i & d_i \end{pmatrix} \begin{pmatrix} x_i \\ y_i \end{pmatrix} + \begin{pmatrix} e_i \\ f_i \end{pmatrix} \quad (2-38)$$

$$W_i = A_i X_i + T_i \quad (2-39)$$

The sets production operation can be obtained by union of these points in sum operation of two linear transformation  $W_1, W_2$  [53]. Table (2-1) shows the code of some sets :-

Table (2-1) Codes of some sets[53].

<b>w</b>	<b>a</b>	<b>b</b>	<b>c</b>	<b>d</b>	<b>e</b>	<b>f</b>
<b>1</b>	<b>1/3</b>	<b>0</b>	<b>0</b>	<b>1/3</b>	<b>0</b>	<b>0</b>
<b>2</b>	<b>1/3</b>	<b>0</b>	<b>0</b>	<b>1/3</b>	<b>2/3</b>	<b>0</b>

where:-

$$W_1 = (1/3)x, \quad \text{and} \quad W_2 = (1/3)x + 2/3$$

It is seen that each code of IFS is divided into many transformations, like triangle transformation to another .[54]

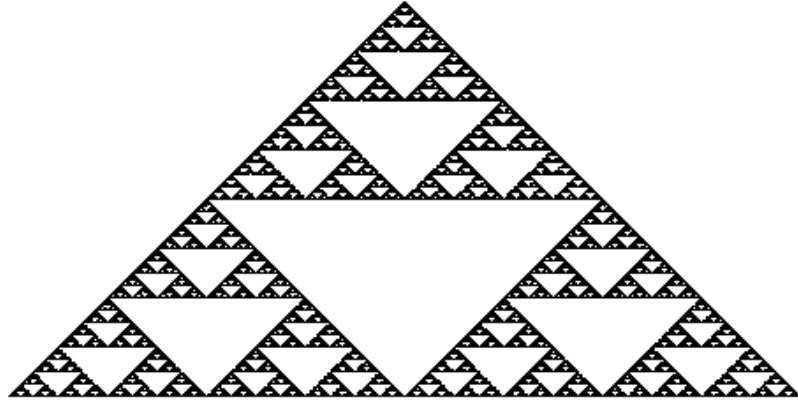


Fig. (2- 18) The Sierpinski gasket[32]

### 2.3.4 Random IFS Algorithm

The Random IFS Algorithm will ( include) that:-

1. We will choose initial point in the fractal.
2. The triangle transformation (IFS code) will be chosen randomly.
3. The choice of transformation is applied to points direction, Then the new point will be sketched.
4. Any point in the fractal consists of IFS axis.
5. These random transformations produce the self shape of image.

This is same samples of fractal shapes with IFS code , they had designed by using (**DUG. Nelson**) program [55].The tables below show the numbers of these codes ,rotational factor data ,and its fractal shape.

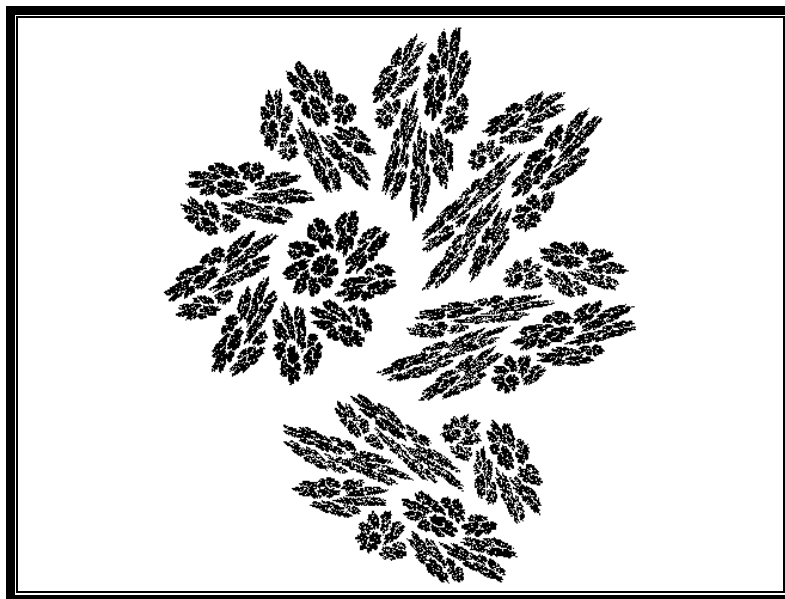


Fig. (2-19) Shape of fractal have two codes[55].

Table (2-2) The IFS codes of Fig. (2-19).

a	b	C	d	e	f
0.787	0.549	-0.575	0.526	-6122	244.78
-0.333	0.416	-0.393	-0.087	349.2	539.932

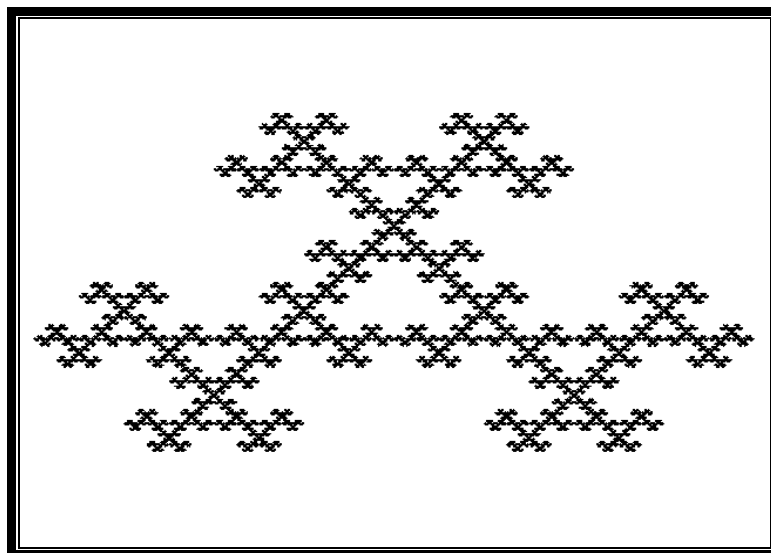


Fig. (2-20) Shape of fractal have three codes[55].



Table (2-3) The IFS codes of Fig. (2-20).

a	b	c	d	e	F
-0.7	-0.25	0.25	591.93	170.06	0.333
-0.7	-0.25	0.25	438.54	323.44	0.333
-0.7	-0.25	0.25	-745.31	323.44	0.333

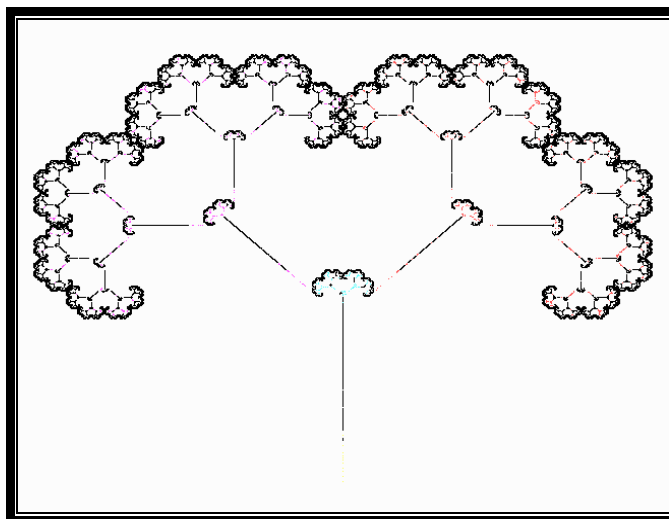


Fig. (2-21) Shape of fractal have four codes[55].

Table (2-4) The IFS codes of Fig. (2-21).

a	b	c	d	e	f
0.0000	0.0000	0.0000	0.5000	319.4737	252.5519
0.4200	0.4283	-0.3540	0.4200	-66.3854	191.7793
0.4200	-0.4983	-0.3540	0.4200	436.9749	-34.4220
0.1000	0.0000	0.0000	0.1000	288.5263	240.3118

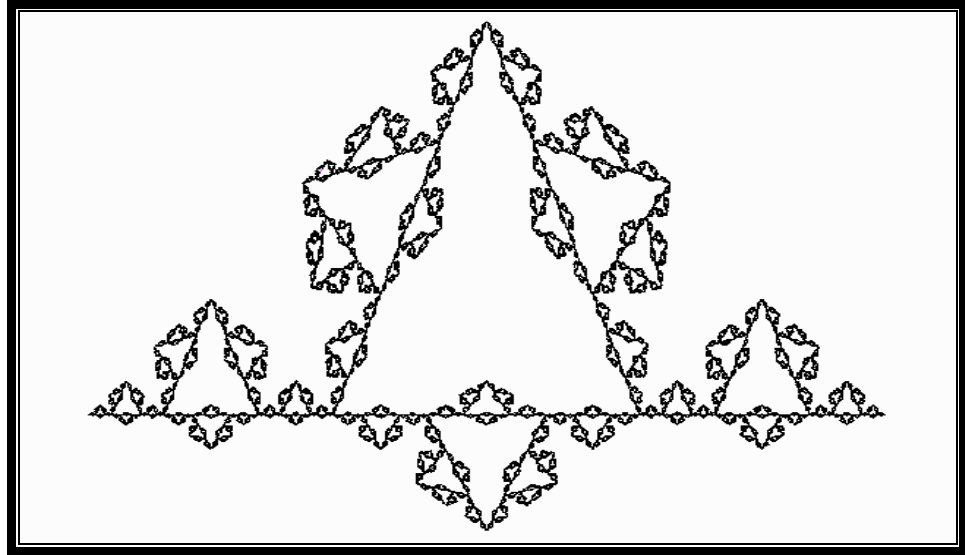


Fig. (2-22) Shape of fractal have five codes[55].

Table (2-5) The IFS codes of Fig. (2-22).

a	b	c	d	e	f
0.3077	-0.0000	-0.0000	0.2941	409.3147	256.6620
0.1923	0.2059	-0.6532	0.0882	130.8280	362.6059
0.1923	-0.2059	0.6538	0.0882	385.1037	-55.0532
0.3077	0.0000	-0.0000	-0.2941	32.9125	256.6620
0.3846	-0.0000	-0.0000	-0.2941	196.5454	470.5471

### 3.1 General Modulator Design

The optical modulator can be represented by real function, this function is called optical modulator function,  $r(x,y,t)$ , which represents the transmittance factor of the object image intensity at the point  $(x,y)$  and time  $(t)$ . Therefore the radiation distribution of the image of the object on the object scene coordinates itself, can be represented by the function  $s(x,y)$ . The radiation flux  $V(t)$ , that is transmitted through the disk and is incident on the optical detector, can be integral and given by[44]:-

$$V(t) = \iint r(x, y, t) \cdot s(x, y) dx dy \quad (3-1)$$

This equation represents the general relationship of the optical modulator. The image of the object function  $s(x,y)$ , with spatial coordinate, can be modulated to temporal signal produced from the detector.

Fig. (3-1) shows the optical modulator system. The aperture (A) has an area and shape independent of the time. The optical modulator is rotated about its axis and scan the aperture, This scan can be done by rotational or translational movement, or may be both[5]

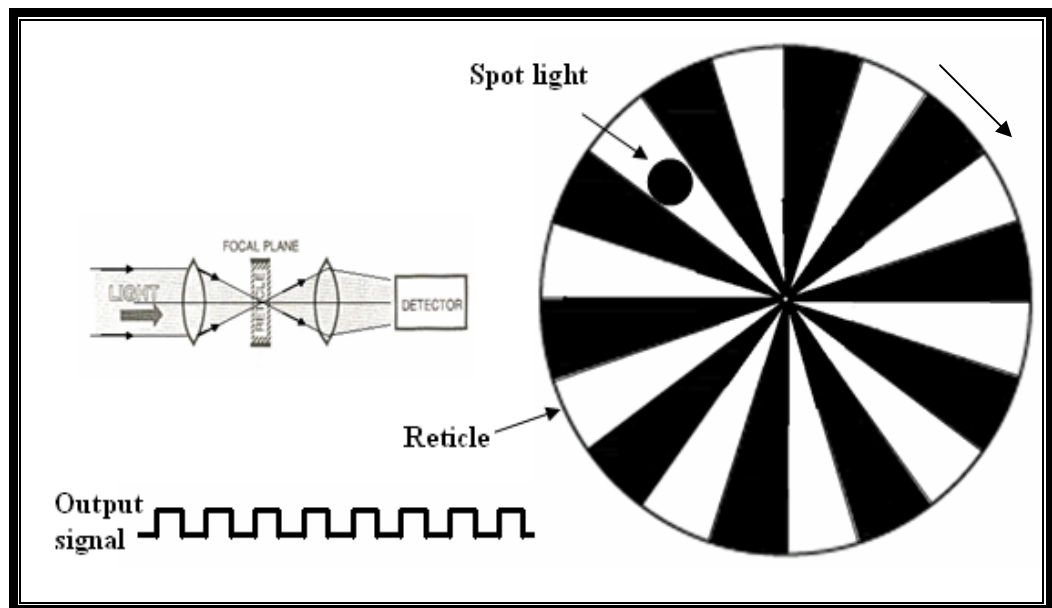


Fig. (3-1) General Optical Modulator System[37].

When the system coordinate is defined on the aperture (A), then the transparent-disk depends on time, on the aperture coordinate, Therefore the object scene depends on time too. The modulation equation can be written as[44] :-

$$V(t) = \iint_A r(x, y, t) \cdot s(x, y, t) dx dy \quad (3-2)$$

where;-

x,y = the aperture (A) coordinate .

R(x,y,t)= the distribution function of object scene radiation

Power.

V(t)= the output signal of the detector.

The optical modulator pattern changes periodically, this concept can be given by:-

$$r(x, y, t) = r(x, y, t + \frac{2\pi}{\omega_0}) \quad (3-3)$$

where:-

$\omega_0$  = the fundamental angular frequency of the disk.

The optical modulator function can be represented by using Fourier series in time (t) and fundamental angular frequency ( $\omega_0$ ):-

$$r(x, y, t) = \sum_{n=-\infty}^{\infty} a_n(x, y) \text{Exp}(jn\omega_0 t) \quad (3-4)$$

where:-

$$a_n(x, y) = \frac{\omega_0}{2\pi} \int_0^{\frac{2\pi}{\omega_0}} r(x, y, t) \text{Exp}(-jn\omega_0 t) dt \quad (3-5)$$

Substituting equation (3-4) into Equation (3-2) gives :-

$$V(t) = \sum_{n=-\infty}^{\infty} bn(t) \cdot \text{Exp}(jn\omega_0 t) \quad (3-6)$$

where:-

$$bn(t) = \int_A an(x, y) \cdot s(x, y, t) dx dy \quad (3-7)$$

Each component of  $\text{Exp}(jn\omega_0 t)$  in Equation (3-6) represents the carrier wave. And this component has been modulated by using temporal function( $bn(t)$ ), which carries object coordinate data.

When the aperture (A) doesn't scan the object of the image space, Then the object function was independent on time. The movement and shape of the optical modulator can be designed by determine the value of ( $\omega_0$ ) and ( $bn(t)$ ).

To study the effect of aperture (A) on modulation operation , you re write the equation (3-7), and enter the aperture function A(x,y). The new equation is given by [44]:-

$$Bn(t) = \int_{-\infty}^{\infty} \int_{-\infty}^{\infty} an(x, y) A(x, y) s(x, y, t) dx dy \quad (3-8)$$

And by using (Parseval Property ) and (Convolution Theorem ), we can given the relationship below:-

$$Bn(t) = \int_{-\infty}^{+\infty} A^*(k_x, k_y) S'(k_x, k_y) \cdot dk_x dk_y \quad (3-9)$$

where:-

$A^*$  = the Fourier transform conjugate

$A^*(k_x, k_y)$  = the Fourier transform conjugate of  $an(x, y)$ .

and

$$S'(k_x, k_y) = \int \int_{-\infty}^{\infty} S(k'_x, k'_y) \cdot O(k_x - k'_x, k_y - k'_y) dk'_x dk'_y \quad (3-10)$$

where:-

$O(k_x - k'_x, k_y - k'_y)$  represents the Fourier transform of convolution integral of spatial signal, produced by the disk.

The spatial signal can be given by :-

$$O(x, y) = \int \int_{-\infty}^{\infty} g(x - x', y - y') S(x', y') dx' dy'$$

When the aperture have slit shape ,and its direction is (x,y), then the Fourier transform is given by :-

$$A(k_x, k_y) = \frac{\sin(\pi x k_x) \sin(\pi y k_y)}{\pi^2 k_x k_y} \quad (3-11)$$

And the Fourier transform of the circular aperture is given by :-

$$A(k_x, k_y) = \frac{\rho J_1(2\pi\rho\sqrt{k_x^2 + k_y^2})}{\sqrt{k_x^2 + k_y^2}} \quad (3-12)$$

where:-

$\rho$  = the radius of the aperture.

$J_1$  = the first order Bessel function.

### 3.1.1 The Optical Modulator Movements

The effect of optical modulator movement can be studied by using the three types of movement, translation, rotational and nutational [10].

In **Translational movement**, in (-y) direction of aperture (A) coordinates, the optical modulator function can be written as:-

$$R(x,y)=r(x,y+Vt) \quad (3-13)$$

where:-

V= the translation movement speed.

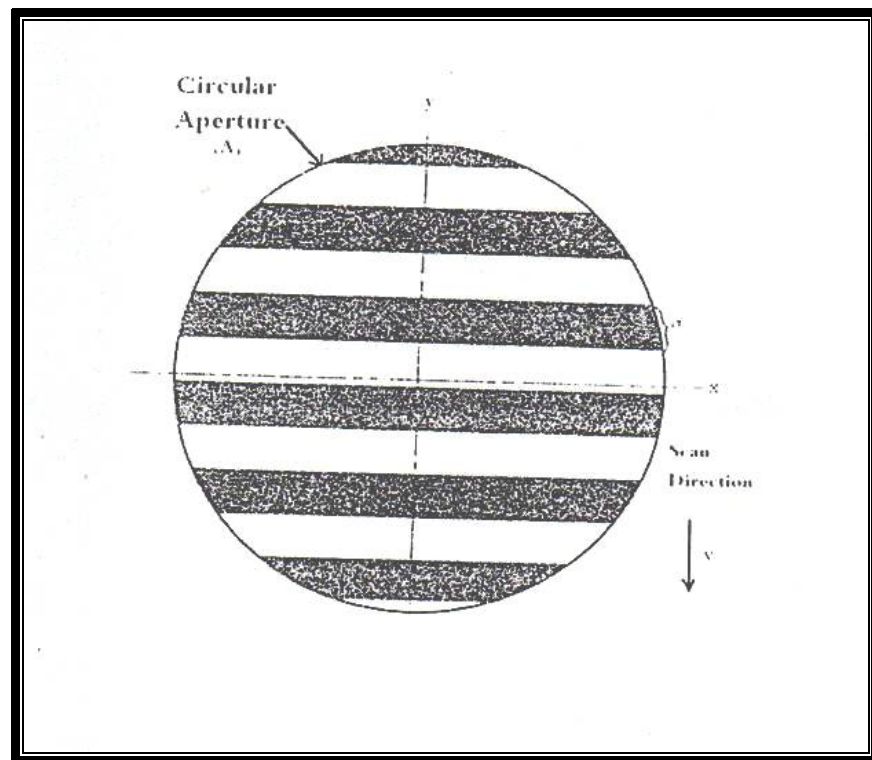


Fig. (3-2) The optical modulator used with translational movement [37].

In **Rotational movement**, When the disk center (Or) position is not equal to aperture center (Oa) position, as shown in Fig. (3-3), the optical modulator function can be written in polar coordinates, and given as :-

$$r(\rho, \theta, t) = r'[\rho'(\rho, \theta), \theta'(\rho, \theta), t] \quad (3-14)$$

where:-

$(\rho, \theta)$  = the polar coordinates of aperture center ( $O_a$ ).

$(\rho', \theta')$  = the polar coordinates of optical modulator center ( $O_r$ ).

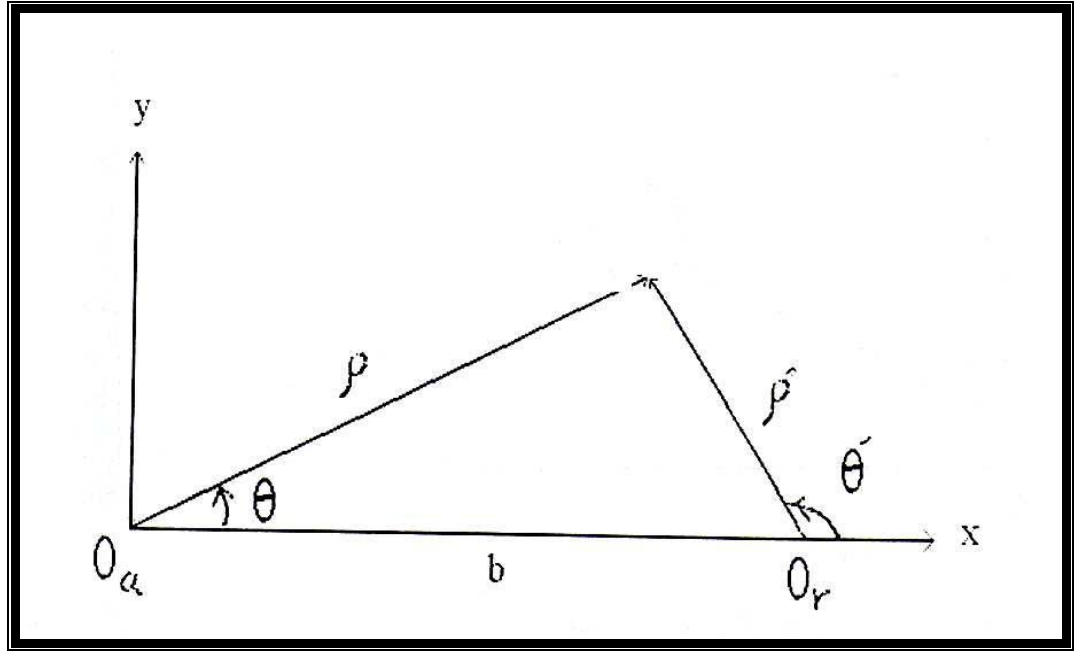


Fig. (3-3) The principle of optical modulator working in rotational movement[37].

Refer to (cosine law) and complex-vector theorem :-

$$\rho' = \rho'(\rho, \theta) = \sqrt{\rho^2 + b^2 - 2\rho b \cos \theta} \quad (3-15)$$

$$e^{-2i\theta'} = e^{-i\theta'(\rho, \theta)} = (\rho e^{-i\theta} - b) \sqrt{\rho^2 + b^2 - 2\rho b \cos \theta} \quad (3-16)$$



In the **Nutational movement**, the position of optical modulator center ( $O_r$ ) is equal to position of aperture center ( $O_a$ ), while the object\_scene was rotated around the optical modulator. Fig. (3-4) shows turning the object image scene center ( $O_s$ ), around the aperture center ( $O_a$ )[10,38].

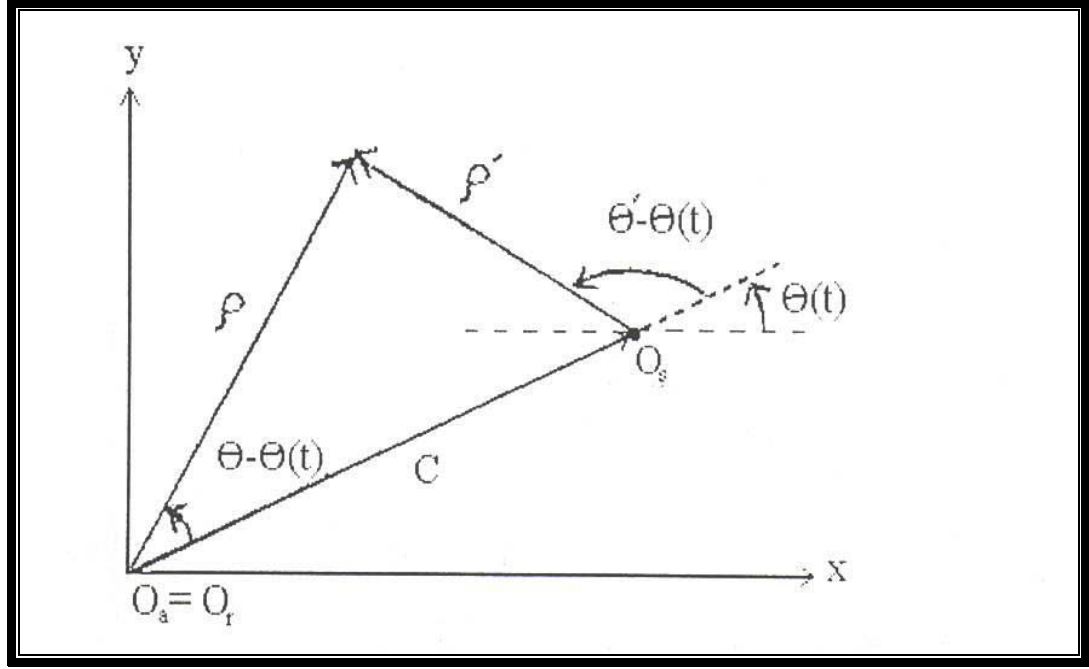


Fig. (3-4) The principle of optical modulator working in nutational movement[37].

The modulation operation of spot source analysis has the two relationships :-

$$\rho = \sqrt{c^2 + \rho'^2 - 2c\rho' \cos[\theta' - \theta(t)]} \quad (3-17)$$

$$e^{-i\theta} = e^{-i\theta(t)} \left[ \rho' e^{-i(\theta' - \theta(t))} - c \right] \left[ c^2 + \rho'^2 - 2\rho'c \cos[\theta' - \theta(t)] \right]^{0.5} \quad (3-18)$$

### 3.2 AM Modulator Design

By using the mathematical analysis of general optical modulator, you can present AM modulation in polar coordinates, as shown below[38]:-

$$r'(\rho', \theta', t) = r'(0, \theta', t) \quad (3-19)$$

where:-

$$\theta' = \frac{2\pi}{q} = \text{the angel of single sector.}$$

$q$  = the number of transparent and opaque sectors.

You can write the Fourier series of this type of modulators, just for angular direction, This equation is given by:-

$$\left. \begin{aligned} r'(0, \theta) &= \sum_{k=-\infty}^{\infty} a_n \cdot e^{jnq\theta'} \\ a_n &= \frac{q}{2\pi} \int_0^{\frac{2\pi}{q}} r'(0, \theta') e^{-jnq\theta'} d\theta' \end{aligned} \right\} \begin{aligned} n &= 2k + 1 \\ k &= \pm 1 \pm 2, \dots \end{aligned} \quad (3-20)$$

where:-

$$r'(0, \theta') = 1 \quad \text{For} \quad 0 \leq \theta' \leq \frac{\pi}{q}$$

$$r'(0, \theta') = 0 \quad \text{Else where}$$

When the number ( $n$ ) is even, then the factor ( $a_n$ ) is equal to zero, therefore:-

$$\left. \begin{aligned} a_0 &= \frac{1}{2} \\ a_{(2k+1)} &= \frac{e^{-j(2k+1)\pi\delta}}{j\pi(2k+1)} \end{aligned} \right\} \quad (3-21)$$

If the angular velocity of the disk is ( $\omega$ ) then:-

$$\theta'(t) = \omega t \quad (3-22)$$

From the Equations (3-19) to(3-22), the function of this types of modulator can be written as shown below:-

$$r(\rho', \omega t - \theta') = \frac{1}{2} + \frac{1}{i\pi} \sum_{k=-\infty}^{\infty} \frac{e^{-i(2k+1)\pi\delta}}{2k+1} e^{-i(2k+1)q\omega t} \quad (3-23)$$

where:-

$q\omega$  = the carrier wave frequency.

### 3.3 FM Modulator Design

FM modulation will be generated by using several optical modulators. One of these modulators, the disk is shown in Fig. (3-5). This optical modulator has many circles, concentric. Each circle is divided to transparent and opaque sectors, Their number are increased far from disk center[44].

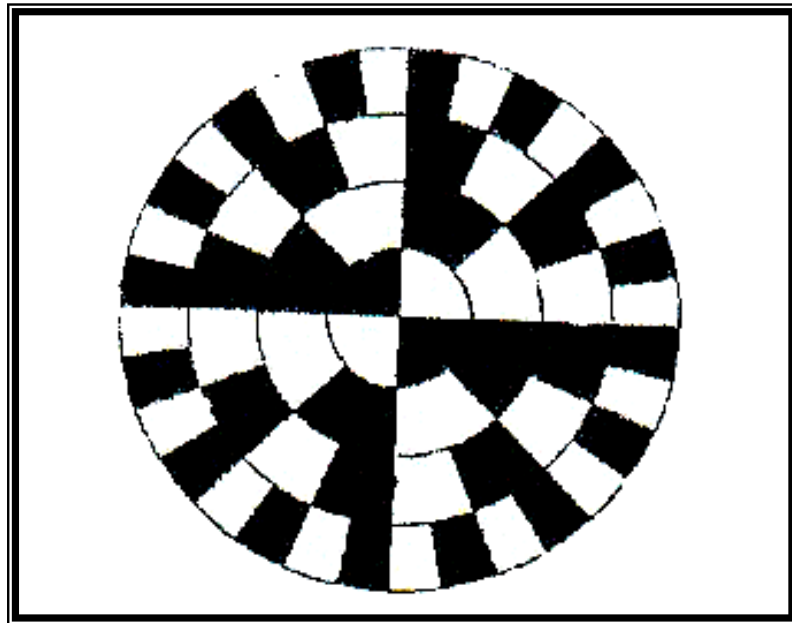


Fig. (3-5) FM optical Modulator.[44].

The mathematical analysis of this type of optical modulator can be given by the relation[37,38,44]:-

$$r(\rho, \theta, t) = \sum_{n=1}^N r_n(\rho, \theta, t) \quad (3-24)$$

This function has ( $q_n$ ) of transparent and opaque spokes. Assume that the optical modulator is rotated about its axis, which identical to aperture center. The phase differences ( $\delta$ ) of this type of disks are equal. Therefore the output electronic signal is given by:-

$$\left. \begin{aligned} V_n(t) &= \int_0^{2\pi} \int_{\rho_{n-1}}^{\rho_n} \rho r_n(\rho, \theta, t) s(\rho, \theta, t) d\rho d\theta \\ V_n(t) &= B_o^{(n)}(t) + \sum_{k=-\infty}^{\infty} B_{2k+1}^{(n)} \text{Exp}[i(2k+1)\rho_n \omega_o t] \end{aligned} \right\} \quad (3-25)$$

where:-

$$\begin{aligned} B_o^{(n)}(t) &= \frac{1}{2} \int_0^{2\pi} \int_{\rho_{n-1}}^{\rho_n} \rho s(\rho, \theta, t) d\rho d\theta \\ B_{(2k+1)}^{(n)} &= \left\{ \frac{\text{Exp}[-i(2k+1)\pi\delta]}{i\pi(2k+1)} \right\} \int_0^{2\pi} \int_{\rho_{n-1}}^{\rho_n} \rho \text{Exp}[-i(2k+1)q_n\theta] s(\rho, \theta, t) d\rho d\theta . \end{aligned}$$

The electronic signal function V(t) can be produced by summation of functions ( $V_n(t)$ ):-

$$V(t) = \sum_{n=1}^N V_n(t) \quad (3-26)$$

### 3.4 Fractal Modulator Design

Simple non-linear deterministic equations can self-generate irregular outputs. Non-linear deterministic system can be simulated when behavior is linear or nearly non-linear. When it increases, though smooth on short time scales, random and unpredictable behavior can be seen over longer periods.

Let  $(H(x), h(d))$  be a metric space, and let  $f : x \rightarrow x$  be a function[44].

Let  $S \subset X$ , then:-

$$f(S) = \{f(x) : x \in S\}.$$

The function  $f$  is **one-to-one**.

If  $x, y \in X$ , and  $f(x) = f(y)$ , so  $x = y$ , then the metric space can be given by the equation:-

$$A' = TA \quad (3-27)$$

where:-

$A$  is a point in initial area.

$A'$  is a new point in under matrix operation  $(T)$

The matrix  $(T)$  is given by:-

$$T = \begin{pmatrix} a & b \\ c & d \end{pmatrix} \quad (3-28)$$

The transformation  $(W)$  in Euclidean plane can be given by[46]:-

$$W(x, y) = (ax + by + e, cx + dy + f) \quad (3-29)$$

The points  $a, b, c$ , and  $d$  define rotation and scaling operations to be applied to the point and are called affine transformation. The  $e$  and  $f$  points define a translation to be applied to the point. The transformation  $(W)$  can be defined in this formula:-

$$W(x) = W \begin{pmatrix} x \\ y \end{pmatrix} = \begin{pmatrix} a & b \\ c & d \end{pmatrix} \begin{pmatrix} x \\ y \end{pmatrix} + \begin{pmatrix} e \\ f \end{pmatrix} \quad (3-30)$$

or

$$W(x) = Ax + T \quad (3-31)$$

where:-

$$Ax = \text{the matrix} \begin{bmatrix} a & b \\ c & d \end{bmatrix} \begin{bmatrix} x \\ y \end{bmatrix}$$

$$T = \text{the horizontal vector} \begin{bmatrix} e \\ f \end{bmatrix}$$

By using this concept and (DUG.Nelson) program[55], we have sketched many shapes of fractal optical modulators, one of which (Fig.(3-6)) is used to design the optical modulator of this research.

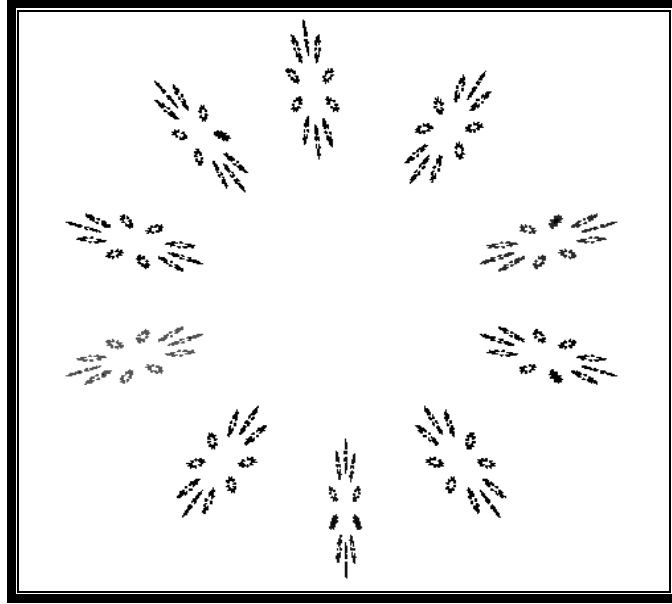


Fig. (3-6) 10-slots Fractal Modulator[55].

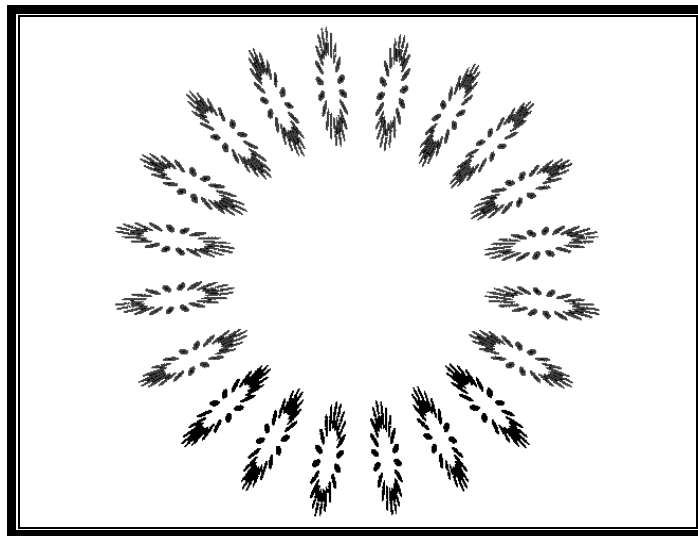
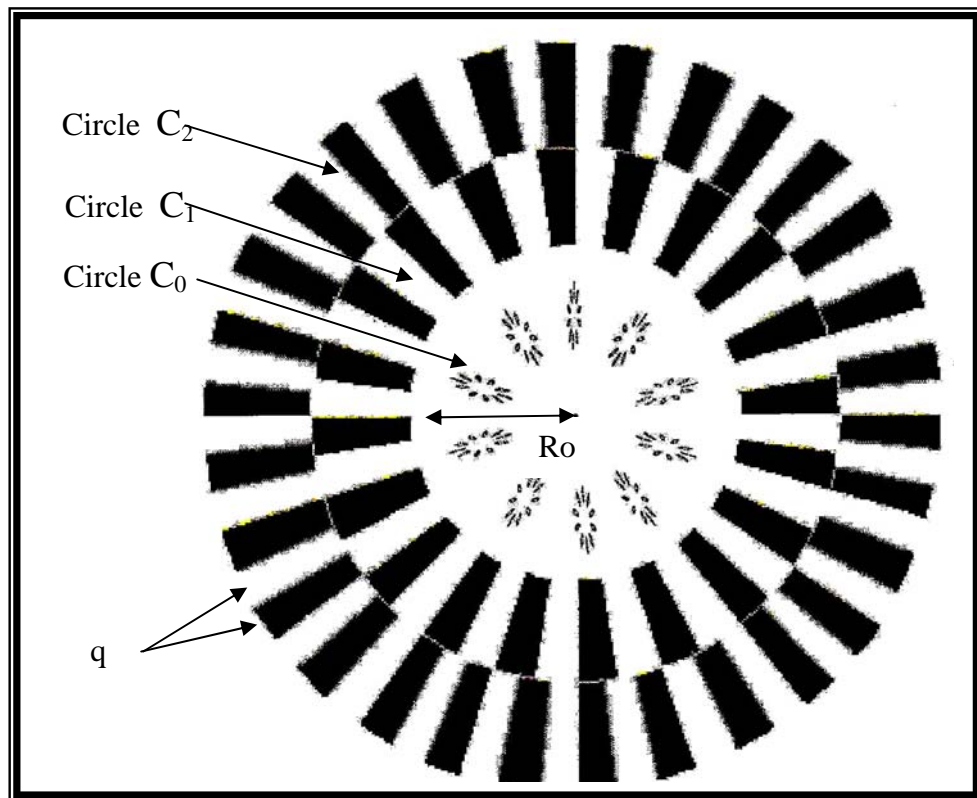


Fig. (3-7) 20-slot Fractal Modulator[55].

### 4-1 Introduction

This chapter reveals the results of this work. At first we have designed optical modulator as shown in Fig. (4-1). This optical modulator consists of three pattern circles ( $C_0, C_1, C_2$ ). Each circle is divided to transparent and opaque block sectors ( $q$ ), and the number of sectors increases progressive ( $nq$ ), where ( $n$ ) represents the number of circles ( $n=1,2,3$ ). In this research ( $q=10$ ) is used. Therefore the numbers of sectors of this three circles are (10,20,30) respectively. It is seen that the number of transmittance and oblique sectors increases with the number of circles (20,40,60) for ( $C_0, C_1, C_2$ ) respectively.

If the central circle radius is ( $R_0$ ), therefore the radius of other circles(dics) is ( $nR_0$ ), (That means the thickness of each circle around the central circle is ( $R_0$ )). The central circle ( $C_0$ ) is designed by using principle of fractal geometry. Special program (Appendix B) is used to sketch the shape of this circle (Fractal Modulator)[55].



**Fig. (4-1) The supposed optical modulator**

Assume that the optical modulator is rotated about its axis, and the rotational velocity is ( $\omega r$ ) in (Rev/sec), then the rotational frequency of optical modulator is ( $fr = \frac{\omega r}{2\pi}$ ). If the spot light source is incident on the optical modulator, then the spot light makes chopping circle, the frequency of the chopping light represents the chopping frequency ( $fc$ ), depending on the number of sectors ( $q$ ). The value of chopping frequency is equal to ( $fc = qfr$ ) and the chopping frequency of each circle is given by the relationship below:-

$$fc_n = n.q.fr \quad (4-1)$$

where:-

$n$  is the number of circles.

$q$  is the number of sectors.

$fr$  is the rotational frequency of the modulator.

Notice that the chopping frequency of the central circle ( $C_0$ ) is different from other circles, because of the property of the fractal shapes, as explained in chapter two, It is seen that each part of the fractal modulator is similar to the total shape, that means the spot light is chopped ten times in each part. By using Q-basic program (Appendix A), we calculate the rotational frequency ( $fr$ ) in (KHZ) for different time( $t$ ) (0.004-0.2). From the equation (4-1), we calculate the chopping frequencies ( $F_{c0}, F_{c1}, F_{c2}$ ) of circles ( $C_0, C_1, C_2$ ), in (KHZ), Table (4-1).



Table (4-1):Rotation frequency and chopping frequencies of optical modulator.

t (sec)	fr(KHZ)	Fc0(KHZ) n=1 q=10	Fc1(KHZ) n=2 q=10	Fc2(KHZ) n=3 q=10
0.004	0.25	2.5	5	10
0.006	0.1666	1.66	3.333	6.666
0.008	0.125	1.25	2.5	5
0.01	0.1	1	2	4
0.02	0.05	0.5	1	2
0.04	0.025	0.25	0.5	1
0.06	0.0166	0.166	0.333	0.666
0.08	0.0125	0.125	0.25	0.5
0.1	0.01	0.1	0.2	0.4
0.2	0.005	0.05	0.1	0.2

First we sketched the relation between the change in time(t) and the rotational frequency of the modulator ( $f_r$ ),and the diagram is shown in Fig.(4-2).Then we sketched the relation between the change in time(t) and the chopping frequency of circles ( $C_0$ ,  $C_1$ ,  $C_2$ ), and the diagram is shown in Figures (4-3,4-4,4-5), It is seen that the frequencies decrease with increased time (t)

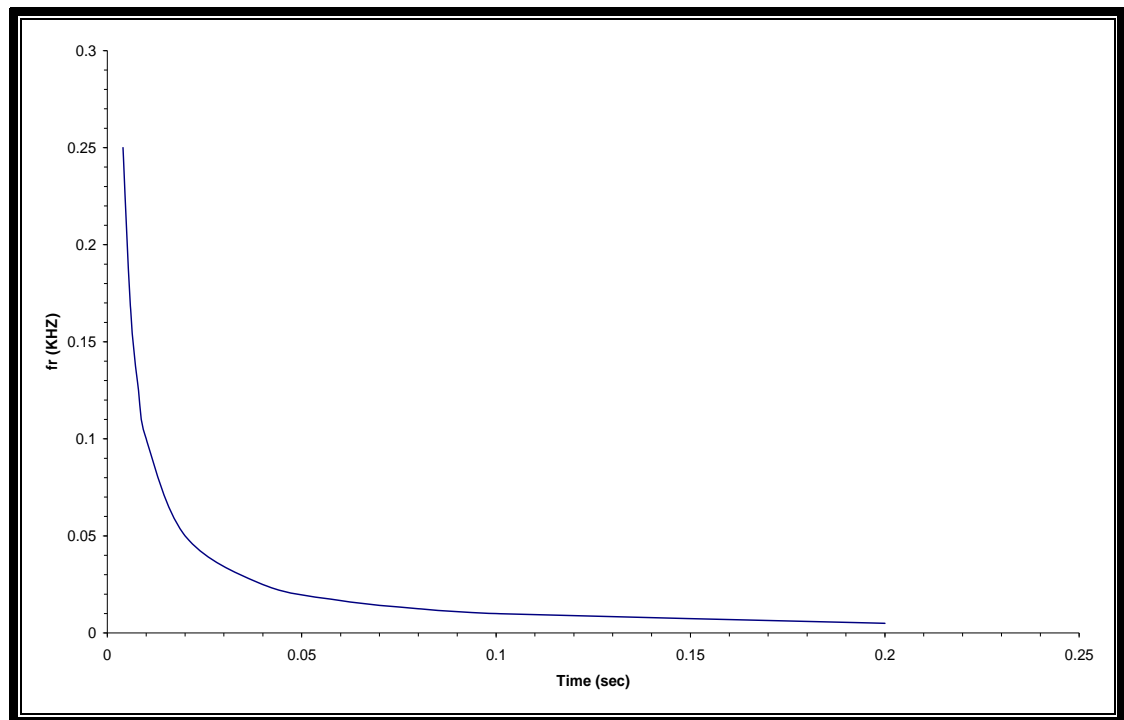


Fig.(4-2): The relation between Rotation frequency (fr) and the change in time.

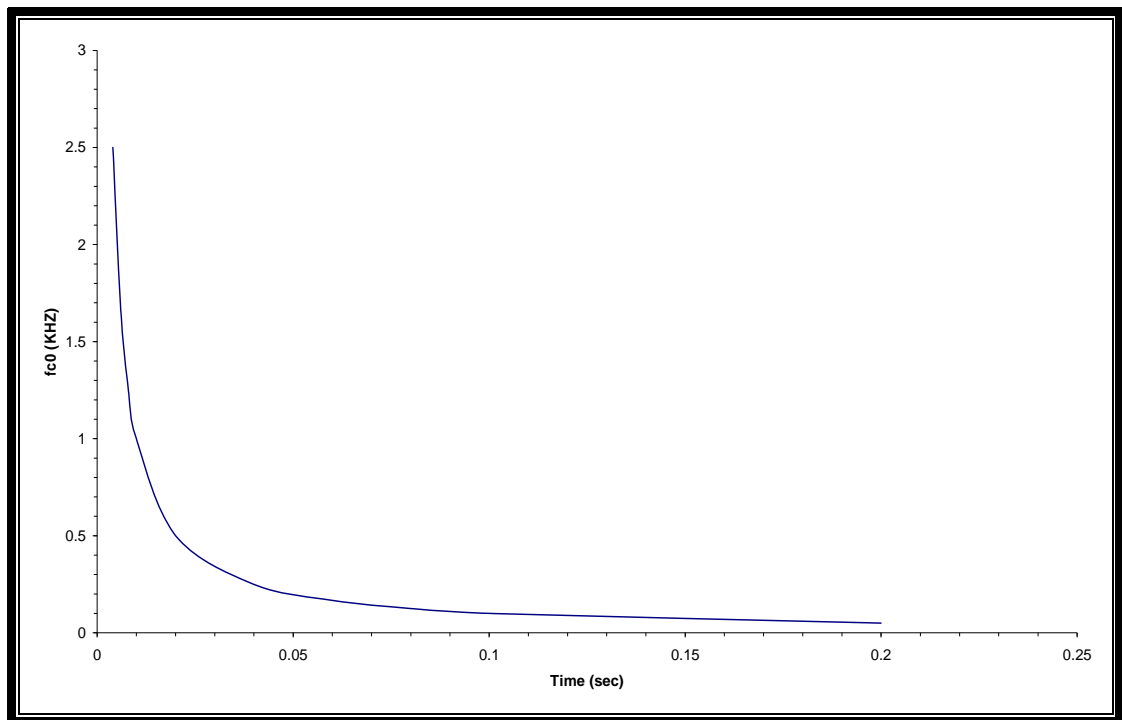


Fig. (4-3): Chopping frequency( $f_{c0}$ ) of central circle( $C_0$ ) with different times.

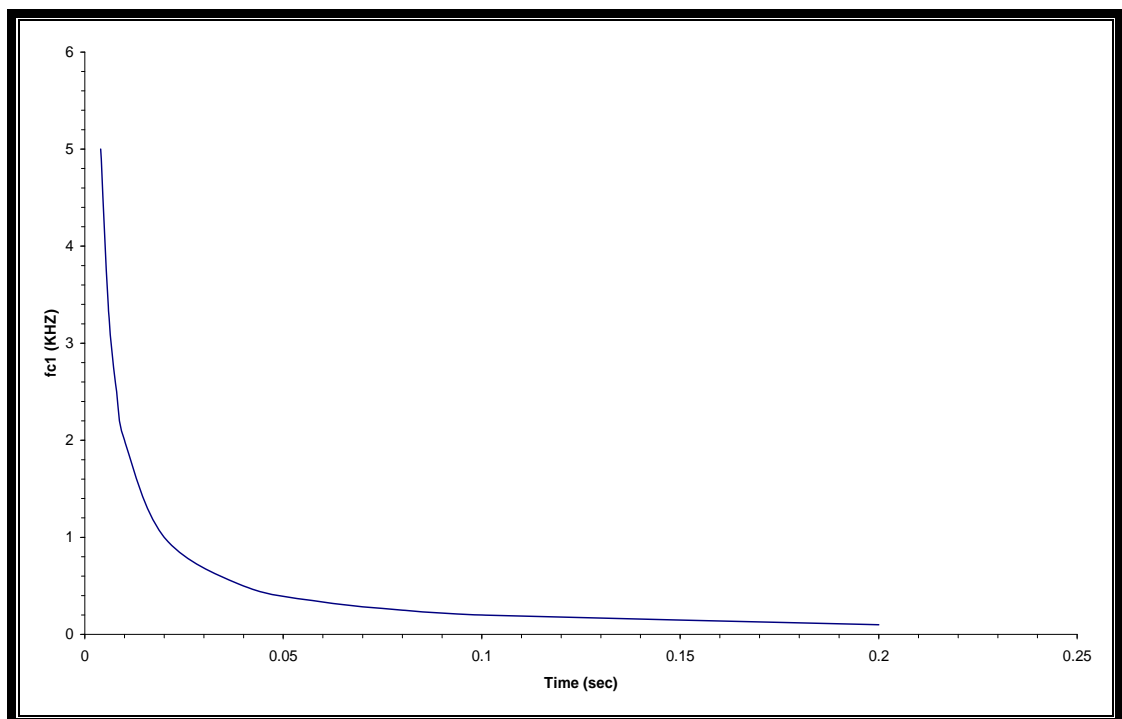


Fig. (4-4): Chopping frequency( $f_{c1}$ ) of circle one( $C_1$ ) with different times.

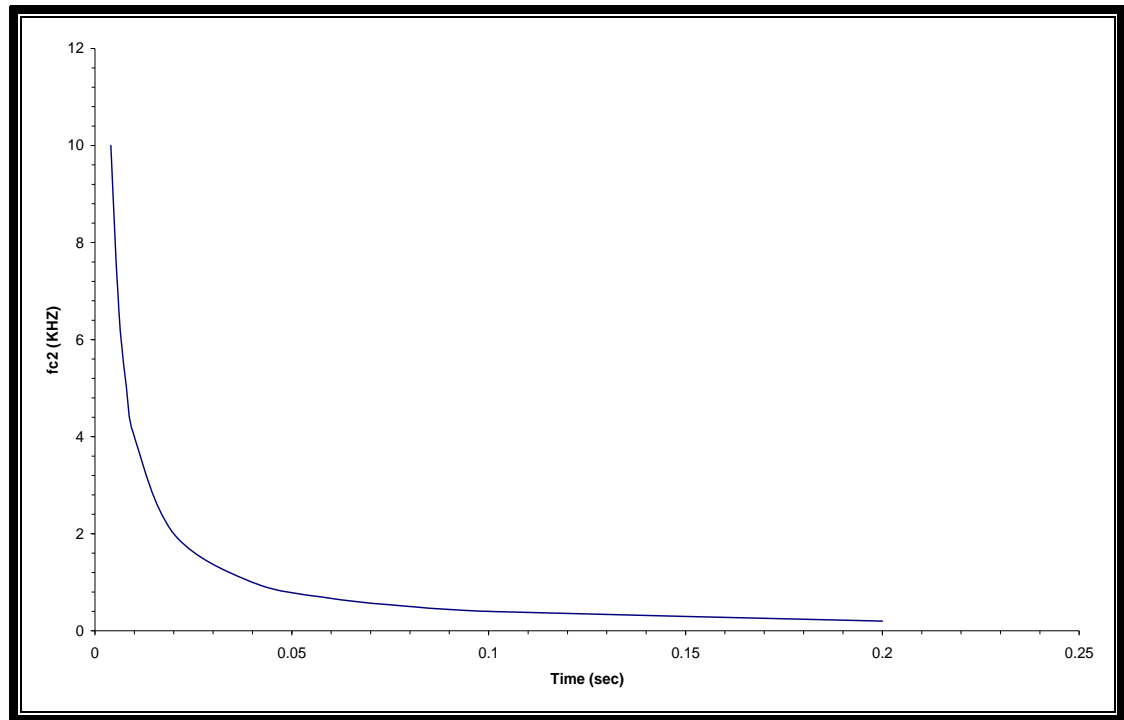


Fig. (4-5): Chopping frequency( $fc_2$ ) of circle two (C2) with different times.

The relation between the chopping frequency and the number of sectors for each circle at time equal to (0.004,0.2) sec is sketched. The diagrams (4-6,4-7) show the chopping frequency ( $f_{co}$ ) at time (0.004,0.2) respectively. It is seen that the frequency chopped is ten times in each part of fractal shape. The chopping frequencies ( $fc_1, fc_2$ ) of circles ( $C_1, C_2$ ) are shown in diagrams (4-8,4-9).

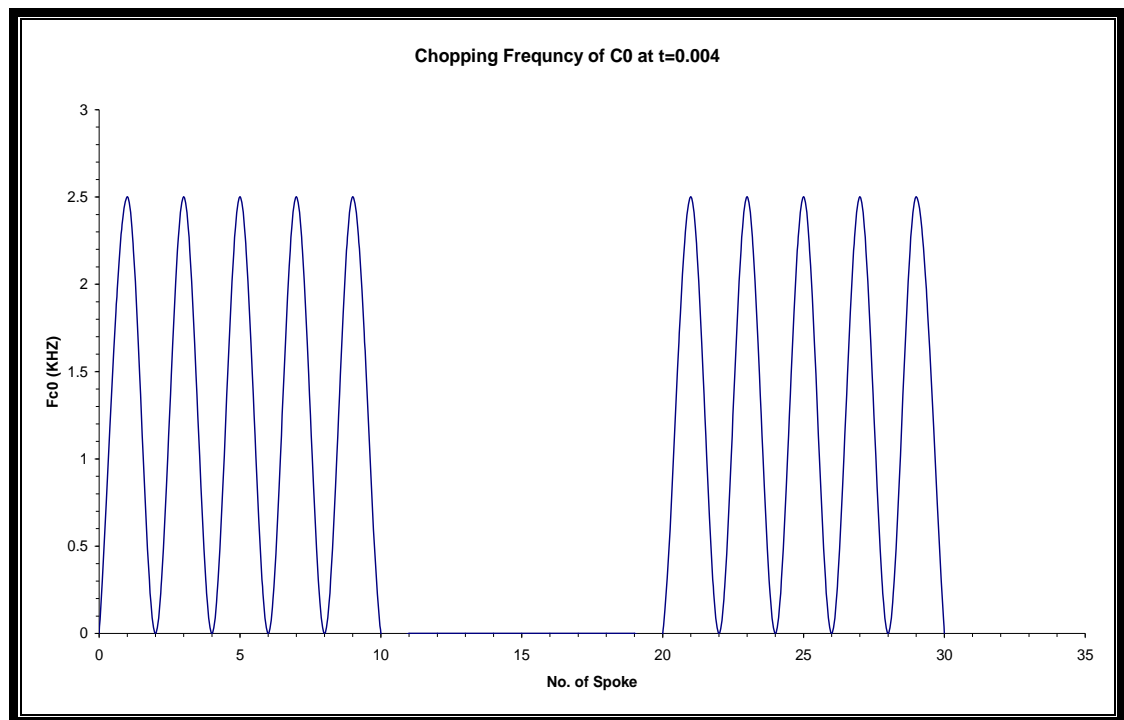


Fig. (4-6): Chopping frequency of C0 at t=0.004 sec.

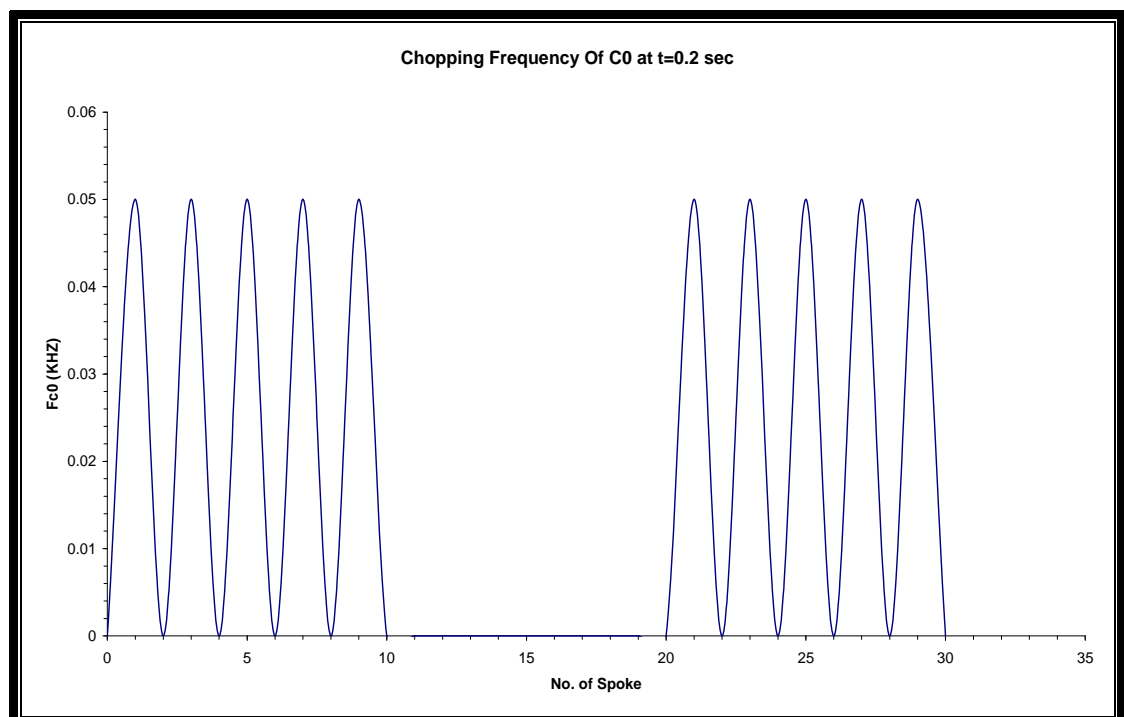


Fig. (4-7): Chopping frequency of C0 at t=0.2 sec.

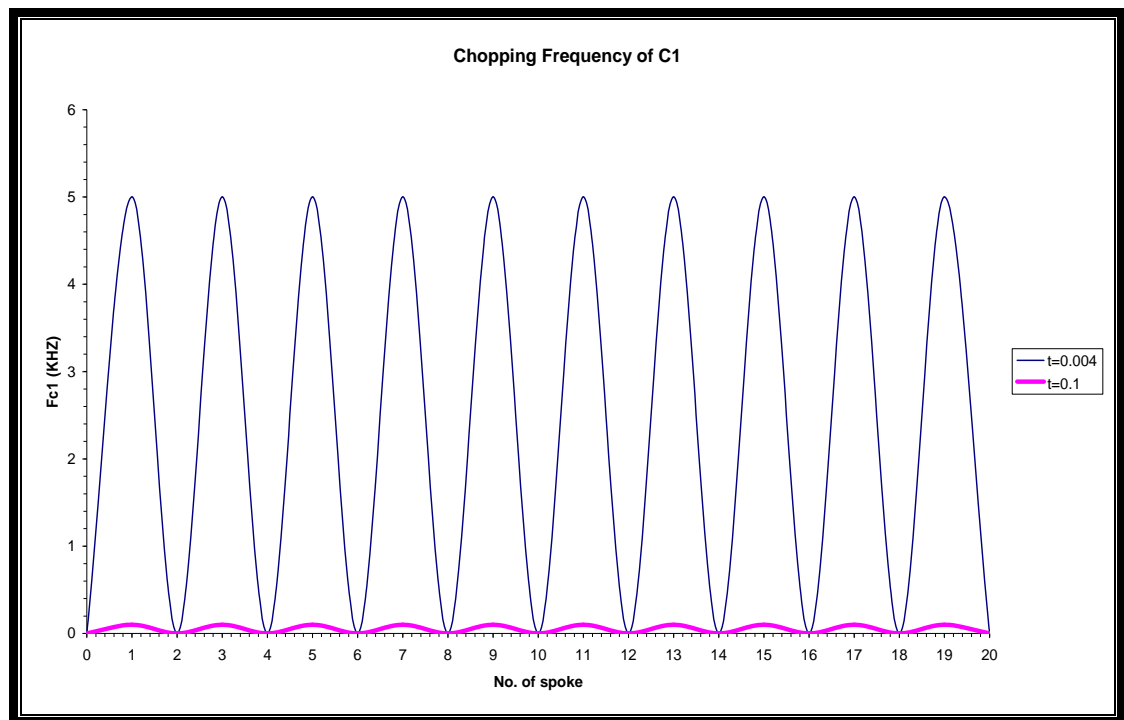


Fig. (4-8): Chopping frequency of C1 at  $t=(0.2,0.004)$  sec.

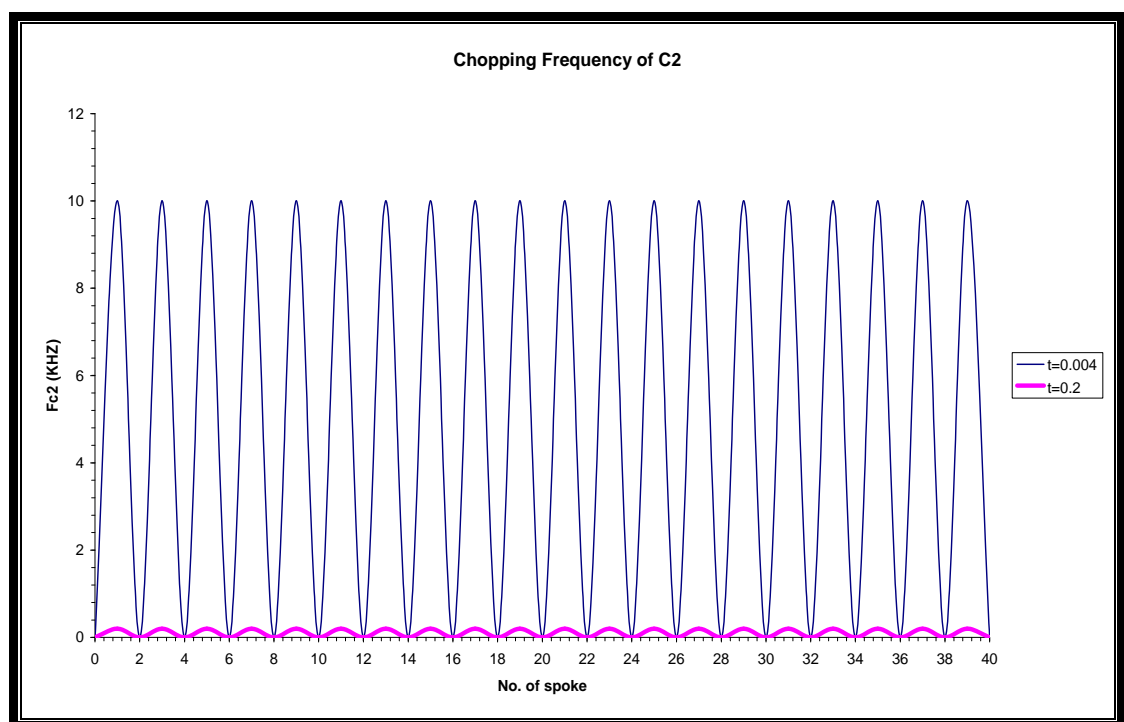


Fig. (4-9): Chopping frequency of C2 at  $t=(0.2,0.004)$  sec.

### 4-2 Evaluation of MTF

The MTF is one of the most useful means for characterizing the optical performance of an optical system. For the supposed optical modulator, the modulation transfer function MTF is calculated for each circle ( $C_0$ ,  $C_1$ ,  $C_2$ ) by calculating the transmittance intensity and by using the relationship:-

$$MTF = \frac{I_{\max} - I_{\min}}{I_{\max} + I_{\min}} \quad (4-2)$$

where:-

$I_{\max}$  is transmittance maximum intensity.

$I_{\min}$  is oblique minimum intensity.

First the area of each circle ( $S_n$ ) is calculated, it is assumed that the optical modulator has diameter equal to (9cm), and radius ( $R_r$ ) equal to (4.5cm), therefore the central circle ( $C_0$ ) has radius ( $R_0$ ) equal to (1.5cm) and the other two circles ( $C_1$ ,  $C_2$ ) have thickness equal to ( $R_0$ ). The area of each circle is given by :-

$$S_0 = (R_0)^2 \cdot \pi = 707 \text{ mm}^2 \quad \text{for } C_0$$

$$S_1 = (2R_0)^2 \cdot \pi - 706 = 211.9 \text{ mm}^2 \quad \text{for } C_1$$

$$S_2 = (3R_0)^2 \cdot \pi - 282.6 = 353.2 \text{ mm}^2 \quad \text{for } C_2$$

The circumference of each circle ( $C_0$ ,  $C_1$ ,  $C_2$ ) is (9.42, 18.87, 28.26)cm respectively. All of these relations are entered to the program in (Appendix A).

In this research the transmittance intensity is measured by the movement of spot light size. The measurement operation begin from the center of modulator ( $R_0=0$ ), and the spot light rotates about the center axis ( $360^\circ$ ) with constant radius (1.5 mm). That means the spot light makes ten circles (rings) in each circle ( $C_0$ ,  $C_1$ ,  $C_2$ ). Measurement of transmittance intensity depends on the ratio between the spot size ( three different spot sizes (1, 1.5, 2) mm<sup>2</sup> are used) and the area of the sub circle ( $S_{cn}$ ) of each

three circle. By using the program in (Appendix A), we calculate  $I_{max}$  (the ratio between the spot size and the transmittance area), and  $I_{min}$  (the ratio between the spot size and oblique area ). Then we measure the modulation transfer function MTF by using equation (4-2), (this equation enter to the program). The MTF was calculated for all three circle (C0,C1,C2).

#### 4-2-1 MTF of Central Circle (C0) (Fractal Modulator)

The fractal modulator (C0) was designed by using (DUG.Nelson) program (Appendix B). From this program, the iterated function systems (IFS) is found and is given in Table (4-2)

Table (4-2) The (IFS) codes of fractal modulator

w	a	b	C	d	e	f
-0.901	- 0.828	0.891	-0.781	277.71	127.05	0.125
-0.891	- 0.781	0.901	-0.828	339.32	351.29	0.125
0.891	- 0.781	0.901	0.828	430.15	235.77	0.125
0.901	- 0.828	0.891	0.781	208.17	245.23	0.125
0.901	- 0.828	0.891	0.781	344.98	129.31	0.125
0.891	0.781	-0.901	0.828	231.73	169.63	0.125
0.891	0.781	-0.901	0.828	208.17	242.56	0.125
-0.901	0.828	-0.891	-0.781	430.15	231.84	0.125
-0.901	0.828	-0.891	-0.781	232.86	308.72	0.125
-0.891	0.781	-0.901	-0.828	405.46	324.56	0.125

To measure the modulation transfer function (MTF), the (fractal element) must be chosen. Here the fractal element is selected as triangle shape, because the (IFS) codes are transformation of triangle.

Assume the fractal element is equilateral triangle, its dimension is (0.9 mm), and its altitude is (0.779 mm), therefore its area is (3.5 mm<sup>2</sup>). The number of triangles in (C0) is (20), these triangles are divided to (10) transmittance and (10) oblique. The modulation transfer function (MTF) is measured with respect to spot size movement. The spot size rotates about the modulation center axis, and in constant radius (1.5 mm). The spot size

movement begins from (0-15)mm. That means there are ten sub circles (rings) in circle (C0).

By using program in (Appendix A), the area of sub circles ( $S_n$ ), and area of transmittance and oblique sectors ( $S_{cn}$ ) are calculated. The maximum intensity ( $I_{max}$ ) represents the ratio between the spot size and transmittance area, and minimum intensity ( $I_{min}$ ) represents the ratio between the spot size and oblique area. Then by using equation (4-2), MTF is measured. We chosen three values of spot size (1,1.5,2) mm<sup>2</sup>, and given in Tables (4-3,4-4,4-5).

Table(4-3): MTF of central circle C0 at spot size (1mm<sup>2</sup>)

Ro(mm)	$S_n(\text{mm}^2)$	$S_{cn}(\text{mm}^2)$	MTF
1.5	7.060	0.353	0.725
3	21.21	1.059	0.40
4.5	35.34	1.766	0.224
6	49.48	2.472	0.163
7.5	63.61	3.179	0.137
9	77.75	3.885	0.09
10.5	91.89	4.592	0.066
12	106.02	5.298	0.046
13.5	120.16	6.005	0.028
15	134.30	6.711	0.0089

The MTF relationship is given in Fig. (4-10).The mean MTF is 0.1887.

Table(4-4): MTF of central circle C0 at spot size (1.5mm<sup>2</sup>)

Ro(mm)	$S_n(\text{mm}^2)$	$S_{cn}(\text{mm}^2)$	MTF
1.5	7.060	0.353	0.815
3	21.21	1.059	0.461
4.5	35.34	1.766	0.313
6	49.48	2.472	0.241
7.5	63.61	3.179	0.176
9	77.75	3.885	0.137
10.5	91.89	4.592	0.098
12	106.02	5.298	0.06
13.5	120.16	6.005	0.03
15	134.30	6.711	0.009

The MTF relationship is given in Fig. (4-11) The mean MTF is 0.234.



Table(4-5): MTF of central circle C0 at spot size ( $2\text{mm}^2$ )

Ro(mm)	Sn( $\text{mm}^2$ )	Scn( $\text{mm}^2$ )	MTF
1.5	7.060	0.353	0.942
3	21.21	1.059	0.652
4.5	35.34	1.766	0.44
6	49.48	2.472	0.32
7.5	63.61	3.179	0.232
9	77.75	3.885	0.169
10.5	91.89	4.592	0.125
12	106.02	5.298	0.081
13.5	120.16	6.005	0.057
15	134.30	6.711	0.032

The MTF relationship is given in Fig. (4-12). The mean MTF is 0.3021, and the relationship of the mean MTF and the spot size of the above Tables are given in Fig. (4-13).

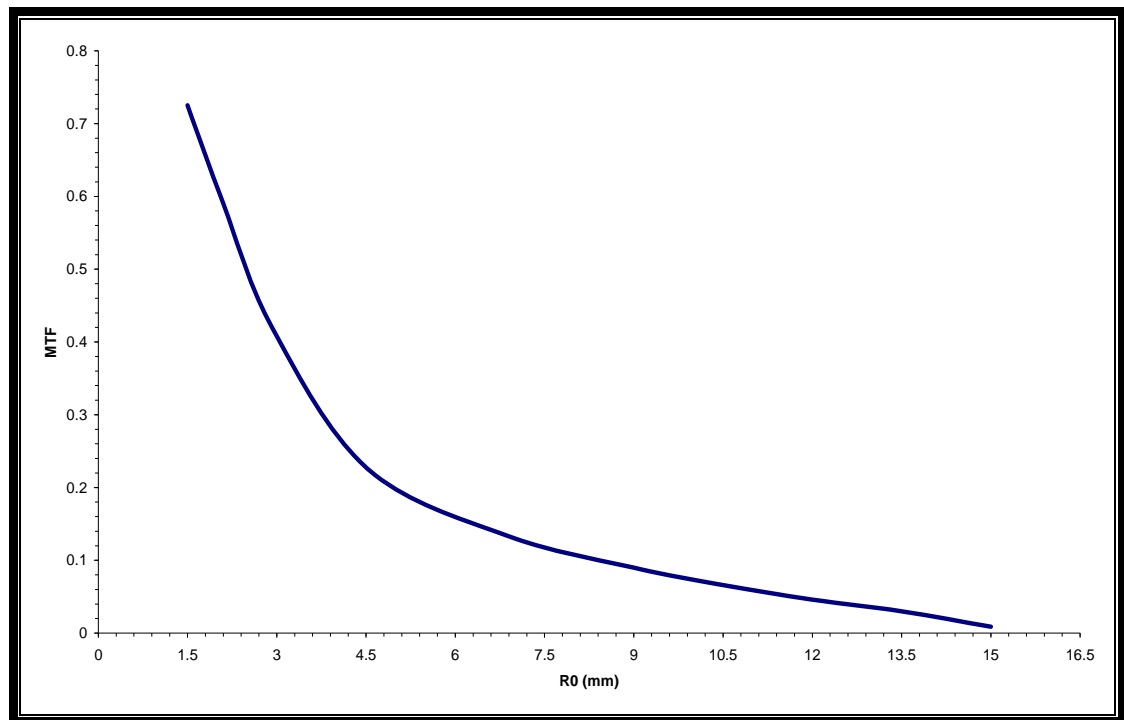


Fig. (4-10): MTF of fractal optical modulator in central circle (C0) at spot size ( $1\text{mm}^2$ )

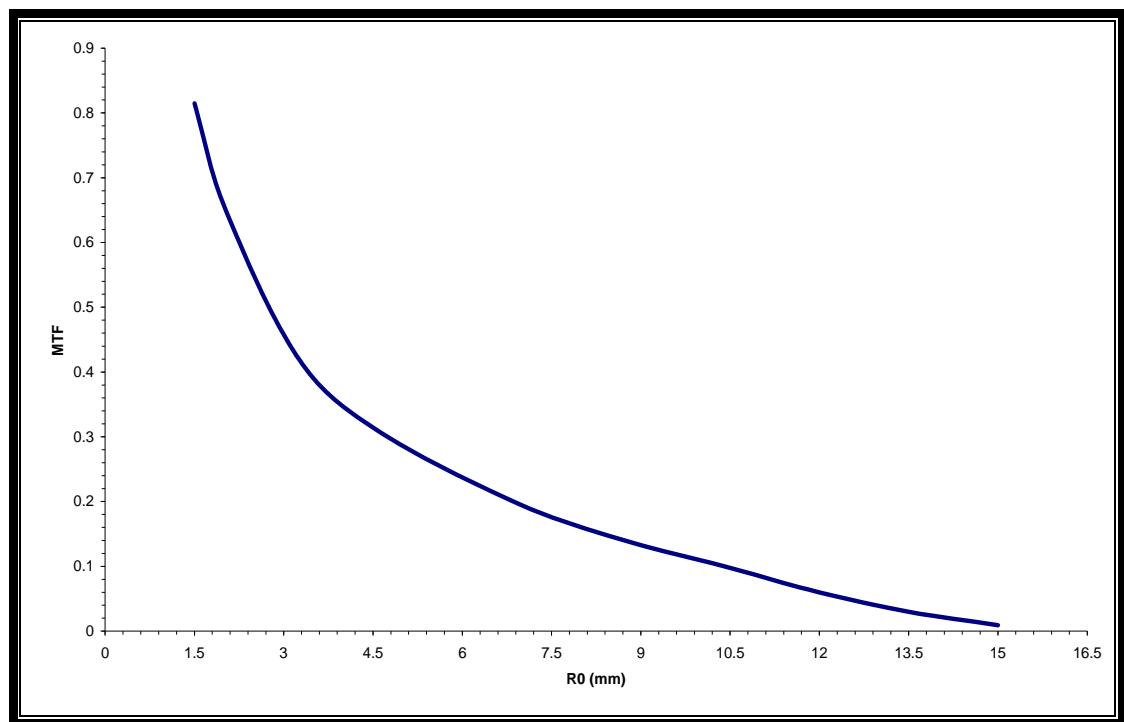


Fig. (4-11):MTF of optical modulator in central circle (C0) at spot size( $1.5\text{mm}^2$ )

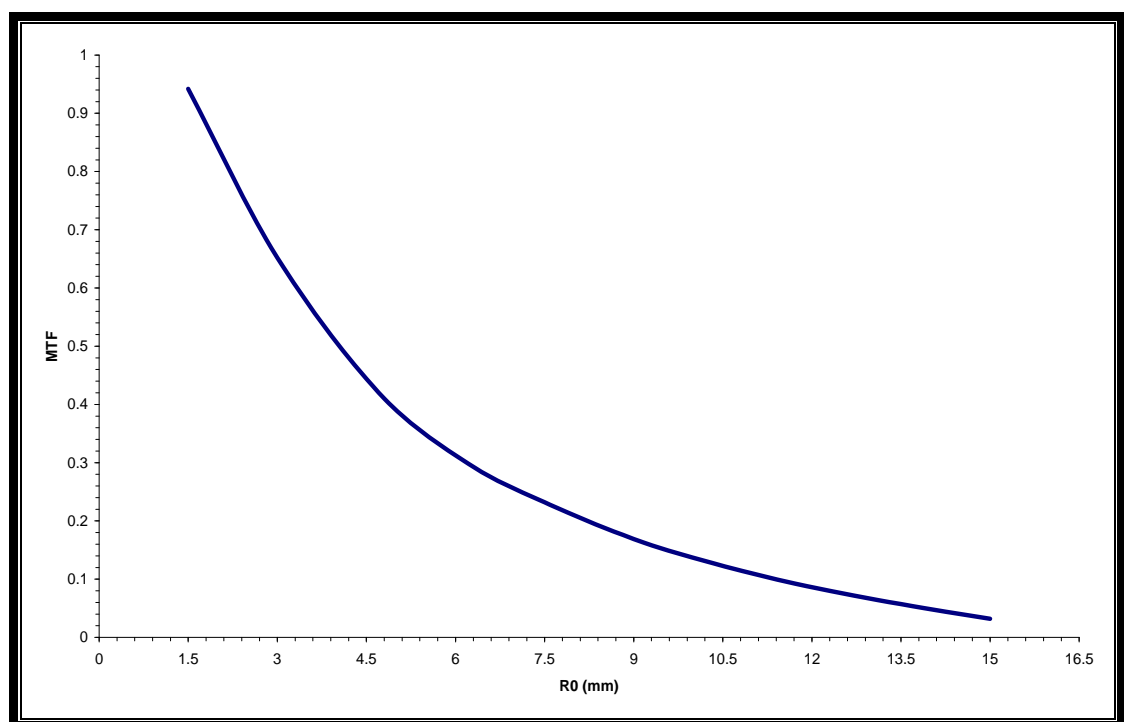


Fig. (4-12):MTF of optical modulator in central circle (C0) at spot size( $2\text{mm}^2$ )

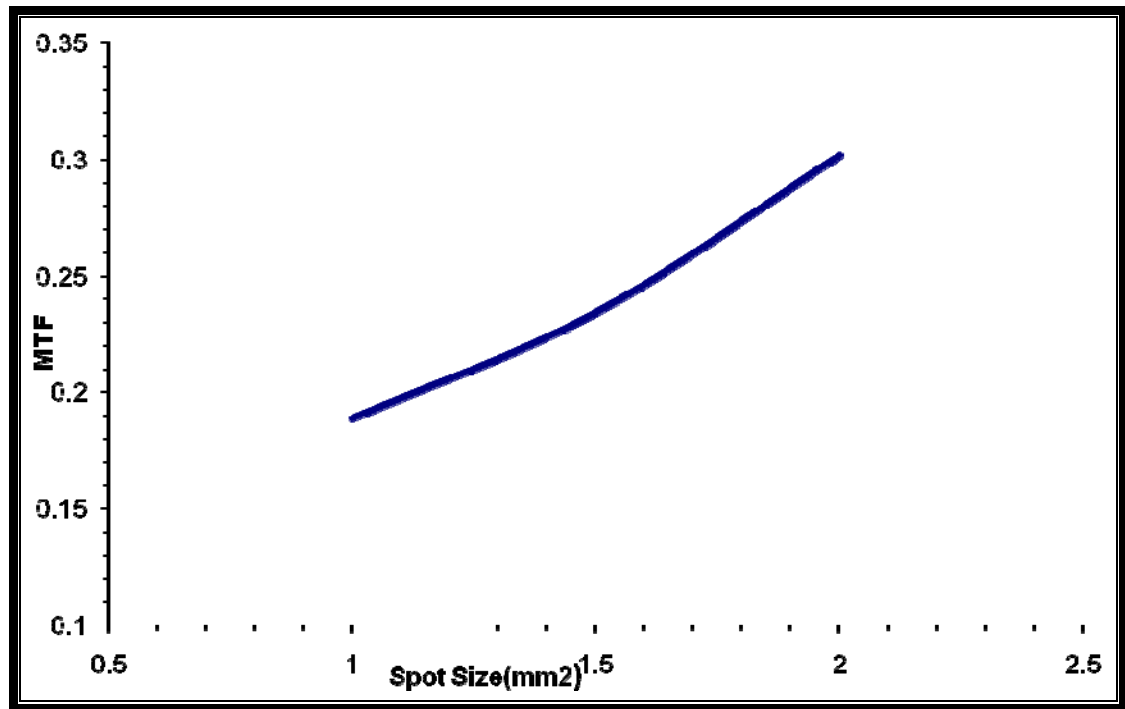


Fig. (4-13):The relationship between the mean MTF and spot size.

#### 4-2-2 MTF of Circle One (C1)(Acquisition Modulator)

This circle contains 20-sectors , that means there are 20 transmittances and 20 obliques. The spot size movement begins from R0=16.5 mm to 30 mm by steps 1.5 mm (ten circles). By using program in (Appendix A), modulation transfer function (MTF) is calculated, Tables (4-6,4-7,4-8), show the (MTF,Sn and Scn), for three different spot sizes (1,1.5,2) mm<sup>2</sup>.

Table(4-6):MTF of circle C1 at spot size (1mm<sup>2</sup>)

Ro(mm)	Sn(mm <sup>2</sup> )	Scn(mm <sup>2</sup> )	MTF
16.5	148.37	3.71	0.648
18	162.50	4.06	0.42
19.5	176.63	4.42	0.252
21	190.76	4.77	0.176
22.5	204.89	5.12	0.121
24	219.02	5.47	0.083
25.5	233.15	5.83	0.068
27	247.28	6.18	0.059
28	261.41	6.53	0.051
30	275.54	6.89	0.044

The MTF relationship is given in Fig. (4-14).The mean MTF is 0.189

Table(4-7):MTF of circle C1 at spot size (1.5mm<sup>2</sup>)

Ro(mm)	Sn(mm <sup>2</sup> )	Scn(mm <sup>2</sup> )	MTF
16.5	148.37	3.71	0.687
18	162.50	4.06	0.541
19.5	176.63	4.42	0.422
21	190.76	4.77	0.202
22.5	204.89	5.12	0.172
24	219.02	5.47	0.130
25.5	233.15	5.83	0.106
27	247.28	6.18	0.091
28	261.41	6.53	0.073
30	275.54	6.89	0.064

The MTF relationship is given in Fig. (4-15).The mean MTF is 0.238

Table(4-8):MTF of circle C1 at spot size (2mm<sup>2</sup>)

Ro(mm)	Sn(mm <sup>2</sup> )	Scn(mm <sup>2</sup> )	MTF
16.5	148.37	3.71	0.917
18	162.50	4.06	0.68
19.5	176.63	4.42	0.485
21	190.76	4.77	0.351
22.5	204.89	5.12	0.251
24	219.02	5.47	0.182
25.5	233.15	5.83	0.135
27	247.28	6.18	0.1
28	261.41	6.53	0.073
30	275.54	6.89	0.051

The MTF relationship is given in Fig. (4-16).The mean MTF is 0.322, and the relationship of the mean MTF and the spot size of the above Tables are given in Fig. (4-17).

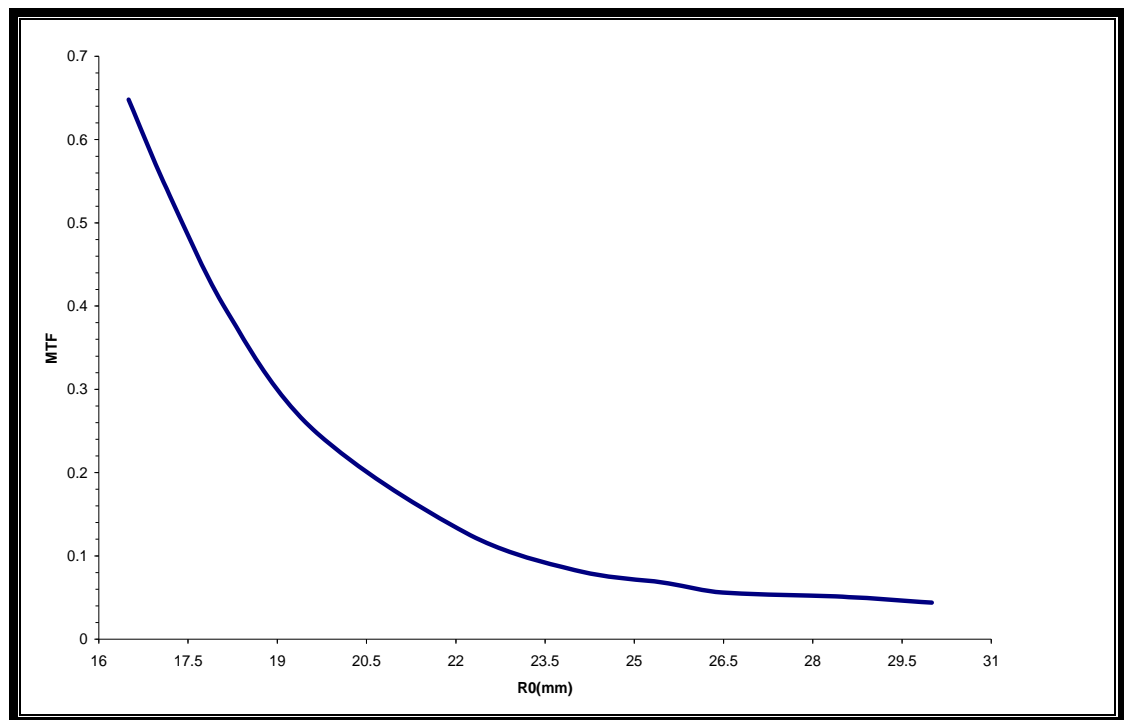


Fig. (4-14):MTF of optical modulator in circle (C1) at spot size( $1\text{mm}^2$ )

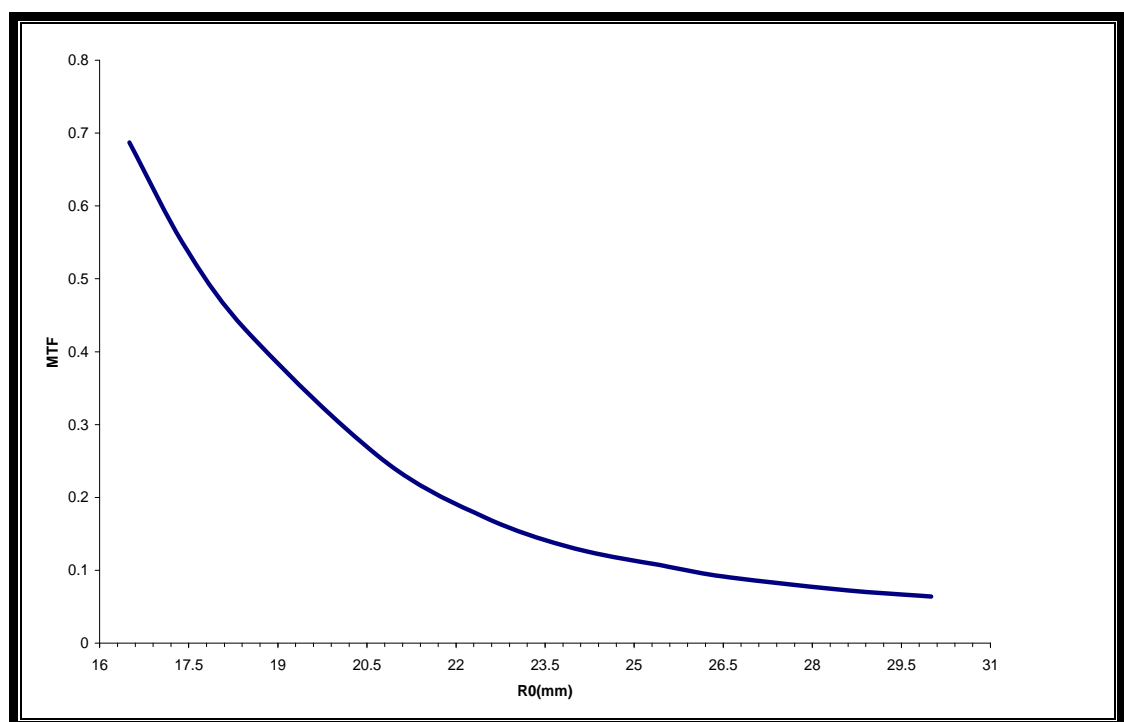


Fig. (4-15):MTF of optical modulator in circle (C1) at spot size( $1.5\text{mm}^2$ )

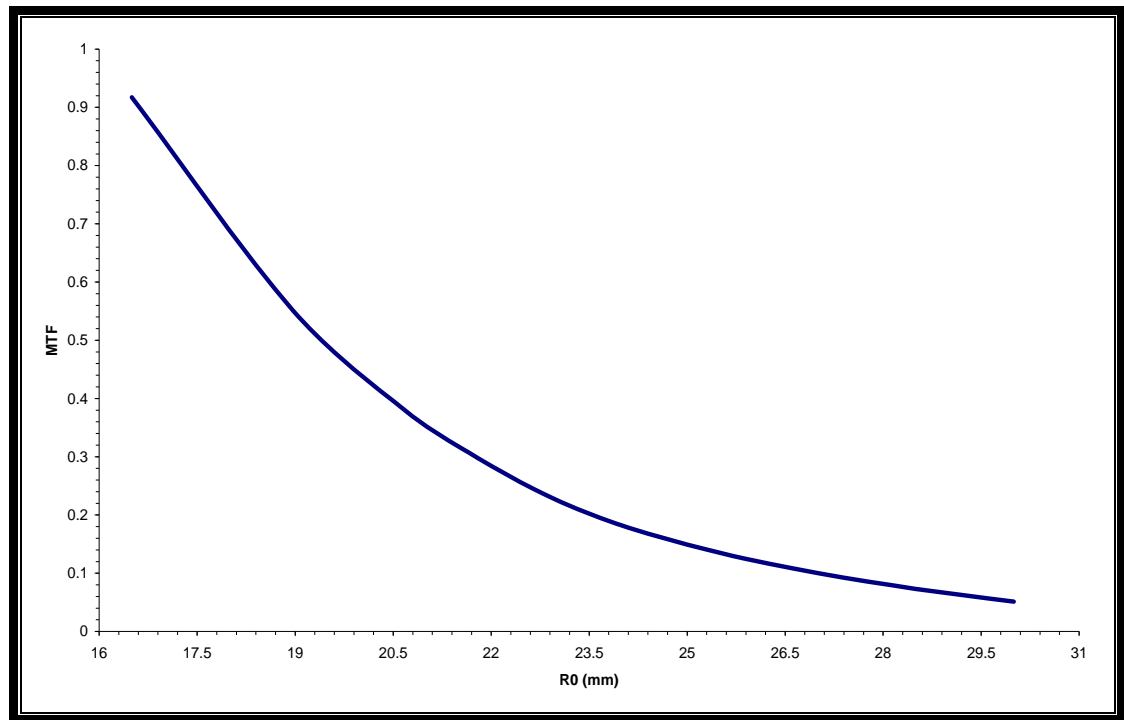


Fig. (4-16):MTF of optical modulator in circle (C1) at spot size( $2\text{mm}^2$ )

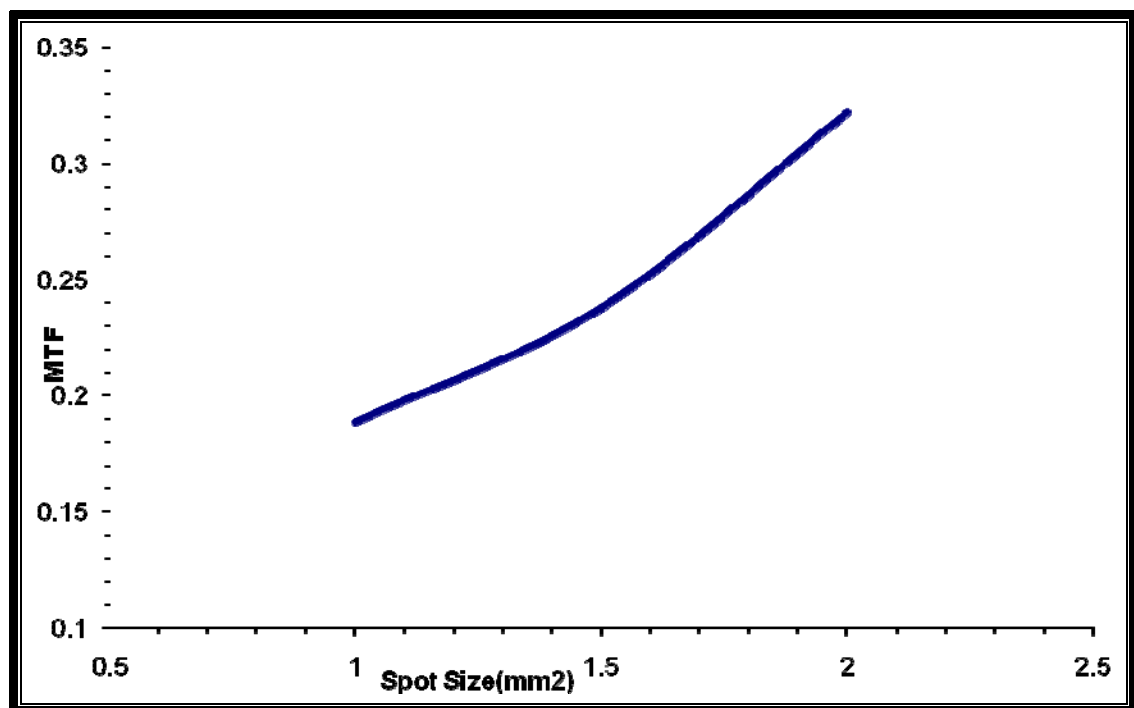


Fig. (4-17):The relationship between the mean MTF and spot size.

**4-2-3 MTF of Circle Two (C2)(Detection Modulator)**

This circle contains 30-sectors, that means there are 30 transmittances and 30 oblique. The spot size movement begins from  $R_0=31.5$  mm to 45 mm by steps 1.5mm (ten circles). By using program in (Appendix A), modulation transfer function (MTF) is calculated, Tables (4-9,4-10,4-11), show the (MTF,  $S_n$  and  $S_{cn}$ ), for three different spot sizes (1,1.5,2)  $\text{mm}^2$ .

Table(4-9):MTF of circle C2 at spot size (1 $\text{mm}^2$ )

Ro(mm)	$S_n(\text{mm}^2)$	$S_{cn}(\text{mm}^2)$	MTF
31.5	289.66	4.827	0.841
33	303.79	5.063	0.461
34.5	317.92	5.298	0.271
36	332.05	5.334	0.171
37.5	346.18	5.796	0.121
39	360.31	6.005	0.075
40.5	374.44	6.240	0.05
42	388.57	6.471	0.037
43.5	402.70	6.711	0.36
45	416.83	6.947	0.17

The MTF relationship is given in Fig. (4-18).The mean MTF is 0.125

Table(4-10):MTF of circle C2 at spot size (1.5 $\text{mm}^2$ )

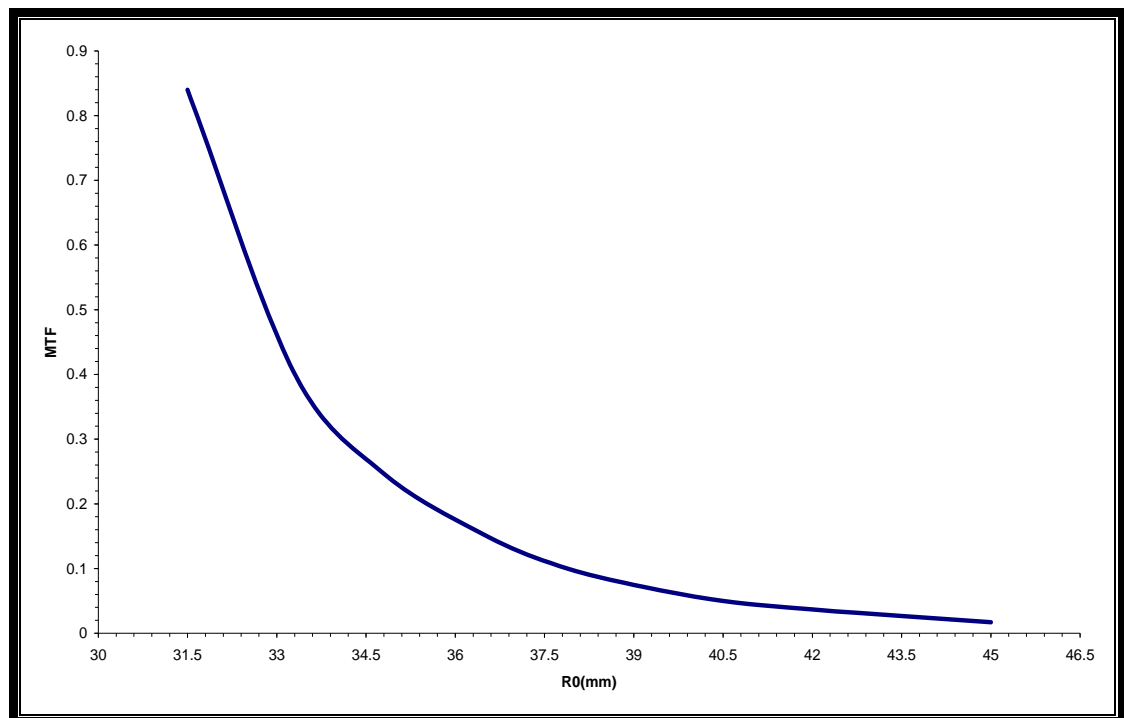
Ro(mm)	$S_n(\text{mm}^2)$	$S_{cn}(\text{mm}^2)$	MTF
31.5	289.66	4.827	0.907
33	303.79	5.063	0.406
34.5	317.92	5.298	0.249
36	332.05	5.334	0.177
37.5	346.18	5.796	0.127
39	360.31	6.005	0.094
40.5	374.44	6.240	0.072
42	388.57	6.471	0.055
43.5	402.70	6.711	0.040
45	416.83	6.947	0.017

The MTF relationship is given in Fig. (4-19).The mean MTF is 0.2088

Table(4-11):MTF of circle C2 at spot size ( $2\text{mm}^2$ )

Ro(mm)	Sn( $\text{mm}^2$ )	Scn( $\text{mm}^2$ )	MTF
31.5	289.66	4.827	0.917
33	303.79	5.063	0.715
34.5	317.92	5.298	0.55
36	332.05	5.334	0.42
37.5	346.18	5.796	0.335
39	360.31	6.005	0.262
40.5	374.44	6.240	0.2
42	388.57	6.471	0.152
43.5	402.70	6.711	0.11
45	416.83	6.947	0.08

The MTF relationship is given in Fig. (4-20).The mean MTF is 0.3731, and the relationship of the mean MTF and the spot size of the above Tables are given in Fig. (4-21).

Fig. (4-18):MTF of optical modulator in circle (C2) at spot size( $1\text{mm}^2$ )



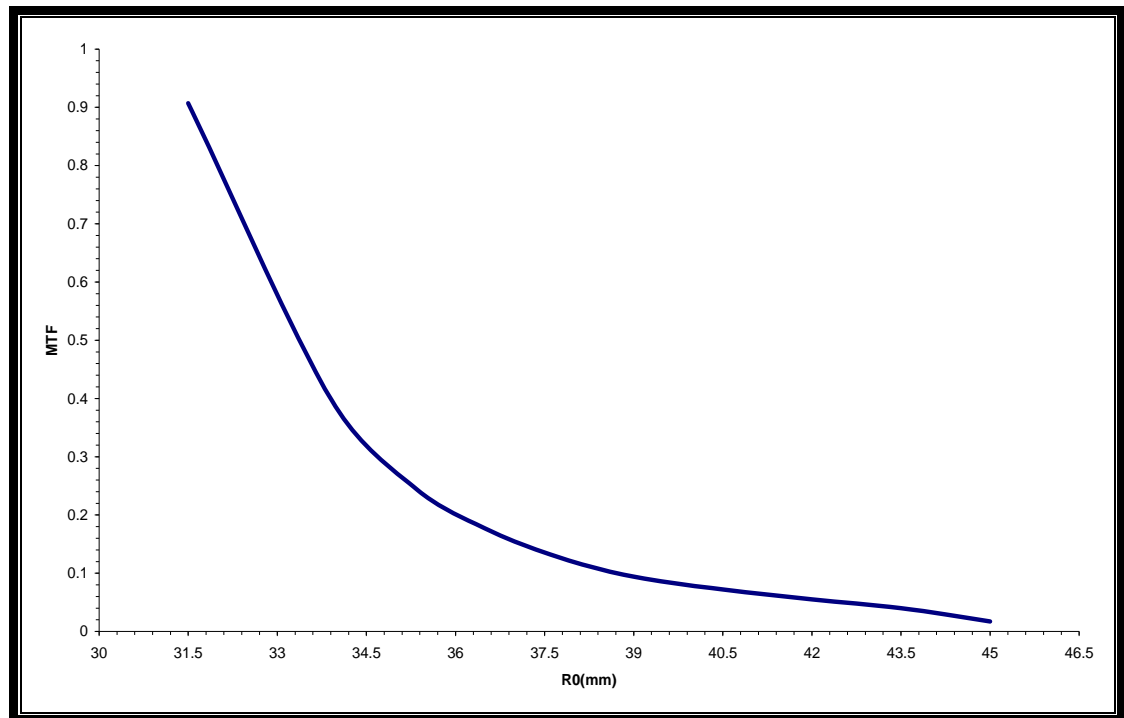


Fig. (4-19):MTF of optical modulator in circle (C2) at spot size( $1.5\text{mm}^2$ )

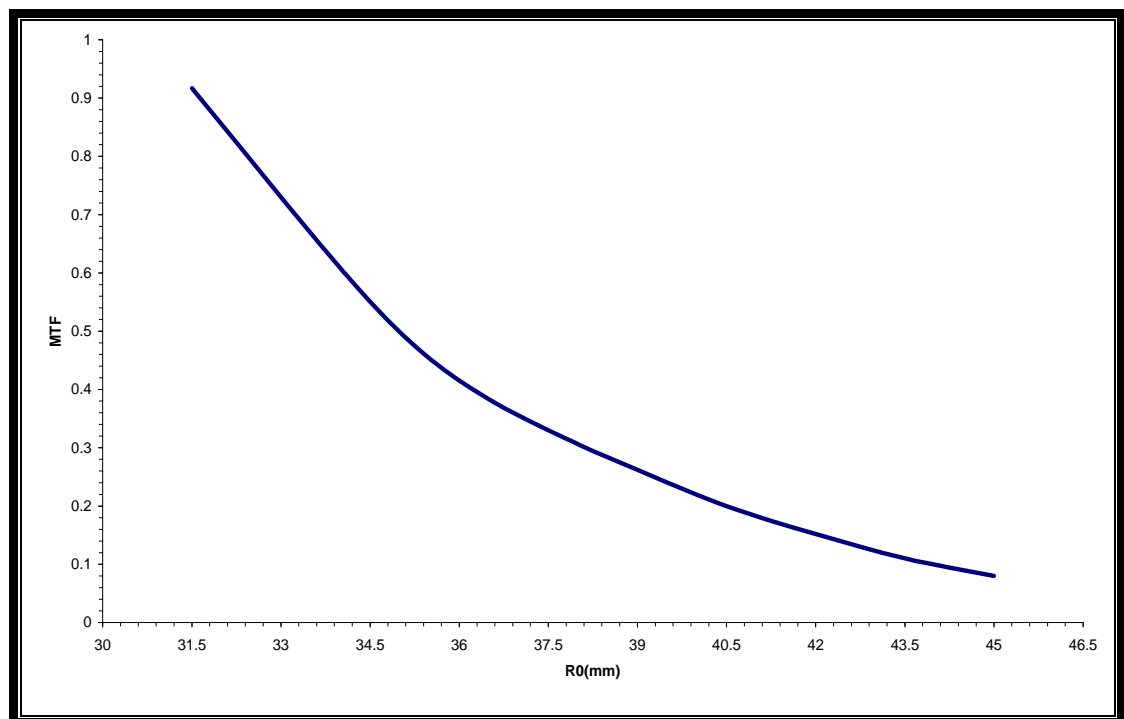


Fig. (4-20):MTF of optical modulator in circle (C2) at spot size( $2\text{mm}^2$ )

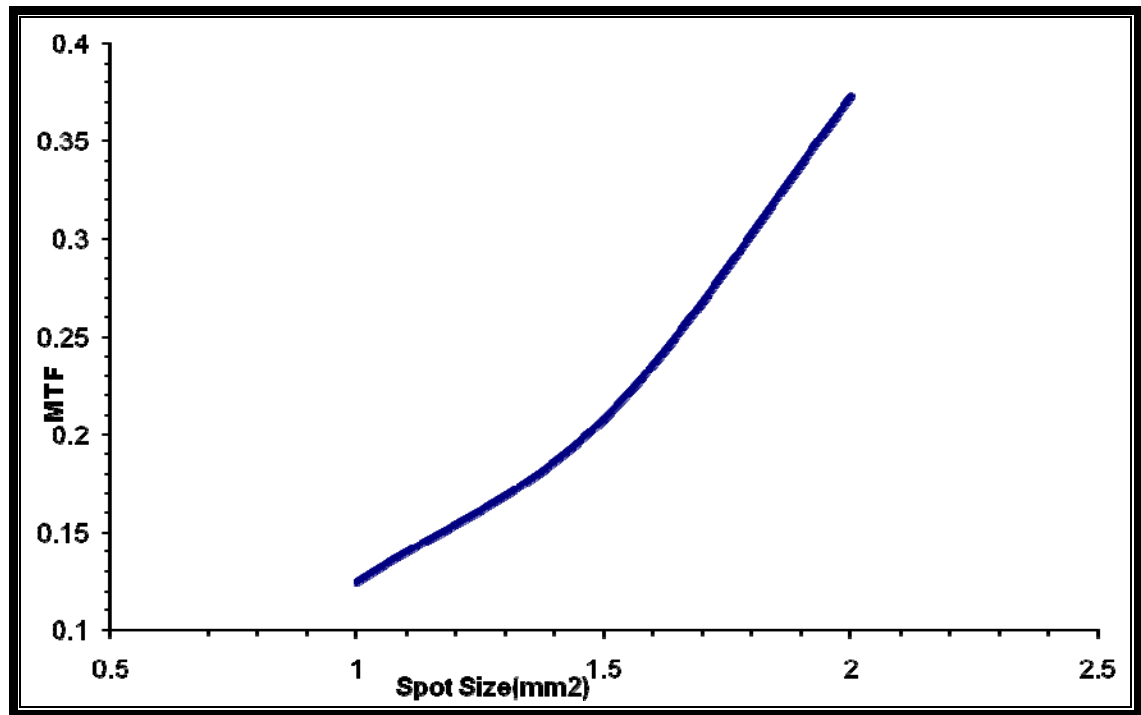


Fig. (4-21):The relationship between the mean MTF and spot size.

**4-3Discussion**

In this section the calculated results, and the relationships in the Figures will be discussed.

Table (4-1) shows the increase in frequency by increasing the number of circles ( $n$ ), when ( $n=1$ ) the value of chopping frequency of optical modulator disk ( $F_{c0}$ ) is 2.5 KHZ, and when ( $n=2$ ) the value of chopping frequency ( $F_{c1}$ ) is 5 KHZ, and when ( $n=3$ ) the value of ( $F_{c2}$ ) is 10 KHZ. The above values are at time( $t$ ) equal to 0.004 sec. As it has been noticed that frequency decreases with increased time, because at time equal to 0.2 sec, the rotational frequency of optical modulator disk is 5 HZ and chopping frequencies ( $F_{c0}, F_{c1}, F_{c2}$ ) is (0.05, 0.1, 0.2) KHZ respectively.

From Figures (4-6, 4-7) it is noticed the change in frequency with difference in the number of sector, and same case is in Figures (4-8, 4-9). Comparison between the three cases (central, one and two circles), the influence of the number of sectors on frequency is notice, where the frequency is different because the number of sectors changes in each circle.

From Table (4-2), we choose the suitable dimensions of fractal element, because the chosen fractal element is equilateral triangle and the Table indicates the IFS codes of the fractal shape, where the IFS codes is transformation of triangle. From the Table (4-2) we used triangle dimension equal to (0.9 mm), and its altitude is (0.779 mm).

From Table (4-3), it is noticed that the modulation transfer function (MTF) decreases with increasing the circle radius ( $R_0$ ), because at  $R_0 = 1.5$  mm, the MTF is 7.20, but when the radius  $R_0 = 15$  mm the MTF is 0.0089, this is will be clear in Figures (4-10, 4-11, 4-12). By comparing among Tables (4-3, 4-4, 4-5), we notice that the MTF increases by increasing spot size. From Tables (4-3, 4-4, 4-5) the mean MTF is (0.1887, 0.234, 0.3021) respectively. And from the Fig. (4-13) it can be seen that the mean MTF is increases with increasing spot size.

From Table (4-6), it is noticed that the (MTF) decreases with increasing the circle radius ( $R_0$ ), where  $R_0 = 16.5$  mm, the MTF is 0.648, but when the radius  $R_0 = 30$  mm the MTF is 0.044, this will be clear in Figures (4-14,4-15,4-16). By comparing among Tables (4-6,4-7,4-8), it is noticed that the MTF increases with increasing spot size. From Tables(4-6,4-7,4-8) the mean MTF is (0.189,0.238,0.322) respectively. And from the Fig. (4-17) it can be seen that the mean MTF is increasing with increasing spot size.

From Tables (4-9), at  $R_0 = 31.5$  mm, the MTF is 0.84, but when the radius  $R_0 = 45$  mm the MTF is 0.017, it can be seen that the MTF decreases with increasing the circle radius ( $R_0$ ), this is clear in Figures (4-18,4-19,4-20). By comparing among Tables (4-9,4-10,4-11), it is noticed that the MTF increases with increasing spot size. From Tables(4-18,4-19,4-20) the mean MTF is (0.125,0.2088,0.3731) respectively. And from the Fig.(4-21) it is can be seen that the mean MTF increases with increasing spot size.

### ***5.1 Conclusions***

1. The MTF of the supposed optical modulator will be increasing with increasing the spot size and decreasing with increasing  $R_0$ .
2. The maximum chopping frequencies in circles ( $C_0, C_1, C_2$ ) are (2.5,5,10)KHZ at ( $t=0.004$ )sec, and minimum chopping frequencies are (0.05,0.1,0.2)KHZ at ( $t=0.2$ )sec, and the best modulation at spot light size equal to ( $2 \text{ mm}^2$ ).
3. The type of supposed optical modulator can be defined by using the suitable spot size.
4. Circle two can be used as detection modulator by using large size of spot size, and circle one can be used as acquisition modulator by using smaller size than spot size, and the central circle (Fractal) can be used as tracking modulator because it is more accurate.
5. The fractal modulator can be used with another normal optical modulator in optical systems.
6. The fractal function can be used to design the optical modulator, especially for fine optical measurement.

### ***5.2 Suggestions for Future Work***

For future work, it is suggested the future work should be extended with:-

1. large number of circle.
2. large number of sectors.
3. different sector shapes.

## *List Of Abbreviation*

<i>symbol</i>	<i>Meaning</i>
<b>AM</b>	<i>Amplitude Modulation</i>
<b>CTF</b>	<i>Contrast Transfer Function</i>
<b>DSF</b>	<i>Disk Spread Function</i>
<b>FM</b>	<i>Frequency Modulation</i>
<b>LSB</b>	<i>Lower Side Band</i>
<b>LSF</b>	<i>Line Spread Function</i>
<b>MTF</b>	<i>Modulation Transfer Function</i>
<b>OPD</b>	<i>Optical Path Difference</i>
<b>OTF</b>	<i>Optical Transfer Function</i>
<b>PSF</b>	<i>Point Spread Function</i>
<b>PM</b>	<i>Phase Modulation</i>
<b>USB</b>	<i>Upper Side Band</i>

## List of Symbols

<i>symbol</i>	<i>Meaning</i>
$A$	<i>Point in initial area</i>
$A'$	<i>Point under matrix(T) operation</i>
$a,b,c,d$	<i>Real numbers have two-dimantional</i>
$B_{ang}$	<i>Angular diameter of Airy disk</i>
$B_{diff}$	<i>Airy disk diameter</i>
$\beta_n(t)$	<i>Temporal function representing the modulation factor of the disk</i>
$\gamma$	<i>Pulse duty factor</i>
$\delta$	<i>Phase different</i>
$\Delta\delta$	<i>Maximum deviation of the frequency</i>
$f$	<i>Focal length</i>
$(f/\#)$	<i>Focal number</i>
$f_c$	<i>Chopping frequency</i>
$f_m$	<i>Modulation frequency</i>
$f_r$	<i>Rotational frequency</i>
$f(x,y)$	<i>The ideal image function</i>
$\phi$	<i>The phase</i>
$\Phi_0$	<i>Radiance power intensity</i>
$G(\xi,\eta)$	<i>Fourier transform of <math>g(x,y)</math></i>
$g(x,y)$	<i>Image irradiance distribution</i>
$H(\xi,\eta)$	<i>Fourier transform <math>h(x,y)</math></i>
$h(x,y)$	<i>Impulse response function</i>
$I_{max}$	<i>Maximum intensity</i>
$I_{min}$	<i>Minimum intensity</i>
$J_n(m_{FM})$	<i>Bessel function of the <math>n</math> kind to the variable(<math>m_{FM}</math>)</i>
$K$	<i>Proportion constant</i>
$\lambda$	<i>Wavelength</i>
$M$	<i>Modulation depth</i>
$m_{AM}$	<i>Amplitude modulation index</i>
$m_{FM}$	<i>Frequency modulation index</i>
$\mu_{mo}$	<i>Modulation factor</i>

$n$	<i>Real number</i>
$o$	<i>Origin point</i>
$o(x,y)$	<i>Spatial signal function</i>
$O(k_x,k_y)$	<i>Fourier transform of spatial signal function</i>
$\omega_o$	<i>Angular frequency</i>
$\omega_r$	<i>Angular frequency of the disk rotation</i>
$\omega_c$	<i>Angular frequency of the carrier wave</i>
$\omega_m$	<i>Angular frequency of the modulation wave</i>
$q$	<i>Number of transmittance and oblique sector</i>
$R_r$	<i>Radius of optical modulator disk</i>
$R_o$	<i>Radius of central circle of the disk</i>
$\rho$	<i>Radius of the aperture</i>
$r(x,y,t)$	<i>The optical modulator disk function</i>
$r(\rho,\theta,t)$	<i>The optical modulator disk function in the Cartesian coordinate</i>
$S_{cn}$	<i>Area of the transmittance and oblique sector</i>
$S_n$	<i>Area of the circle(n)</i>
$S(x,y)$	<i>The object scene function</i>
$s(\rho,\theta,t)$	<i>Object scene function in the Cartesian coordinate</i>
$t$	<i>Time</i>
$T$	<i><math>n \times n</math> matrix</i>
$T_p$	<i>The time-interval between pulses</i>
$\tau_p$	<i>Band width of the single pulse</i>
$V(t)$	<i>Output signal of the detector</i>
$W$	<i>Transformation on the Euclidean plane</i>
$W_a$	<i>Wave aberrations</i>
$Z$	<i>Limit of resolution</i>



---

References:

1. V.Gerbig ,A.W.Lohman , " App. Optics", Vol.28, No.24, PP.5198, (1989)
2. R.Kingslake , "Applied Optics and Optical Engineering", Vol.III, PP.183, (1965) .
3. K.S.Kapany and J.J.Burke, Optics . Soc. Am ., Vol.52 ,No.12, PP.1351, (1962).
4. A. H. AL-Hamdani., "Numerical Evaluation of lenses Quality Using Computer Software", Ph.D.Thesis Al-Mustansiriyah University", (1997).
5. M.J. Riedl, "Optical Design Fundamentals for Infrared Systems", 2nd ed., SPIE, the International Society for Optical Engineering, Bellingham, Washington, USA, (2001).
6. F. P. Twyman , Optics.Soc. Vol.6, PP.35,49, (1923).
7. M. Daniel, optical shop testing, John Wileg and sons, 1978 .
8. J.M Woznick and T.Henri, "Motional effect in retardation plates and mode locking in ring lasers ",J. Modern Optics, Vol.46, No.6, PP.1031 ,(1999)
9. R.E. Fischer and B. Tadic-Galeb, "Optical System Design", McGraw -Hill,2000.
10. R.D. Hudson, "Infrared System Engineering", John Wiley and Sons, (1969).
11. L.F. Pau, "An Introduction to Infrared Imaging Acquisition and Classification Systems", Research Studies Press LTD,(1983).
12. E. Hecht ,Optics, Third Edition, Addition-Wesky Publishing Company,(1998).
13. S.A. Habbana, "Design and Evaluation of Image Quality for IR Scanner ", Ph.D. Thesis, Military College of Engineering, Baghdad, Iraq, (2001).

- 
14. *C. S. Williams and O. A. Bechlund, Optics, short course for engineers & Scientists , John Wiley and Sons, Inc (1972).*
  15. *J.W. Blaker, "Geometric Optics", The Matrix Theory, Macel Dekker, Inc. New York (1971).*
  16. *F. A. Jankins. "Fundamentals of Optics" 4<sup>th</sup> ed. McGraw- Hill, (1957).*
  17. *J. M. Skjaclund, App. Opt. , Vol. 27 , No. 12 , PP. 2580 , (1988) .*
  18. *R.R. Shannon , Spie Vol. 531, Geometrical optics PP. 27, (1985).*
  19. *W.J. Smith, "Modern Optical Engineering", McGraw- Hill, (2000).*
  20. *M. Born, E. Wolf, "Principles of Optics", 6<sup>th</sup> ed., Pergman, London, (1970).*
  21. *D.E. Stoltzman, "Applied Optic and Optical Enginerring" edt. by R.R. Shannon, New York: Academic Press, Vol. 9, (1983).*
  22. *R.E. Fischer and B. Tadic-Galeb, "Optical System Design", McGraw-Hill, (2000).*
  23. *J. Simcik, Curriculum Morphing Project, " Electro-Optic and Acousto-Optic Devices", Vol. 4, PP 7, (1992).*
  24. *M.B. Kathryn and L.H. Steven, "The Essenc Of Optoelectronice", Prentice Hall, (1998).*
  25. *K.P. William, "Laser Communication System", John Wiley & Sons, (1969).*
  26. *J. Wilson and J.F. Hawkes, "Laser Principles and Application", Prentice Hall (1987).*
  27. *W. Hollyer, "Optical Choppers and Optical Shutters", Global Spec Inc (1999).*
  28. *R. Carpenter, "Comparison of AM and FM Reticle System", Applied Optics, Vol. 2, No. 1, PP. 229-236, March, (1963).*
  29. *F. Schwarz. and G. Jankowitz, "Performance of a Wire-Guided Missile Control System", IRIS Proc., Vol. 2, No. 1, PP. 83-90. Nov. (1967).*

- 
30. P. Garnell. and D.J. East, "Guided Weapon Control Systems", Pergamon Press. (1977).
  31. M. Hewish, R. Luria and G. Turbe, "Anti-Tank Guided Weapons", Part 1, *International Defense Review*, pp(1631,12), (1989).
  32. B.B. Mandelbrot, , "The Fractal geometry of nature", W.H. Freeman and Company, (1983).
  33. F. Liedtke, "Computer Simulation of an automatic Classification Procedure for Digitally Communication Signals with Unknown Parameters", *Signal Processing Magazine*, Vol. 6, pp. 311-323, 1984.
  34. P. Lollo, "Signal Classification by Discrete Fourier Transform ", *IEEE Int. Conf. on MILCOM*, May 1999.
  35. Y. Fukui "Modulation Transfer Function (MTF)" March 20, 2003.
  36. M. L. Jebbar, " Evaluation of MTF for Fractal Optical Modulator of Semiconductor", M.Sc. Thesis, Al-Mustansiriya University 2007.
  37. Y.Yakushenkov, "Electro-Optical Devices, Theory and Design", Mir Publishers, Moscow, (1983).
  38. W.L .Wolfe. and G. J. Zissis.,Eds, "The Infrared Handbook", (IRIA) Center, Environmental Research Institute of Michigan, (1968).
  39. S. Lapatine , "Electronics in Communications", John Wiley and Sons (1986).
  40. O. Glossary " Newport "PP. 604 (2003).  
Email :Sales @ Newport .com.
  41. "Stanford Research systems". (2003).  
Visit on line [www. Thinksys .com](http://www.Thinksys.com).
  42. J. L. Alward. And R. R. Legault , "Stat-of-the Art Report on Spatial Filtering ", *IRIS* Vol.9, No. 1, pp. 83-86, (1964).
  43. H. G. Eldering , "The Theory of Optimum Spectral Filtering", *Infrared Physics*, Vol. 4, No. 4, pp. 231-237, (1964).
  44. L. M. Biberman, "Reticles in Electro-Optical Devices" , Pergamon

- Press, (1966).
45. D. H. Pollock, J.S.Accetta & D.L.Shumaker, "Optical Engineering Press, Bellingham ", (Countermeasure System). Vol. 7. (Infrared & Electro-Optical Systems Handbook). PP.235-286, (1993).
46. B.H, Walker, "Image Quality", Proc. Vol.549, PP.154-150 (1985).
47. J. W. Goodman, "Introduction to Fourier Optics", Mc Graw-Hill Physical and Quantum Electronics Series, (1968).
48. C.S. Williams, and O. A. Becklund, "Introduction to the Optical Transfer Function", Wiley Series in pure and Applied Optics, (1989).
49. Modulation Transfer Function, "Melles Griot" 3-4 , 3-5 (2000) .
- 50.K. Falconer, "Fractal geometry Mathematical ", Foundations & Applications, John Wiley and Sons Ltd, Chester (1999).
51. A. Kenneth and D.A. Gregory, "The calculation of fractal dimension in the presence of non – fractal cluster", SPIE, Vol.3765, pp. 216-227, (1999).
52. A. Workshop presented at the Society for Chaos Theory in Psychology and the Life Sciences meeting, July 31, (1997).
53. C.M. Francis, "Chaotic and fractal dynamics", John Wiley& Sons, (1992).
54. M.F. Barnsley, and L. P. Hurd, "Fractal image compression" Ak peters Ltd. (1993).
55. Doug Nelson "Fractal Design". (CompuServe ID). 704313374.(1996).  
<http://archives.math.utk.edu/software/msdos/dynamics/fdesign/fdesi313.zip>

## الخلاصة

قرص التضمين البصري (**Optical Modulator**) عنصر مهم في المنظومات البصرية، وهو عبارة عن آلة تقوم بتحويل الزاوية بين خط النظر إلى الهدف، والمحور البصري إلى إشارة كهربائية، ويأخذ عدة أشكال دائرية وذلك بحسب الحاجة إليه. يقوم قرص التضمين البصري بتضمين الإشارة الضوئية بتردد معين حسب شكل وعدد المقاطع.

قمنا خلال بحثنا هذا بتصميم قرص تضمين بصري يتكون من ثلاثة دوائر متحدة المركز (**C0, C1, C2**)، وكل دائرة من هذه الدوائر تم تقسيمها إلى أزواج من القطاعات الشفافة والمعتمة، تم اختيار عدد القطاعات مساوي الى (20,40,60) على التوالي، وعدد هذه القطاعات يزداد تصاعدياً مع زيادة عدد الدوائر. وتم اختيار سمك كل دائرة من الدوائر الثلاثة مساوي الى  $(R_o=1.5) \text{ cm}$ ، هذا يعني أن نصف قطر قرص التضمين البصري هو  $(R_r=4.5) \text{ cm}$ .

تم تصميم الدائرة المركزية (**C0**) باستخدام دالة الهندسة الكسورية (**Fractal**)، وذلك باستخدام برنامج خاص تم تعديله لرسم وتوضيح الأشكال الكسورية، ومن ضمنها المقطع الكسوري (**Fractal Modulator**)، والشكل النهائي لقرص التضمين المقترح تم تصميمه باستخدام برامجيات (**Auto-CAD**).

تمت دراسة كفاءة قرص التضمين البصري من خلال حساب دالة الانتقال المعدلة له (**Modulation Transfer Function MTF**)، فقد وجدنا من خلال البيانات والأشكال البيانية لهذه الدالة أن أعلى تردد قطع تم الحصول عليه للدوائر ( $C_0, C_1, C_2$ ) هو (2.5,5,10) KHZ على التوالي عند الزمن  $(t=0.004) \text{ sec}$ ، وأقل تردد قطع تم الحصول عليه هو (0.05,0.1,0.2) KHZ عند الزمن  $(t=0.2) \text{ sec}$ ، وأن أفضل تضمين تم الحصول عليه هو عندما يكون حجم البقعة الضوئية مساوي الى  $(2 \text{ mm}^2)$ ، وان قرص التضمين المقترح يمكن استخدامه في المنظومات البصرية.